Structure-Activity Relationship Studies on Daptomycin

by

Ghufran Barnawi

A thesis
presented to the University of Waterloo
in fulfillment of the
thesis requirement for the degree of
Master of Science
in
Chemistry

Waterloo, Ontario, Canada, 2018

AUTHOR'S DECLARATION

I hereby declare that I am the sole author of this thesis. This is a true copy of the thesis, including any required final revisions, as accepted by my examiners.

I understand that my thesis may be made electronically available to the public.

Abstract

Daptomycin (Dap) is a Ca^{2+}-dependent cyclic lipodepsipeptide antibiotic used for treating skin infections caused by Gram-positive pathogens. It is also used to treat endocarditis caused by *Staphylococcus aureus* including methicillin-resistant *S. aureus* (MRSA). The mechanism of action (MOA) for Dap is still somewhat unclear. Thus, the MOA for Dap has been a focus of considerable study, and many MOAs have been proposed. Nevertheless, a considerable amount of evidence has been amassed that suggests Dap binds to bacterial cell membranes and forms oligomeric pores that allow for the passage of small cations. This results in the depolarization of the cell membrane and cell death. The first goal of this study was to identify the contribution of each amino acid in Dap to its biological activity and membrane affinity. This was achieved by performing an alanine scan on an active Dap analog, Dap-E12-W13, whereby each residue was replaced with alanine through chemical synthesis. The antibacterial activity of the alanine analogs was determined against *Bacillus subtilis*. These studies revealed that positions 2, 6, and 11 are amenable to substitution. These studies, in conjunction with those performed earlier on Dap, also suggested that position 8 is amenable to substitution as long as the correct stereochemistry is maintained. Membrane binding studies using model liposomes revealed that the position 2, 6 and 11 analogs were able to interact with membranes in a manner very similar to that of the parent peptide Dap-E12-W13, in that they did not require high concentrations of calcium to achieve maximal membrane binding. This was in contrast to the other Ala mutants which required much greater than physiological Ca^{2+} ion concentrations to achieve maximal interactions and good biological activity.

The second goal of this study was to create one or more Dap analogs that have activity equal to or greater than that of Dap, with the long-term goal of creating a Dap analog that is active against resistant bacterial strains and in the presence of lung surfactant. Towards this end, Ser11 of an active Dap analog, Dap-K6-E12-W13, was substituted with 17 common amino

acids. Although none of the resulting analogs were more active than Dap, these studies revealed that position 11 was amenable to substitution with positively charged amino acids (His, Arg, Lys) as these substitutions resulted in either no or minimal loss of activity. Moreover, the Asn, Thr, Cys, Met and Gly analogs were also relatively active being only 2.7-fold less active than Dap-K6-E12-W13 at 1.25 mM Ca^{2+}.

Acknowledgements

I would like to thank my supervisor, Prof. Scott Taylor, for giving me this opportunity and for his advice and encouragement. In the past two years Prof. Taylor has helped me improve as a graduate student and for that I am very grateful.

I would like to thank my remaining advisory committee members, Dr. Michael Palmer and Dr. Gary Dmitrienko. Also, thank you to all the Taylor lab members especially Dr. Chuda Raj Lohani for their constant help and support.

I would also like to thank the Government of Saudi Arabia for providing me with a full scholarship and allowing me to fulfil my dream of continuing my education overseas.

Finally, thank you to all my family and friends who unconditionally give me encouragement and motivation.

Table of Contents

List of Figures

List of Schemes

List of Tables

List of Abbreviations

3MeGlu	3-Methylglutamate
Ala	Alanine
Alloc	Allyloxycarbonyl
Asp	Aspartate
B. subtilis	*Bacillus subtilis*
Boc	*tert*-Butyloxycarbonyl
CCCP	Carbonyl cyanide *m*-chlorophenylhydrazone
CD	Circular Dichroism
cLPAs	Cyclic Lipodepsipeptide Antibiotics
Dap	Daptomycin
D-Ala	D-Alanine
D-allo-Ile	D-allo-Isoleucine
D-Arg	D-Arginine
D-Asn	D-Asparagine
D-Cys	D-Cysteine
D-Gln	D-Glutamine
D-Glu	D-Glutamate
D-His	D-Histidine
D-Leu	D-Leucine
D-Met	D-Methionine
D-Phe	D-Phenol alanine
D-Pro	D-Proline
D-Ser	D-Serine
D-allo-Thr	D-allo-Threonine
D-Trp	D-Tryptophan
D-Tyr	D-Tyrosine
D-Val	D-Valine
Dap	Daptomycin
DCM	Dichloromethane
DMAP	4-Dimethylaminopyridine
DMF	*N,N*-Dimethylformamide
DIC	Diisopropylcarbodiimide

DMBA	1,3-Dimethylbarbituric acid
DMPC	Dimyristoyl phosphatidylcholine
DMPG	Dimyristoyl phosphatidylglycerol
DIPEA	Diisopropylethylamine
DOPC	Dioleoyl phosphatidylcholine
DOPG	Dioleoyl phosphatidylglycerol
DTT	Dithiothreitol
FDA	Food and Drug Administration
Fmoc	Fluorenylmethyloxycarbonyl-protecting group
FRET	Fluorescence resonance energy transfer
Glu	Glutamate
Gly	Glycine
HOAt	1-Hydroxy-7-azabenzotriazole
HOBt	1-Hydroxybenzotriazole
Ile	Isoleucine
ITC	Isothermal titration calorimetry
Kyn	Kynurenine
LUVs	Large Unilammelar Vesicles
MBC	Membrane Binding Curve
MIC	Minimum Inhibitory Concentration
MOA	Mechanism of Action
mprF	Multi-peptide resistance factor
N_3Trp(Boc)OH	Azido tryptophan
Orn	Ornithine
$Pd(PPh_3)_4$	Tetrakis(triphenylphosphine)palladium
PyAOP	(7-Azabenzotriazol-1-yloxy)tripyrrolidinophosphonium hexafluorophosphate
RP-HPLC	Reversed-phase high performance liquid chromatography
S. aureus	*Staphylococcus aureus*
SAR	Structure-activity relationship
SPPS	Solid-phase peptide synthesis
TFA	Trifluoroacetic acid
THF	Tetrahydrofuran

Trp	Tryptophan
Val	Valine

Chapter 1

Daptomycin

1.1 Antibiotics

Throughout much of human history the number one cause of death to humankind was bacterial infections.[1] Fortunately, many infections that used to be fatal can now be treated with antibiotics. The discovery and development of antibiotics have been credited as the reasons for the increase in the human lifespan over the last century.[1] Consequently, it is safe to say that one of the most important advances ever made in medical science was the discovery and development of anti-bacterial drugs.

It was not until the late 19th century that scientists began to scientifically search for and study antibacterial chemicals.[1] One of the first scientists to do so was the German physician Paul Ehrlich. He found that certain chemical dyes often colour some bacterial cells but not others.[2,3] Among his accomplishments was the discovery that certain dyes could be used as drugs which would kill a specific organism while leaving other tissues unharmed.[4] Suggesting that it is possible to create substances or compounds that can kill certain bacteria selectively without harming other cells.[2,3] In 1909, he discovered that a chemical called arsphenamine or Salvarsan was an effective treatment for syphilis. This became the first modern anti-bacterial drug.[5,6] Ehrlich referred to his discovery as 'chemotherapy' – the use of a chemical to treat a disease. The word “antibiotics” was first used over 30 years later by the Ukrainian-American inventor and microbiologist Selman Waksman, who in his lifetime discovered over 20 antibiotics.[5,7]

Less than 20 years later, Alexander Fleming, a Scottish biologist, defined new horizons for antibiotics with his discovery of penicillin (in 1928).[8-10] Penicillin, which is isolated from the fungus *Penicillium notatum,* has been used to treat bacterial infections such as syphilis and gangrene.[8-10]

In 1943, Selman Waksman discovered streptomycin, an antibiotic synthesized by the soil organism *Streptomyces griseus.* It was the first major antimicrobial agent developed after penicillin, and the first antibiotic effective for treating tuberculosis.[11-13] It is also used for treating infections of heart valves (endocarditis), the plague, tularemia, and brucellosis.[12,13]

The discovery of these three antibiotics, salvarsan, penicillin and streptomycin, set the stage for future antibiotic research which resulted in the discovery of a large number of antibiotics from microbes, specifically from members of the actinomycetes and fungi class.[14] Many antibiotics discovered up to the early 1970s reached the market, and their chemical scaffolds were later used as leads for creating new generations of clinically applicable antibiotics by chemical modification.[14] Indeed, the period between 1944-1970 is considered to be the golden era of discovery of antibiotics. Very few new classes have been discovered since then.[15]

One of the most serious issues facing the medical community today is widespread resistance to many of the more commonly used antibiotics. This is mainly due to the over use of antimicrobial drugs in many parts of the world.[16-18] This has brought about the rise of bacteria, called “super bugs”, that are resistant to just about every antibiotic available.[19] This has resulted in warnings of a return to the pre-antibiotic era by medical experts; and a

recent database lists the existence of more than 20,000 potential resistance genes for almost 400 different types or more of bacteria, predicted from available bacterial genome sequences.[20]

The World Health Organization (WHO) created a list of several important antibiotics to combat super bugs. These antibiotics are called "last resort" antibiotics, which are only used when other more commonly used antibiotics are ineffective. By restricting the use of these important antibiotics, it is expected that the bacteria will not rapidly develop widespread resistance to them. This leads the conversation to one of these last resort antibiotics, called daptomycin (Dap), which is the focus of this thesis.

1.2 The History of Daptomycin

Dap was first isolated from a soil bacterium *Streptomyces roseosporus* from Mount Ararat (Turkey) by researchers at Eli Lilly in the early 1980s.[21,22] It was subjected to clinical trials; however, these clinical trials were then stopped at Phase II after patients exhibited high levels of creatine phosphokinase (CPK) in their system that caused muscle pain.[23] In later years, Cubist Pharmaceuticals purchased the rights to Dap and demonstrated that the side effects could be minimized by altering the dose regimen.[23] Dap was then approved in the USA by the Food and Drug Administration (FDA) in 2003 and in Europe in 2006 for treating severe skin infections including methicillin-resistant and susceptible *Staphylococcus aureus* (MRSA and MSSA) and vancomycin-resistant *Enterococci* (VRE). Dap is marketed under the trade name Cubicin® and was, until recently, sold by Cubist Pharmaceuticals which was purchased by Merck & Co. in 2014. Unfortunately, Dap is not

active *in vivo* against community-acquired pneumonia (CAP), which could be due to the inhibition of Dap by lung surfactant.[24]

Dap, whose structure is shown in figure 1.1, is a member of the A21978C factor family of calcium (Ca^{2+})-dependent cyclic lipodepsipeptide antibiotics (cLPAs) isolated from cultures of *Streptomyces roseosporus*.[21,22] It was initially isolated as a minor component of the A21978C factors, but its production can be increased by supplementing the growth medium with decanoic acid.[21,22] Dap consists of 13 amino acids, six of which are non-proteinogenic: D-Asn2, Orn6, D-Ala8, D-Ser11, (2S,3R)-methylglutamate (3MeGlu12), and kynurenine (Kyn13).[25] Ten of these amino acids create the macrocyclic core, which is closed with a depsi-bond (ester bond) between the side chain of the threonine (Thr) residue at position 4 and the C-terminal of the kynurenine (Kyn) residue at position 13. The remaining three amino acids are part of a tripeptide attached to Thr4 and attached to the *N*-terminus of the Trp1 residue is a decanoic tail.

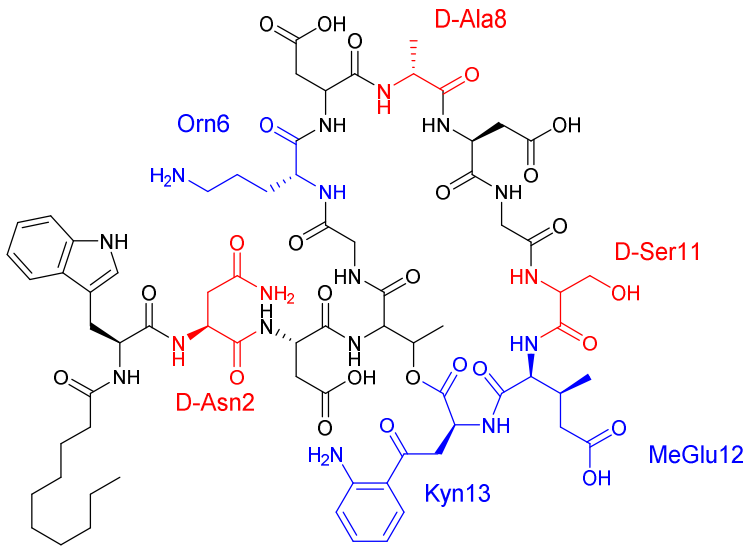

Figure 1.1. The structure of Dap. D amino acids are shown in red. Non-proteinogenic L-amino acids are shown in blue.

1.3 Daptomycin's Mechanism of Action

The mechanism of action (MOA) of Dap is still not known with certainty, and many MOAs have been proposed.[26] We will not discuss all of the proposed mechanisms. Instead we will focus upon those mechanisms which are supported by the most evidence.

Using radio-labelled Dap, Canepari *et al.* demonstrated that Dap interacts with the cell wall and membrane but not with the cytosolic components.[27] It is known that Dap requires its lipid tail for activity.[25] Furthermore, the presence of the phospholipid phosphatidylglycerol (PG) in the bacterial membrane is also important for Dap activity. Dap preferentially binds to PG-enriched membrane domains in *B. subtilis* cells.[28] Studies suggest that decreasing membrane PG content is a mechanism by which certain strains of *S. aureus* develop resistance to Dap.[29,30] The requirement for PG may be the reason behind Dap's low toxicity to humans as PG is found at very low concentrations in mammalian cells.[31]

The requirement of PG for Dap activity has been supported by model membrane studies. Dap inserts into model membranes composed of phosphatidylcholine (PC) and phosphatidylglycerol (PG) in a calcium-dependent manner, as evidenced by a simultaneous increase and blue shift in the fluorescence emission signal of the Kyn residue.[32] In model membranes containing PC and PG, a significant increase in the fluorescent quantum yield of the Kyn residue occurs compared to membranes containing just PC.[33] This suggests that Kyn inserts more deeply into PC/PG membranes compared to membranes that contain only PC. Using circular dichroism spectroscopy (CD), it has been shown that Dap undergoes a

significant conformational change in the presence of calcium and membranes that contain PC and PG.[33]

Isothermal titration calorimetry (ITC) studies using liposomes (large unilamelar vesicles, LUVs) containing PC and PG have shown that Dap binds PG with a stoichiometry of 1:2.[34] In contrast, fluorescence studies using a Dap analog containing a fluorescent label on the lipid tail and a lipid bicelle system found the ratio of PG to Dap to be 1:1.[34] This discrepancy may be a result of the two techniques monitoring Dap-liposome binding at different stages, or perhaps Dap is interacting with only the outer leaflet of the liposome but with both leaflets of the bicelle. Very recently, Huang and coworkers reported, using CD and small unilammelar vesicles (SUVs) containing PC and PG, that Dap binds to PG stoichiometrically. However, this interaction was not examined at Ca^{2+} concentrations above 100 μM, and therefore may not have reached saturation.[35]

Dap exhibits its maximal antibacterial effect at physiological Ca^{2+} concentration which is about 1.2 mM.[21,22] Like other Ca^{2+}-dependent cLPAs, Dap contains a highly conserved DXDG motif that is believed to be involved in binding Ca^{2+}.[36,37] Studies conducted by Grunewald *et al.* showed that when the aspartate residues within this motif are replaced with asparagine, activity is completely lost.[38] This suggests that these two residues, Asp7 and Asp9, are important for Dap's binding to Ca^{2+}.

The x-ray crystal structure of free Dap (apo-Dap), Dap bound to calcium, or of a Dap-calcium-PG complex has not been reported. However, the 3-D structure of free Dap by NMR has been reported by three different groups and all three arrived at different structures, probably because they were obtained under different conditions.[39-41]

The structure of Ca^{2+}-bound Dap by NMR has also been determined by two groups and, again, two different structures were obtained again, under different conditions.[39,40] The Ca^{2+}-Dap structures and the corresponding apo-Dap structures were very similar.

Attempts to obtain the NMR structure of Dap in the presence of Ca^{2+} and PG has not been successful mainly because of the tendency of the Dap-Ca^{2+}-PG complexes to precipitate out of solution at Dap concentrations necessary for NMR studies.[42] Overall, the NMR studies did not provide any significant insights into the MOA of Dap.

In 1987, Allen *et al*. reported, using a K^+ selective electrode, that Dap caused K^+ leakage from *S. aureu*s and this was accompanied by a collapse of the membrane potential, as evidenced by the release of the membrane-permeant cation tetraphenylphosphonium.[43] They also reported that Dap inhibits the cellular uptake of amino acids by active transport, a phenomenon that depends on the membrane potential. These results suggested to them that Dap functions by permeabilizing the cell membrane, resulting in membrane depolarization and cell death.[43]

In 2003, Silverman *et al.*, employing a fluorescence potentiometric probe and a K^+-sensitive fluorescent probe, demonstrated that 5 μg/ml of Dap triggers membrane depolarization and K^+ release from *S. aureus* (at pH 7.2).[44] On the basis of these results, and those of others such as Allen *et al*'s, Silverman proposed that, upon binding Ca^{2+}, that Dap inserts into the cell membrane, where upon it may bind an additional Ca^{2+} which results in its oligomerization and the formation of a cation-selective pore.[44]

In 2011, the Palmer group, using Dap labeled with a nitrobenzoxadiazole (NBD) moiety on the side chain of the Orn residue (NBD-Dap, figure 1.2), demonstrated Ca^{2+}- and

PG-dependent fluorescence resonance energy transfer (FRET) between the Kyn residue (donor) of unlabeled Dap and the NBD residue (acceptor) of NBD-Dap in the presence of PC/PG LUVs.[45] This suggests that Dap is oligomerizing when bound to calcium and PG membranes. When just NBD-Dap was used, oligomer formation was also evident by self-quenching of the NBD fluorescence. Using the FRET assay, they were able to determine that the number of subunits contained in one Dap oligomer was approximately 6-7 in PG/PC (1:1) liposomes.[45] They were also able to detect FRET with hybrid oligomers consisting of Dap and CB-182,462, a closely related Ca^{+2}-dependent cLPA on bacterial cells and LUVs.[45]

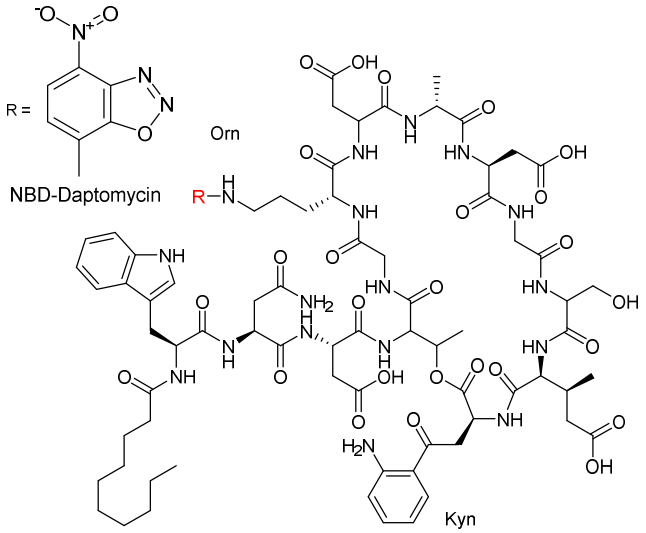

Figure 1.2. Structure of NBD-Dap

The Palmer and Taylor groups also reported that an active Dap analog bearing a perylene acyl tail (perylene-Dap, figure 1.3) exhibited excimer fluorescence in the presence of PC/PG LUVs or bacterial membranes and Ca^{2+}.[46] The formation of perylene excimers on model membranes was inhibited by unlabeled Dap. Perylene-Dap exhibited very little excimer formation in the presence calcium and of LUVs that did not contain PG.[46]

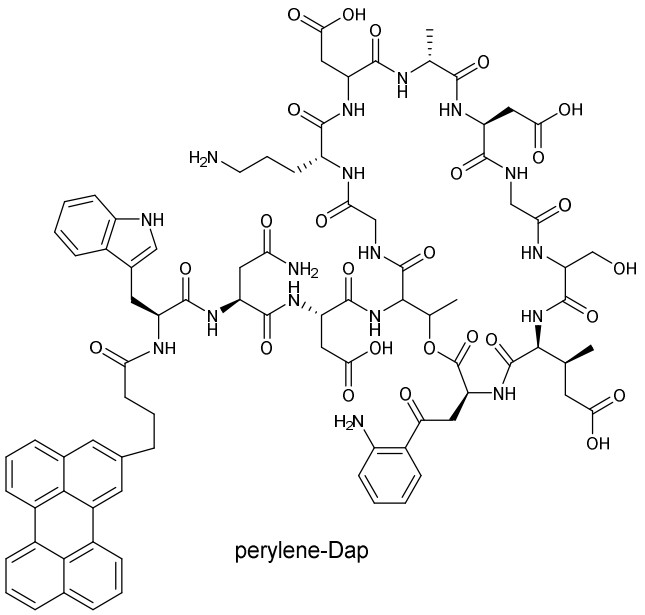

Figure 1.3. Structure of the perylene-dap derivative used for excimer fluorescence studies

The Palmer group also provided evidence that Dap can translocate between the inner and outer leaflets of PC/PG liposomes by showing that only 50% of the fluorescence of NBD-Dap bound to PC/PG liposomes can be quenched by dithionite.[47] This suggests that one half of the NBD-Dap was in the outer leaflet and the other half was in the inner leaflet of the membrane where it is not accessible to dithionite.

The Palmer group has developed an assay that allows one to detect Dap-induced permeabilization of LUVs for small cations, such as K^+ and Na^+.[48,49] In this assay, the pH-sensitive fluorophore pyranine was entrapped in PC/PG LUVs in an internal buffer at pH 6 that did not contain the cation in question. These LUVs were diluted in an external buffer containing the cation in question at pH 8. When Dap, the proton ionophore carbonyl cyanide m-chlorophenylhydrazone (CCCP) and Ca^{2+} were added, the fluorescence increased, presumably due to the formation of pores by Dap which allow the external cation

in question to enter the liposome in exchange for protons (via CCCP).[48] This results in an increase in the pH inside the liposome which results in an increase in the fluorescence intensity of pyranine (see figure 1.4 for more detail).

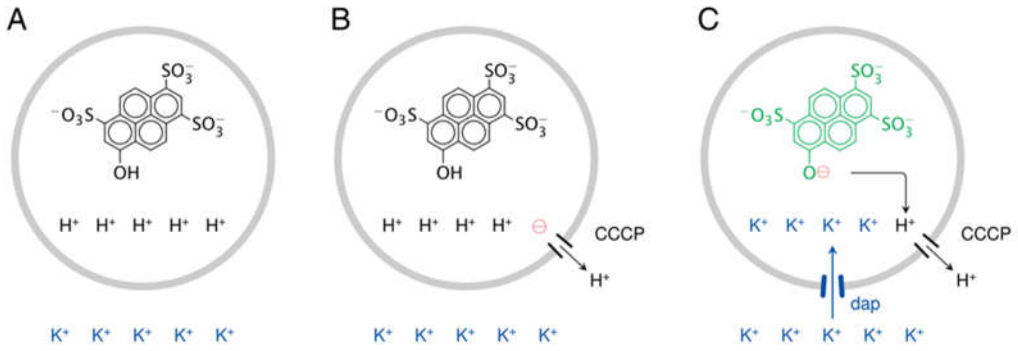

Figure 1.4. Schematic representation of the pyranine assay for pore formation.[48] (A) Encapsulated pyranine with a H^+ gradient inside and K^+ gradient outside. (B) Application of the protonophore CCCP alone allows insignificant loss of protons. (C) If Dap allows influx of the opposing K^+ gradient, efflux of the proton gradient occurs increasing pH and causing pyranine fluorescence. Figure provided by Dr. M. Palmer. Used with permission.

On the basis of the above mentioned studies, Zhang has suggested that Dap binds to Ca^{2+} and oligomerizes and forms pores in a multistep process (figure 1.5).[47] First, Ca^{2+} binds to Dap, which neutralizes the negative charges in Dap and allows Dap to loosely associate with the membrane. Second, another Ca^{2+} binds to Dap which results in deeper membrane insertion, through a specific interaction between PG and the Dap-Ca^{2+} complex. This results in a large conformational change in Dap. Third, the inserted Dap monomers form oligomers which then translocate the lipid-layer and form a pore.

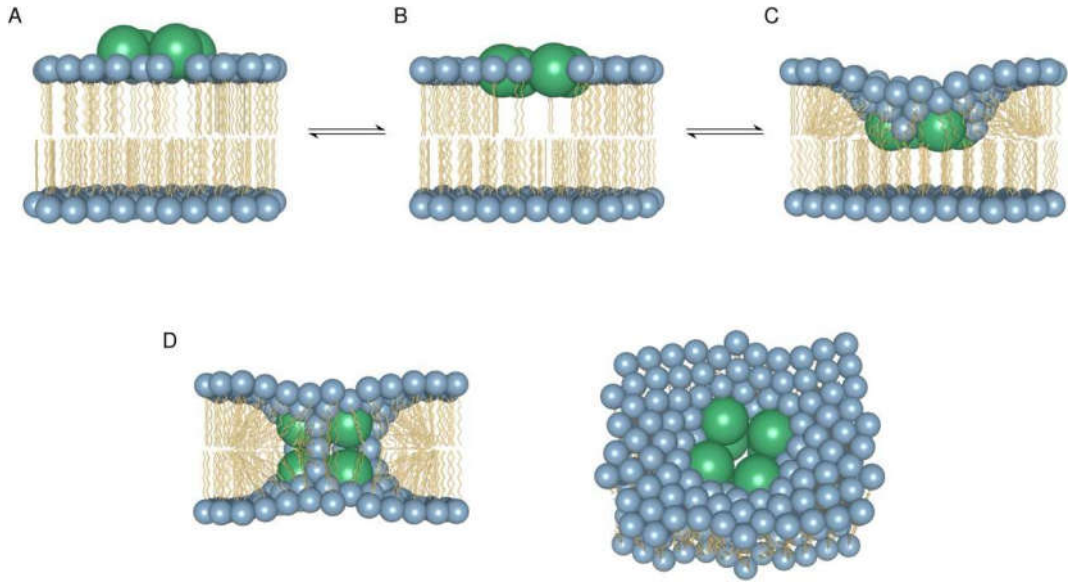

Figure 1.5. Dap mechanism proposed by Palmer and coworkers. Panels A and B show the tetramer formation after the binding of the first Ca^{2+} ion to Dap, resulting in tetramer formation. Panels C and D shows binding of the second Ca^{2+} which results in membrane translocation and pore formation. Figure provided by Dr. M. Palmer. Used with permission.

Recently, Muller *et al*. proposed a different MOA for Dap.[50] Using a variety of fluorescent lipid probes, they showed that binding of Dap to bacterial membranes led to a disorganization of fluid lipid domains, affecting membrane fluidity. This led to the rapid detachment of lipid II synthase (MurG) and phospholipid synthase (PlsX), two enzymes involved in bacterial cell wall synthesis and phospholipid synthesis, from the cytoplasmic side of the cell membrane. They concluded that Dap exerts its bactericidal effects primarily by causing the dissociation of these two enzymes from the bacterial membrane which disrupts cell wall synthesis.[50]

Muller *et al*. also reported that they were unable to detect leakage of specific cations upon subjecting *B. subtilis* to sublytic concentrations of Dap (3 μg/mL) for 5 min as determined using inductively coupled plasma optical emission spectroscopy (ICP-OES).[50]

Moreover, using a fluorescent probe and Dap concentrations that block cell growth (2 μg/mL) but not cell lysis, they found that only incomplete membrane depolarization of *B. subtilis* occurs after 30 min. Complete dissipation of the membrane potential only occurred at lytic Dap concentrations, and, even then, depolarization of the membrane was gradual and complete only after ~25 min. In contrast, the well-know pore-forming peptide, gramicidin S, caused almost instantaneous depolarization. On the basis of these results they concluded that Dap does not form specific pores.[50] Although the mechanism proposed by Muller *et al.* is entirely possible, there are some issues with their study. The ICP-OES study was performed with only low micromolar concentrations of calcium and incubation for only 5 min and it was already well-known that Dap does not depolarize bacterial membranes as rapidly as gramicidin. Dap is effective on vegetative cells and bacterial L-forms (bacteria that do not have a cell wall), which suggests that Dap is not involved in cell wall synthesis inhibition.[51,52] These facts support the notion that the dislodgment of MurG is not required for Daps activity. On the other hand, PlsX is likely to be active in bacteriostatic cells and L-forms.

1.4 The Synthesis of Dap Analogs and Structure-Activity Relationship (SAR) Studies

One obvious and potentially powerful approach for studying Dap's MOA, and for producing novel antibiotics with improved properties, is by performing SAR studies. This requires the preparation of analogs or modified versions of Dap and then determining their biological activity and how they interact with bacterial membranes and/or model membranes. Dap analogs have been prepared by semi-synthesis and by total synthesis.

Since the main focus of this thesis is on SAR studies of Dap, the Dap analogs that have been previously constructed and studied (before the studies described in this thesis) are discussed in some detail below.

1.4.1 Dap Analogs by Semi-Synthesis

Many Dap analogs have been made by semi-synthesis. The majority of these studies have focused on changing the acyl tail or attaching chemical entities to the Orn residue, whose side chain contains the sole amino group of the entire molecule.

Modification of the acyl tail involves first protecting the Orn reside with a Boc group and then de-acylating (removing the decanoyl tail) from the resulting protected Dap using a de-acylase. The resulting free amino group is reacted with activated esters of carboxylic acids and then the Boc group is removed.[53] This approach has been used to prepare surotomycin, which contains an (E)-3-(4-pentylphenyl)but-2-enoyl tail. Surotomycin has high activity against *Clostridium difficile*. Unfortunately, it failed to be non-inferior to current therapies in Phase III clinical trials and so further studies on this antibiotic were discontinued.[54]

Many Dap analogs have been made by attaching chemical entities to the Orn residue using a variety of different chemical procedures.[55,56] None of these compounds made it to human clinical trials, though several had *in vitro* activity equal to or better than Dap. These results suggested that the Orn residue is not essential for antibacterial activity.

The Trp residue in Dap has been replaced with a range of natural and unnatural aromatic amino acids.[57] They were prepared by first protecting the Orn reside with an allyloxy group. The decanoyl tail was then removed enzymatically, followed by removal

of Trp1 by Edman degradation and then attachment of the *N*-protected unnatural aromatic amino acid to the *N*-terminus of the Asn residue. The *N*-protecting group on the unnatural amino acid residue was removed, the decanoyl tail was attached to the resulting free amino group, and the allyl group removed from the Orn residue. Several of these analogs exhibited activity close to that of Dap and also had increased activity in the presence of lung surfactant compared to Dap. These results suggest that the Trp residue is not essential for activity.[57]

1.4.2 Total Synthesis of Dap Analogs

The total synthesis of Dap analogs has been achieved using three different approaches: chemo-enzymatic synthesis, combinatorial biosynthesis and total chemical synthesis.

1.4.2.1 The Chemo-Enzymatic Approach to Dap Analogs

The earliest approache used for preparing Dap analogs is the chemo-enzymatic approach. In this approach, solid phase peptide synthesis (SPPS) is used to prepare a linear Dap analog having a thioester C-terminus. After removal from the solid support and HPLC purification, the resulting thioester peptide is cyclized using a thioesterase/cyclase. In 2004 and 2006 Grunewald, *et al*. reported the synthesis and biological activity of nine Dap analogs using this approach.[38,58] The analogs that were prepared and tested are shown in table 1.1.

Table 1.1. MIC's of the analogs created by the chemo-enzymatic approach.

Entry	Compound	MIC (μg/mL)[a]
1	Dap-L-N2-E12	20
2	*Authentic Dap*	3
3	Dap- L-N2-N3-E12	80
4	Dap- L-N2-N7-E12	>960
5	Dap- L-N2-N9-E12	>960
6	Dap- L-N2-Q12	30
7	Dap- L-N2-D11-E12	>320
8	Dap- L-N2-E12-W13	100
9	Dap- L-N2-K6-E12-W13	100

[a] The analogs were tested against *B. subtilis* PY79 at 73.6 mg/L calcium.[38,58]

At the time of this work, Asn2 in Dap was believed to be an L amino acid, and so L-Asn was used. It was later determined that Dap contains D-Asn at this position.[59] Moreover, in all of their analogs, 3MeGlu13 was replaced with Glu, since the synthesis of 3MeGlu with the correct stereochemistry is labour-intensive. Consequently, most of their Dap analogs were triple mutants containing Glu in place of 3-MeGlu12, the unintended L-Asn2 substitution, and the substitution of interest at a third position within the peptide. Perhaps the most significant information obtained from these studies was that when Asp 7 or Asp 9 were replaced with Asn, all activity was lost (entries 4 and 5). Asp7 and Asp9 are believed to be important for Ca^{2+} binding, as they are part of the DXDG sequence found in the EF hand motif of many calcium binding proteins as mentioned earlier. These results support this supposition. The relatively minor decrease in activity found when Asp3 and 3MeGlu12 were replaced with Asn and Gln, respectively (entries 3 and 6 in Table 1.4) suggests that these residues are not directly involved in Ca^{2+} binding.

This chemoenzymatic approach to Dap analog synthesis has some drawbacks. One is that the cyclases are non-specific. Moreover, the overall yields can be quite low. Finally, the peptides have to be purified by HPLC both before and after cyclization, which does not make it a very practical approach to making large numbers of analogs.

1.4.2.2 The Biosynthetic Approach to Dap Analogs

Dap is naturally produced by *Streptomyces roseosporus* via several non-ribosomal peptide synthetases (NRPSs).[60,61] Three large, multifunctional, synthetase enzymes, DptA, DptBC and DptD, govern its assembly (figure 1.6).[61] Each synthetase contains several modules and each module has a condensation-adenylation-thiolation (CAT) domain and each module incorporates an amino acid. There is also an optional epimerization (E) domain. An enzyme called DptE that initiates the synthesis by activating decanoic acid in an ATP-dependent manner. The activated decanoic acid is then transferred to an enzyme called DptF. The C-domain of DptA catalyzes the condensation between the enzyme-bound decanoyl tail and tryptophan. After this initial condensation, the peptide chain is elongated by DptA, DptBC, and DptD operating in a linear fashion. Once the linear peptide chain is completed, the thioesterase (TE) in DptD directs the intramolecular attack of the hydroxyl group of threonine on the carbonyl of the enzyme-bound thioester. This leads to cyclization and release of the cyclic lipopeptide. [60,61]

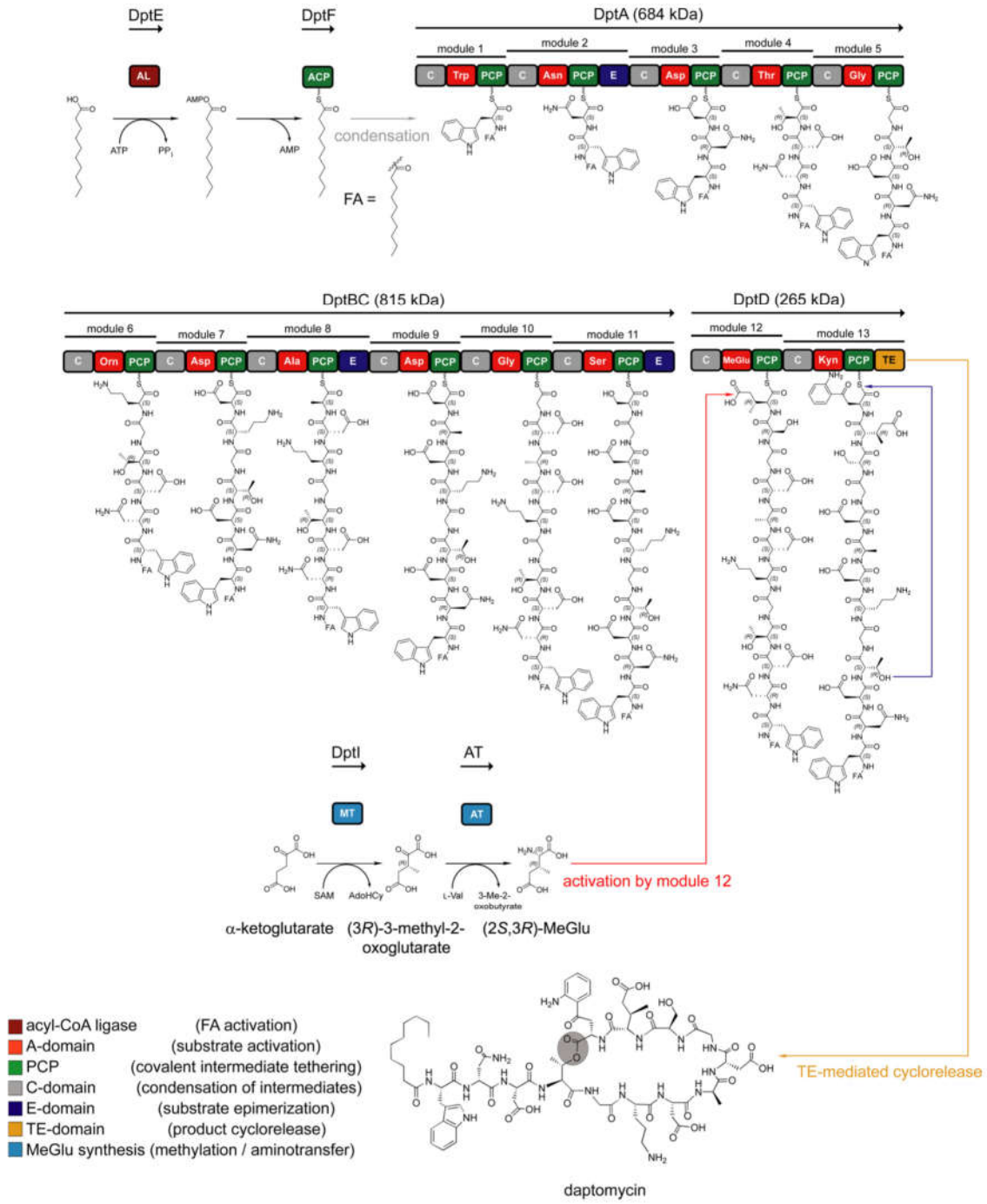

Figure 1.6. The biosynthesis of Dap. See text for details. The figure was used with permission.[61]

Dap analogs have been prepared by combinatorial biosynthesis.[59,62,63] In this approach, the modules responsible for the incorporation of the amino acids are swapped with NRPS systems encoding similar, naturally occurring lipopeptides. Cubist Pharmaceuticals used this approach to prepare analogs of Dap. Their objective was to prepare a Dap analog that remained active in the presence of lung surfactant.[59] The Dap analogs created by this approach and their MIC's against *S. aureus* in the absence and presence of synthetic lung surfactant are given in table 1.2.

Table 1.2. Dap analogs created through combinatorial biosynthesis and their MIC's against *S. aureus* in the absence and presence of lung surfactant.

	amino acid at position listed[b]									*S. aureus* MIC (μg/mL)[c]		
compound[a]	2	3	5	6	8	9	11	12	13	− surf	+ surf	ratio (+/−)
daptomycin	D-Asn	Asp	Gly	Orn	D-Ala	Asp	D-Ser	3mGlu	Kyn	0.5	64	128
CB-181,220	D-Asn	Asp	Gly	Orn	D-Ala	Asp	D-Ser	3mGlu	Kyn	0.5	64	128
CB-182,098	D-Asn	Asp	Gly	Orn	D-Ala	Asp	D-Ser	3mGlu	***Trp***	1	32	32
CB-182,107	D-Asn	Asp	Gly	Orn	D-Ala	Asp	D-Ser	3mGlu	***Ile***	2	8	4
CB-182,106	D-Asn	Asp	Gly	Orn	D-Ala	Asp	D-Ser	3mGlu	***Val***	4	8	2
A21978C1(Asn13)	D-Asn	Asp	Gly	Orn	D-Ala	Asp	D-Ser	3mGlu	***Asn***	128	ND	ND
CB-182,130	D-Asn	Asp	Gly	Orn	D-Ala	Asp	D-Ser	***Glu***	Kyn	8	16	2
CB-182,166	D-Asn	Asp	Gly	Orn	D-Ala	Asp	***D-Ala***	3mGlu	Kyn	1	16	16
CB-182,290	D-Asn	Asp	Gly	Orn	D-Ala	Asp	***D-Asn***	3mGlu	Kyn	1	16	16
CB-182,123	D-Asn	Asp	Gly	Orn	***D-Ser***	Asp	D-Ser	3mGlu	Kyn	1	32	32
CB-182,257	D-Asn	Asp	Gly	Orn	***D-Asn***	Asp	D-Ser	3mGlu	Kyn	8	ND	ND
CB-182,286	D-Asn	Asp	Gly	Orn	D-Ala	Asp	***D-Asn***	3mGlu	***Ile***	4	ND	ND
CB-182,251	D-Asn	Asp	Gly	Orn	D-Ala	Asp	***D-Asn***	***Glu***	Kyn	32	ND	ND
CB-182,263	D-Asn	Asp	Gly	Orn	***D-Asn***	Asp	D-Ser	3mGlu	***Ile***	16	ND	ND
CB-182,269	D-Asn	Asp	Gly	Orn	***D-Asn***	Asp	D-Ser	***Glu***	Kyn	128	ND	ND
CB-182,296	D-Asn	Asp	Gly	Orn	***D-Lys***	Asp	***D-Asn***	3mGlu	Kyn	1	32	32

[a] Dap or Dap analog. [b]Amino acid changes are shown in bold italics. [c] MICs were determined against *S. aureus* in the presence or absence of 1% synthetic lung surfactant. Reprinted with permission from Baltz, R. H. *Am. Chem. Soc. – Synth. Biol.* 2014, *3*, 748-758. Copyright 2014, American Chemical Society.

When Kyn13 was replaced with a other hydrophobic residues (Trp, Ile, Val) the activity in the absence of surfactant decreased 2 to 8-fold, while the activity in the presence of lung surfactant increased. The W13 mutant was only 2-fold less active than Dap itself. The N13 mutant was almost devoid of activity, suggesting that a non-polar residue is

necessary at this position. Replacing 3MeGlu12 with Glu reduced the activity 16-fold, but the activity in the presence of surfactant increased 4-fold. Interestingly, substituting D-Ser11 with D-Ala or D-Asn resulted in almost no loss of activity in the absence of surfactant and a 4-fold increase in activity in the presence of surfactant. This suggests that D-Ser11 is not required for activity and suggests that this position is a potential site for further modification.

Although Dap analogs can be prepared using combinatorial biosynthesis, there are several shortcomings that limit the usefulness of this approach. Combinatorial biosynthesis is dependent on specificity of the host organism for certain modules, with no guarantee that added modules will be accepted by this bacterium. Although some amino acid substitutions can be made, no dramatic changes can be done. For example, Cubist Pharmaceuticals was unable to exchange 3MeGlu12 for anything other than Glu.[59] It was also not possible to alter the stereochemistry of the residues.

1.4.2.3 Dap Analogs by Total Chemical Synthesis

The first total chemical synthesis of Dap was achieved in 2013 by Lam, *et al.*[64] The most challenging aspect of the synthesis was formation of the ester bond. They were unable to form the ester bond between Thr4 and Kyn13 either on a solid support or even in solution. Instead, they had to prepare a tetrapeptide in solution which contained an ester linkage between the α-COOH group of a Trp residue and the side chain of Thr4. The Trp residue was then converted to a Kyn residue by ozonolysis. The resulting tetrapeptide was used as a building block in their solid phase synthesis of a linear, branched, uncyclized precursor. After cleavage from the support the uncyclized peptide was purified by HPLC then cyclized

via a solution phase serine ligation reaction.[64] This combination of solid and solution phase chemistry made for a very laborious synthesis and is therefore not well suited to the preparation of large numbers of analogs.

In 2014, Martin, *et al.* reported the total chemical synthesis of two Dap analogs and their enantiomers.[65] Branched, acyclic versions of the Dap analogs were prepared in the solid phase, which, after cleavage from the solid support, were cyclized in solution. Each one had a diaminopropionic acid (DAPA) residue in place of Thr4. This resulted in the ester bond in Dap being replaced with an amide bond. One analog contained DAPA and Glu in place of 3MeGlu at position 12 (entry 2, table 1.3). Another contained DAPA, Glu at position 12 and Trp at position 13 (entry 3, table 1.3). The other two analogs were the enantiomers of these analogs (entries 4 and 5, table 1.3). The analogs containing the natural stereochemistry were 100-200 times less active than Dap, indicating that the ester bond and/or the methyl group of the Thr side chain is crucial for activity. The enantiomers of these analogs were inactive, which suggests that Dap is interacting with a chiral target such as a chiral lipid (perhaps PG), or a protein (such as Plsx).

Table 1.3. MIC's of the analogs created by the synthetic approach by Martin, *et al*.

Entry	Compound	MIC (μM)[a]
1	Daptomycin [b]	3
2	Dap-DAPA4-E12	201
3	Dap-DAPA4-E12-W13	101
4	Dap-DAPA4-E12 (ent)	Not active
5	Dap-DAPA4-E12-W13 (ent)	Not active

[a]Tested against *S. aureus* ATCC 29123 at 50 mg/L calcium. [b]Isolated for natural source.

In 2015, the Taylor group published the first total synthesis of Dap performed entirely on the solid phase (scheme 1.1).[66,67] As this synthesis and subsequent routes to Dap developed in the Taylor group are very relevant to this thesis, these syntheses are in some detail below.

The original route planned by Taylor to synthesize Dap is shown in scheme 1.1. Dipeptide **1.1**, which consists of Asp9 and Gly10, was attached to chlorotrityl resin via the side chain of the Asp residue. Fmoc SPPS was used to prepare peptide **1.2**. Unfortunately, they were unable to make the ester bond between the Thr4 side chain in peptide **1.2** and FmocKyn(Boc, CHO)OH to get peptide **1.3**. This forced them to design an alternative route to Dap.

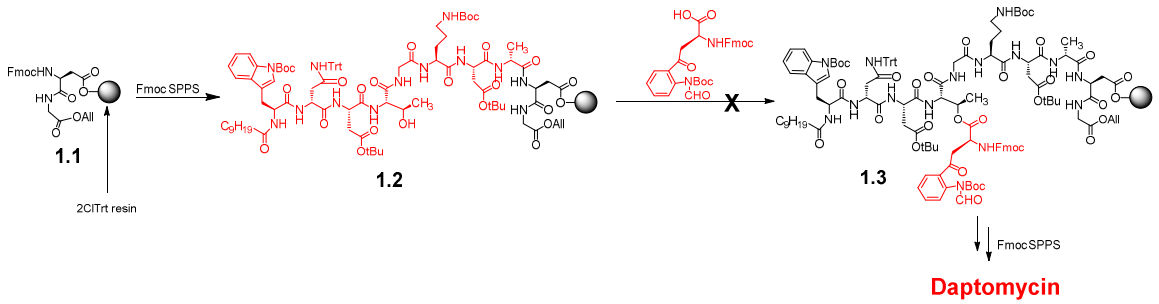

Scheme 1.1. First attempt by the Taylor group to prepare Dap by Fmoc SPPS.

In the revised route (scheme 1.2), peptide **1.4** was prepared using Fmoc SPPS. N_3Asp(tBu)OH (an azido acid) was attached to this peptide to give peptide **1.5**. Because peptide **1.5** did not contain Asn2, Trp1 and the decanoyl tail, which had been found to interfere with ester bond formation, it was possible to make the ester bond between FmocKyn(Boc,CHO)OH and the side chain of Thr4, using the symmetric anhydride of FmocKyn(Boc,CHO)OH, to give peptide **1.6** in quantitative yield. The azido group in peptide **1.6** was reduced to the amine using PMe_3 in dioxane/water and then Asn2 was installed as an azido acid. The azido group on the Asn residue was reduced as before and then Trp1 was installed as an azido acid, followed by azido group reduction and installation of the decanoyl tail to give peptide **1.3**. The Fmoc group on peptide **1.3** was removed and then 3MeGlu12 and Ser11 were installed using Fmoc SPPS to give peptide **1.7**. The allyl group was removed from Gly10 and the resulting peptide **1.8** was cyclized on resin to give **1.9**. As the cyclization involved activation of Gly10, no racemization occurred during the cyclization process. After removal of all the protecting groups and cleavage from the resin using TFA, Dap was obtained in a 3.7 % overall yield.

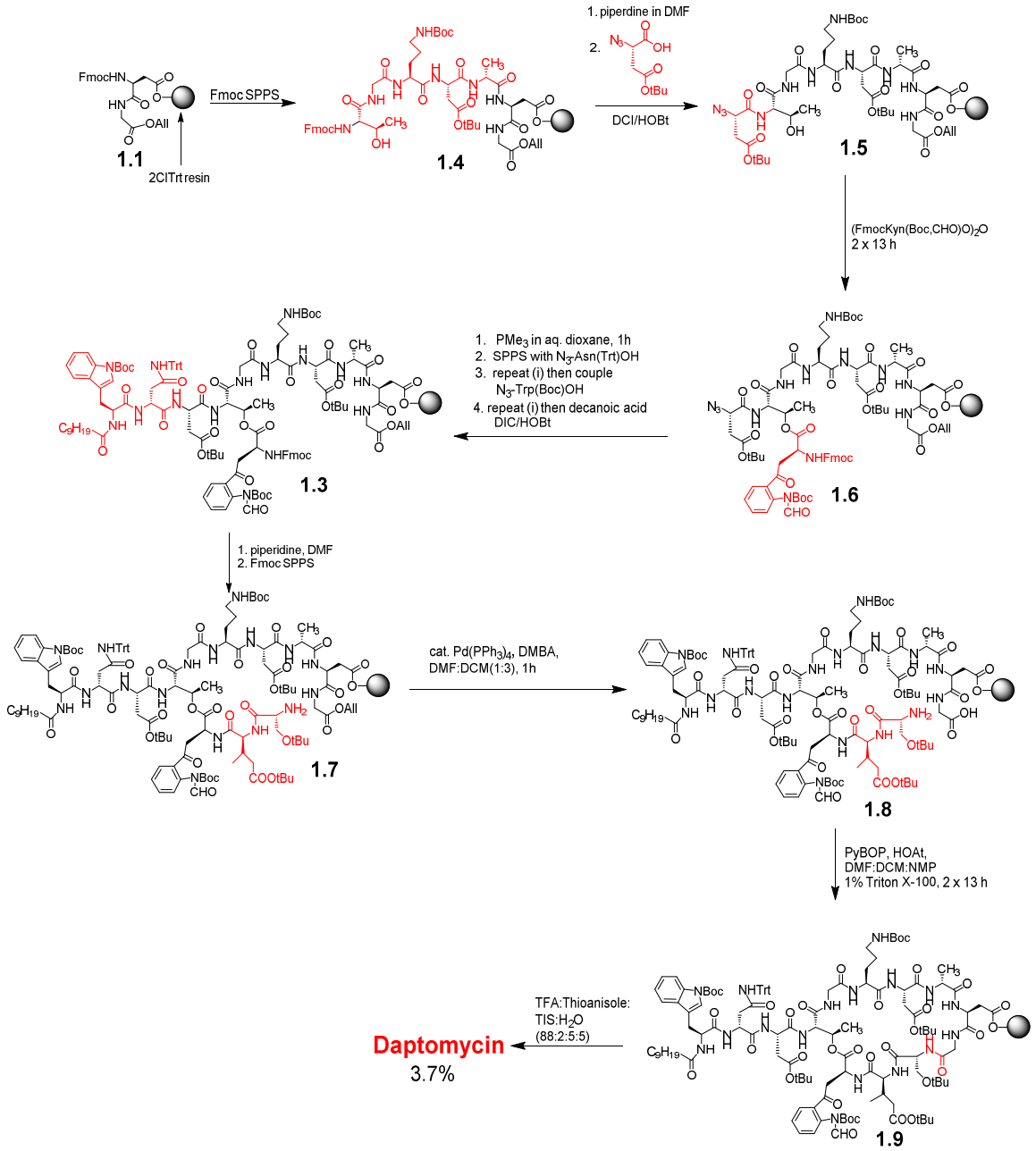

Scheme 1.2. The total solid phase synthesis of Dap by the Taylor group

In addition to Dap itself, several Dap analogs were synthesized using the approach outlined in scheme 1.2 and their activity tested against two *B. subtilis* strains (table 1.4).[66] When the stereochemistry of the side chain of 3MeGlu was reversed (entry 2, table 1.4),

the activity was greatly reduced. It has been observed previously that the substitution of 3MeGlu with Glu decrease activity while substitution of Kyn13 with Trp had little effect on activity.[58,63] Unexpectedly, when both were simultaneously replaced (Dap-E12-W13, entry 3, table 1.4), the activity was approaching that of Dap at 5 mM calcium. When both 3MeGlu and Kyn13 were replaced with Glu and Tyr respectively, the activity was much below that of Dap (entry 4, table 1.4). Surprisingly, all of the analogs were found to be much more active at high Ca^{2+} ion concentrations (25 and 100 mM). This suggests that these substitutions reduce Dap activity, at least in part, by reducing calcium affinity.[66,67]

Table 1.4. MIC's of the analogs created by the route outlined in scheme 1.2 by Taylor and coworkers.

		MIC (μg/mL)	
Entry	Compound	*B. subtilis ATCC 1046*	*B. subtilis PY79*
1	Daptomycin	0.75[a], 0.5[b,c]	0.75[a]
2	Dap-(2S,3S)-MeGlu	40[a], 5.0[b], 5.0[c]	>40[a]
3	Dap-E12W13	1.5[a]	3.0[a]
4	Dap-E12Y13	35[a], 3.0[b], 1.3[c]	ND

[a]5 mM Ca^{2+}. [b]25 mM Ca^{2+}. [c]100 mM Ca^{2+}

One drawback to the synthesis outlined in scheme 1.2 was that it utilized three azido acids as building blocks. Azido acids are not commercially available and have to be synthesized. This provided the impetus for the Taylor group to design an improved synthesis of Dap analogs that required only a single azido acid.[66,67] This approach is outlined in scheme 1.3 for the synthesis of Dap-E12W13. In this approach, Trp13 is introduced into peptide **1.11** (from peptide **1.10**) as an azido acid. Asn2, Trp1 and the decanoyl tail are then installed using standard Fmoc SPPS to give peptide **1.12**.

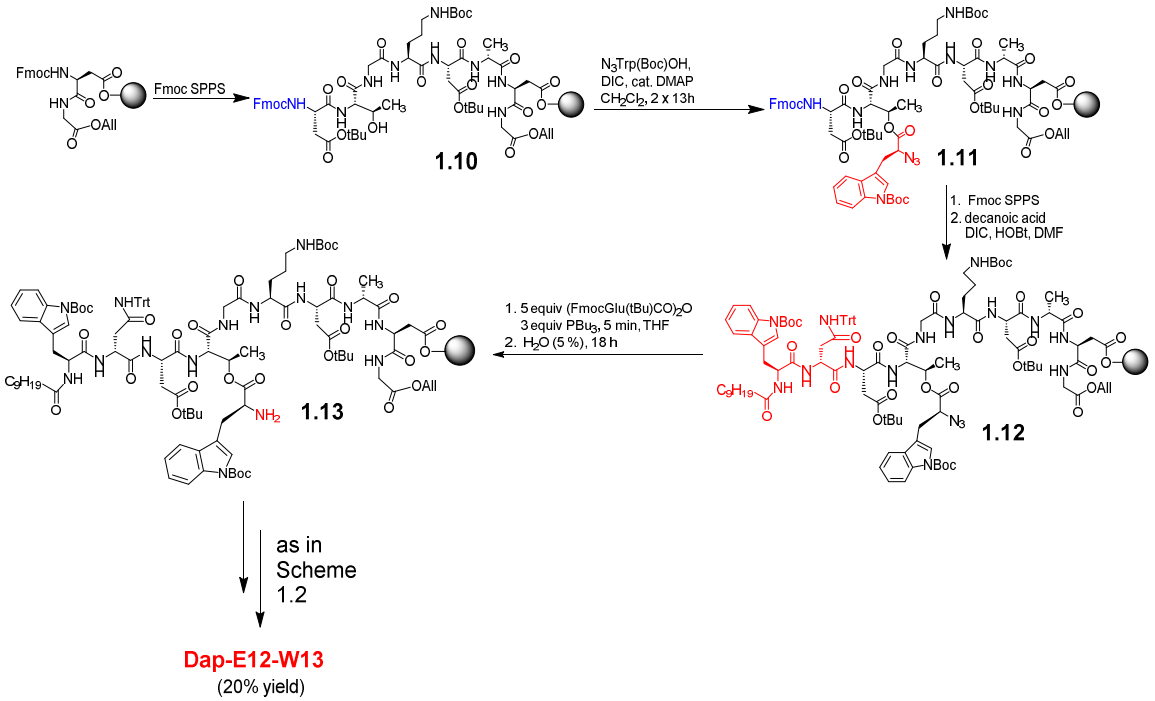

Scheme 1.3. Taylor and coworkers improved synthesis of Dap-E12-W13.

The reduction of the azido group in peptide **1.12** to give peptide **1.13** was preformed using unusual conditions: 5 equiv of the symmetric anhydride of FmocGlu(tBu)OH, 3 equiv Bu_3P, in THF for 5 min followed by the addition of water and shaking for 18 h. The Bu_3P/water should reduce the azido group to give the amine, which one would expect would react with the symmetric anhydride of FmocGlu(tBu)OH; this in turn should result in the incorporation of Glu12 into peptide **1.12**. However, this does not occur. The azido group is reduced to the amine but Glu12 is not installed. Peptide **1.13** is almost the sole product.[68] If the reduction is done using standard reduction conditions (PMe_3 or PBu_3 in dioxane/water or DTT/DIPEA) then a side reaction occurs in which 50% of the ester bond in peptide **1.12** is cleaved and peptide **1.14** and triazole **1.15** are produced (scheme 1.4) in 1:1 ratio.[68]

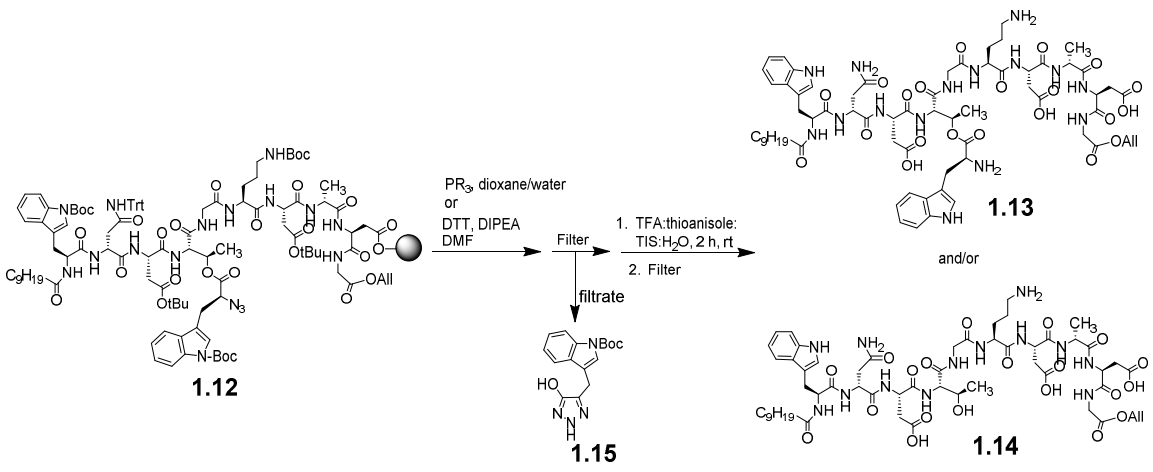

Scheme 1.4. Cleavage of the ester bond in peptide **1.12** using standard azido group reduction conditions.

This side reaction is a result of the intermediate aminophosphorane cyclizing and attacking the carbonyl carbon of the ester bond followed by loss of peptide **1.13** and formation of triazole **1.14** (scheme 1.5).[68,69]

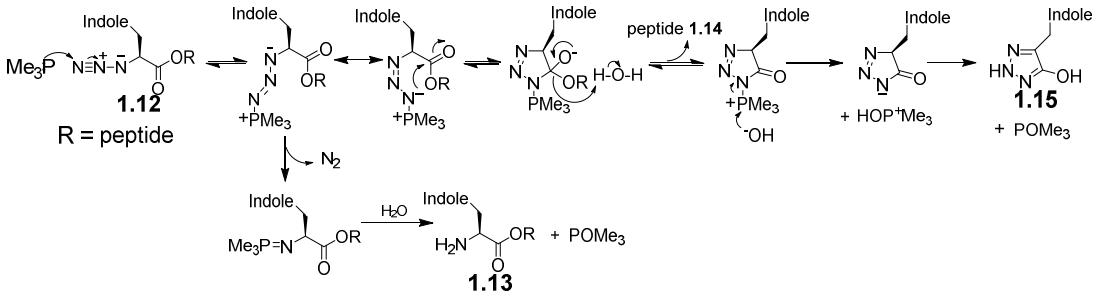

Scheme 1.5. Proposed mechanism for the formation of peptide **1.14** and triazole **1.15**.

Using the approach outlined in scheme 1.3, several new Dap analogs, based upon Dap-E12-W13, were prepared in yields as high as 20 % (table 1.5).[66,67] When 3MeGlu was replaced with Gln, Thr4 replaced with Ser, or Asp3 replaced with Glu (entries 2, 3 and 4 in table 1.5), the resulting analogs were considerably less active than Dap at 5 mM Ca^{2+} but almost as active as Dap at 100 mM Ca^{2+}. However, when Asp7 was replaced with Ala

(entry 5, table 1.5), activity was completely lost, even at high Ca^{2+} concentrations. This supports the supposition that this amino acid is directly involved in binding Ca^{2+} as discussed in sections 1.3 and 1.4.2.1. The poor activity of the Ser4 analog revealed that the methyl group on the side chain of Thr4 is essential for good activity.

Table 1.5. MIC's of the analogs created by the route outlined in scheme 1.3 by Taylor and coworkers.

		MIC (μg/mL)[a]		
Entry	Compound	*1.8*[b]	*5.0*[b]	*100.0*[b]
1	Daptomycin	1.0	0.75	0.5
2	Dap-Q12W13	ND	7	0.75
3	Dap-S4E12W13	>100	65	3
4	Dap-E3E12W13	>100	40	1.5
5	Dap-A7E12W13	>100	>100	>100

[a]Against *B. subtilis ATCC 1046*. [b]Calcium concentration

1.5 Proposed Mechanisms of Resistance to Daptomycin

Although clinical isolates of Dap-resistant bacteria are still relatively rare, they are appearing with greater frequency. This is a cause for concern as Dap is a last resort antibiotic. If widespread resistance to last resort antibiotics occurs, few alternatives are available. If it can be determined how bacteria develop resistance to Dap, then this information might provide vital clues to elucidating Dap's MOA, and it may be possible to rationally develop Dap analogs that retain activity against bacteria resistant to native Dap. Some of these resistance mechanisms are discussed below.

Mutations in the pgsA gene have been shown to occur in Dap-resistant *B. subtilis* and *S. aureus*.[28-30] The *pgsA* gene encodes a phosphatidyl transferase that is involved in the biosynthesis of PG. These mutations might cause a decrease in the amount of PG in the membrane, which would decrease the effectiveness of Dap.

Isolates of *S. aureus* that are resistant to Dap show an increase in the percentage of lysyl-PG in the cell membrane.[70-72] Lysyl-PG is a common phospholipid commonly found in Gram-positive bacteria. These Dap-resistant bacteria up-regulate a protein called MprF. Depletion of MprF causes hypersensitivity to Dap.[71] MprF converts PG to lysyl-PG and then flips the lysyl-PG to the outer leaflet of the cell membrane. Lysyl-PG bears a positive charge; in contrast, PG bears a negative charge. Therefore, an increase in the amount of lysyl-PG in the cell membrane results in an increase in the positive charge on the surface of the cell membrane. It has been proposed that this affects the ability of Dap to interact with the membrane. However, Mishra *et al*. found that not all mutations in MprF alter the membrane charge ratio.[71] Therefore it is possible that up regulation of MprF simply results in a reduction of the percentage of PG in the membrane.

In *E. faecium*, mutations in yycFG operon, which encodes two proteins called YycG and YycF, have been found in Dap-resistant strains.[73] Dap-resistant mutants of *S. aureus* derived in vitro exhibited changes affecting the histidine kinase of the system (YycG).[70,74] TycG and YycF are part of a regulatory system required for viability in Gram-positive bacteria. In *B. subtilis*, YycG is localized to the cell division septum where it regulates cell division and cell wall restructuring.[75] Baltz has suggested that there is a relationship between YycG and Dap's MOA.[60] First, Dap and YycG are found near the cell division

septum of bacteria. Second, both Dap-treated bacteria and bacteria depleted of YycG have also been shown to exhibit minor morphological changes in both *S. aureus* and *B. subtilis*, leading to unnatural division septa. Third, the depletion of YycG has been shown to cause cell death without lysis, like Dap. Fourth, the YycFG system positively regulates biofilm formation while Dap treats *S. aureus* biofilms effectively. Baltz therefore suggested a dual mechanism of action for Dap: disruption of YycG and membrane depolarization.

When *B. subtilis* was treated with Dap, the expression of a membrane-associated transcriptional regulator called LiaRS increased >400 fold.[28,76] This two-component regulator is thought to be involved in the cell membrane adaptive responsive to antibiotics. Arias *et al.* characterized several LiaRS mutations found in clinical isolates of *E. faecalis* and *E. faecium* that induce resistance to Dap.[77] When LiaRS was activated, the expression of two proteins called LiaI and LiaH were greatly increased.[77] These proteins are known to segregate to separate domains of the plasma membrane but their role in Dap resistance is, to date, unknown. Friulimicin, another Ca^{2+}-dependent lipopeptide antibiotic was found not to up-regulate the production of LiaRS which suggests that Dap's activation of these proteins regulator is specific.[76]

Tran, *et al.* noted that some non-clinical isolates of some bacteria have developed enzymes that hydrolyze the ester bond in Dap, thus destroying the antibiotic.[78] This mode of resistance has not been found to occur in clinical isolates to date.

Up-regulation of the *dlt* operon has been found to occur in Dap-resistant *S. aureus* strains.[79-82] Proteins coded by the *dlt* operon are involved in the attachment of D-alanine to cell wall teichoic acids of Gram-positive bacteria. This results in LTA bearing a positive

charge (from the α-amino group of alanine). It has been suggested that this could repel Dap from the membrane, reducing Dap's activity.

1.6 Research Objectives and Thesis Overview

There are two objectives of the work presented in this thesis. The first is to ascertain the functional contribution of each amino acid residue at each successive stage of Dap action, that is, in membrane binding, oligomerization, and pore formation. Towards this end, in chapter 2, an alanine scan was performed on Dap-E12-W13, in which each amino acid was substituted with Ala. The resulting Dap analogs were then assessed for their biological activity and interaction with model membranes in the presence of Ca^{2+}. The second objective is to develop a Dap analog with improved activity. Since the results from the alanine scan identified position 11 as one possible site for modification, Ser11 was replaced with 17 other common amino acids and the resulting Dap analogs were then assessed for their biological activity and their ability to interact with model membranes in the presence of calcium. These studies are still ongoing in the Taylor group.

Chapter 2
An Alanine Scan of Daptomycin

2.1 Introduction

In Chapter 1, section 1.4, it was discussed that only limited SAR studies have been performed on Dap to date. More in-depth SAR studies would be helpful towards resolving Dap's MOA, and for the development of Dap analogs that are active against Dap-resistant bacteria and/or can function in the presence of lung surfactant.

In this chapter, an attempt is made to answer the following questions about Dap: Which amino acids in Dap are amenable to substitution? In other words, which amino acids can be substituted with another amino acid without significantly adversely affecting Dap's biological activity? Which amino acids effect Dap's ability to interact with membranes? Is there a correlation between biological activity and calcium affinity and membrane binding?

One approach that has been used extensively in biochemistry to determine the contribution of certain residues to a protein's activity and action mechanism is to perform an alanine scan. In an alanine scan, each residue in question is replaced with alanine one-at-a-time and the effect of the substitution on the activity of the resulting peptide is assessed. Alanine is chosen because it is small and inert, and its main effect usually consists in the removal of the specific features of the residue it replaces. Alanine scans have been used to investigate the contribution of residues to the activity and mechanism of action of peptide antibiotics. For example, an alanine scan of the clinically important cationic cLPA

polymyxin revealed how much each of its residues contributes to its biological activity and its association with lipopolysaccharides, polymyxin's biological target.[83]

In this chapter, we attempt to answer the above questions by performing an alanine scan on Dap-E12-W13. Dap-E12-W13 was used instead of Dap for these studies because it does not contain 3MeGlu at position 12, which is very labor intensive to prepare, yet it exhibits biological activity approaching that of Dap at 5 mM Ca^{2+}. The *in vitro* antibacterial activity of the Dap analogs prepared in this study was determined. To determine which amino acids effect Dap's ability to interact with membranes and if there is a correlation between biological activity and membrane binding, each analog was examined for its ability to interact with model liposomes in the presence of varying amounts of Ca^{2+}.

2.2 Materials and Methods

2.2.1 Chemicals and Instruments

2'-Chlorotrityl chloride polystyrene resin (2ClTrt-PS, 1.5 milliequiv/g) and 2'-chlorotrityl chloride Tentagel resin (2ClTrt-TG, 0.19 millequiv/g) as well as all Fmoc amino acids, reagents and solvents used for SPPS were purchased from commercial sources, such as, Combi-Blocks, Creosalus, and Chem-Impex Int'l Inc. All used without further purification unless stated otherwise. Dichloromethane (DCM) was distilled from calcium hydride under nitrogen. Manual peptide syntheses were performed manually using a rotary shaker for agitation.[84] Automated peptide synthesis was performed on a Protein Technologies Quartet peptide synthesizer. High performance liquid chromatography (HPLC) was performed using a Waters 600 System equipped with a UV detector set to 220 nm. A Higgins Analytical Inc. (Mountainview, CA, USA) Clipeus C18 column (10 μM,

250 x 4.6 mm) was used for analytical HPLC at a flow rate of 1.0 mL/min. A Higgins Clipeus C18 column (10 μM, 250 x 20 mm) was used for semi-preparative HPLC at a flow rate of 10 mL/min. All HPLC chromatograms shown in the appendix section were obtained using a linear gradient of 10% acetonitrile (ACN)/90% H_2O (0.1% TFA) to 90% acetonitrile (ACN)/10% H_2O (0.1% TFA) over 50 min. High resolution positive ion electrospray (ESI^+HRMS) mass spectra (see appendix A and C) were obtained using a Thermoscientific Q-Exactive orbitrap mass spectrometer. 1:1 MeOH/H_2O + 0.1% formic acid was used as a solvent for HRMS. 1,2-dimyristoyl-sn-glycero-3-phosphocholine (DMPC), 1,2-dimyristoyl-sn-glycero-3-phospho-(1'-rac-glycerol) (sodium salt; DMPG), 1,2-dioleoyl-sn-glycero-3- phosphocholine (DOPC), and 1,2-dioleoyl-sn-glycero-3-phospho-(1'-rac-glycerol) (sodium salt; DOPG), whose structures are shown in figure 2.1, were obtained from Avanti Polar Lipids (Alabaster, Alabama). Large unilammelar vesicles (LUVs) were prepared by using equal proportions of phosphatidylcholine (PC) and phosphatidylglycerol (PG) lipids. They were then added to a round bottom flask and dissolved in 3 mL chloroform. The dissolved lipids were dried under purified nitrogen and kept under high vacuum overnight. The dried lipid film was then suspended in HEPES-buffer (20 mM HEPES, 150 mM NaCl, pH 7.4) and vortexed until all lipids were detached from the flask and suspended in buffer. These multilamellar vesicles were extruded under pressurized nitrogen through polycarbonate membranes (0.1 nm in diameter), fifteen times, to produce LUVs.

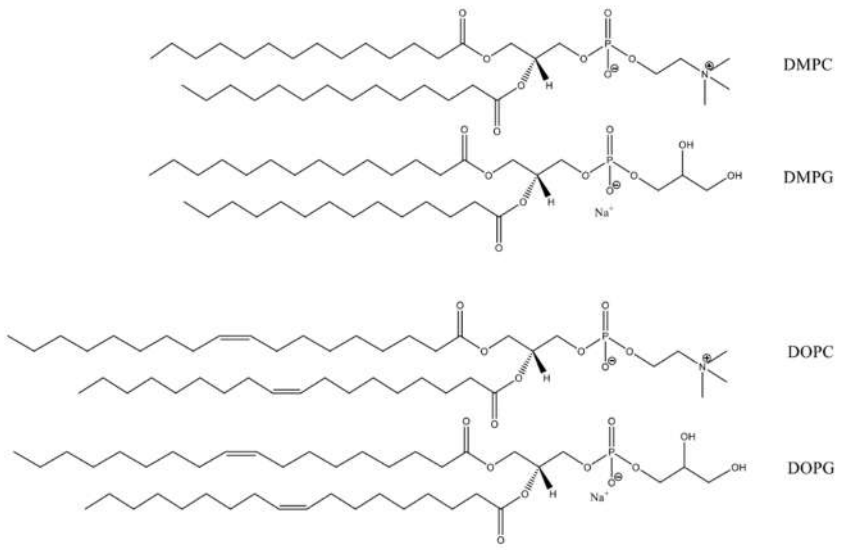

Figure 2.1. Structure of PC (phosphatidylcholine) and PG (phosphatidylglycerol) lipids.

2.2.2 General Procedure for the Synthesis of Dap Analogs

Peptide **2.1** (scheme 2.1),[66,67] which contains residues 9 and 10, was used for the preparation of all analogs with the exception of Dap-A10-E12-W13. 2ClTrt-PS (133 mg, 0.200 mmols), 2ClTrt-TG (526 mg, 0.100 mmols) or Rink Amide-PS were used as resins. For the synthesis of Dap-A10-E12-W13, the Gly residue in peptide **2.1** was replaced with Ala. Residues 8 to 1 were incorporated using standard Fmoc SPPS using Fmoc amino acid (4 equiv), O-(1H-6-chlorobenzotriazole-1-yl)-1,1,3,3-tetramethyluronium hexafluorophosphate (HCTU, 4 equiv) and 4-methylmorpholine (4 equiv) in dimethylformamide (DMF, 1.5 mL) and 1 h coupling times. After each coupling the resin was filtered and washed with DMF (3 x 3 min) and DCM (3 x 3 min). FmocThrOH was used for the incorporation of Thr4. The Fmoc group was removed with 20% 4-methylpiperidine in DMF (1.5 mL, 1 x 5 min). The resin was washed with DMF (1 x 15 min, 3 x 3 min) and DCM (3 x 3 min) after each deprotection. The decanoyl tail was

introduced using decanoic acid (4 equiv), diisopropylcarbodiimide (DIC, 4 equiv) and hydroxybenzotriazole (HOBt, 4 equiv) in DMF (1.5 mL) for 13 h followed by the usual washing procedure. The depsi bond was introduced by first reacting either FmocTrp(Boc)OH (10 equiv) or FmocAlaOH (10 equiv) and DIC (10 equiv) in dry DCM (2 mL) for 35 min. This mixture was then added to the swollen resin-bound peptide. DMAP (0.1 equiv) was added followed by the addition of Triton X-100 (20 μL) (unless stated otherwise in Table 1) and the mixture was agitated for 13 h. The mixture was filtered and washed with DMF (3 x 3 min) and DCM (3 x 3 min). The coupling was repeated if the efficiency of the reaction was less than 80 % (see Table 1 for the number of couplings used for each analog). Residues 12 to 11 were incorporated using standard Fmoc SPPS using Fmoc amino acid (4 equiv), 4 equiv DIC (4 equiv) and 4 equiv HOBt (4 equiv) in DMF (1.5 mL) and 3-4 h coupling times. After each coupling the resin was filtered and washed with DMF (3 x 3 min) and DCM (3 x 3 min). For residues 12 and 11, the Fmoc group was removed using 20% 2-methylpiperidine in DMF (1.5 mL, 3 x 10 min) followed by the usual washing procedure. The alloc group was removed using dimethylbarbituric acid (DMBA, 10 equiv) in the presence of a catalytic amount of $Pd(PPh_3)_4$ in DCM:DMF (3:1 v/v, 2 mL) for 50 min. The resin was filtered and washed with DCM (3 x 3 min), and then with a 1.0 % solution of sodium diethyldithiocarbamate trihydrate in DMF (2mL, 3 x 15 min) to remove excess Pd catalyst, and then DMF (3 x 3 min) and DCM (3 x 3 min). On resin cyclization was performed using (7-azabenzotriazol-1-yloxy) tripyrrolidinophosphonium hexafluorophosphate (PyAOP)/1-Hydroxy-7-azabenzotriazole (HOAt)/2,4,6-collidine (5/5/10 equiv) with 1% Triton X-100 in DMF (2 mL) (2 x 1.5 h). Crude analog was

obtained by treating the resin-bound peptides with a solution of trifluoroacetic acid (TFA): triisopropylsilane (TIS): H_2O (95:2:5:2.5, 2 mL) for 2 h. The mixture was filtered, and the resin was rinsed with DCM. The combined filtrates were concentrated to one fourth the original volume using a stream of N_2 gas. The peptide was precipitated by adding cold ether (3 mL). The precipitated peptide was collected by centrifugation and washed twice with cold ether. Pure analog obtained using semi-preparative HPLC employing a linear gradient of ACN/H_2O (0.1% TFA) (70% Acetonitrile and 30% H_2O (0.1% TFA) to 35% Acetonitrile and 65% H_2O (0.1% TFA) in over 50 min). Fractions containing the desired analog were collected, concentrated by high vacuum and lyophilized to give pure analog as a white powder (see Appendix A for the analytical HPLC chromatograms and HRMS spectra for each analog).

2.2.3 Antibacterial Activity

The minimum inhibitory concentration (MIC) of the Dap analogs against *B. subtilis* strains were determined as previously described by Muraih *et al* using serial dilutions in microtiter plates..[85] Each reported MIC is the average of three determinations.

2.2.4 Liposome Binding Studies

Liposome binding studies were performed as previously described by Muraih *et al*.[85] To a suspension of DMPG/DMPC or DOPG/DOPC (1:1) LUVs (250 μM total lipid) in HEPES (20 mM, pH 7.4)/NaCl (150 mM), was added Dap, or Dap analog (3 μM final concentration). A solution of $CaCl_2$ was added to the final concentrations indicated in Figure 2.2 (0-100 mM). Samples were incubated at 37 °C for 3 minutes. Fluorescence spectra were acquired on a PTI QuantaMaster 4 instrument (excitation wavelength: 365 nm;

emission wavelength: 400-600 nm for Dap; excitation wavelength: 280 nm; emission wavelength: 300-400 nm for the Dap analogs). (see Appendix B for the fluorescence spectra and membrane binding curves (MBCs) for each analog).

2.3 Results and Discussion

2.3.1 Synthesis of Dap-E12-W13 Analogs

In Chapter 1, we presented two different routes (schemes 1.2 and 1.3) to Dap that were developed in the Taylor group.[66,67] Each route utilized at least one azido acid as a building block. However, it was desirable to have a route to Dap that does not require any azido acids and relies solely on Fmoc building blocks as they are commercially available while azido acids are not.

One of the Dap analogs that the Taylor group wished to prepare was one in which all of the uncommon amino acids (not including the D amino acids), Orn6, 3MeGlu12, and Kyn13, are replaced with one of the common 20 amino acids. In Dap-E12-W13, a fairly active Dap analog, 3MeGlu12 and Kyn13 in Dap are replaced with Glu and Trp. Hence, all that was left was replacing the Orn residue in Dap-E12-W13 with Lys. The synthesis of this analog, Dap-K6-E12-W13, was undertaken by Dr. Chuda Lohani in the Taylor group. While working on the synthesis of this analog, he revisited the route outlined in scheme 1.1 as it was designed to use only Fmoc building blocks. Using equimolar quantities of FmocTrp(Boc)OH (10 equiv) and DIC (10 equiv), cat. DMAP (0.1 equiv), 0.1 % triton X-100, in CH_2Cl_2, he was able to prepare peptide **2.3** from peptide **2.2** after one overnight (16 h) coupling with almost no epimerization (scheme 2.1). Peptide **2.3** was then carried

forward to give Dap-K6-E12-W13 in over a 20 % yield. It is worthy of note that these conditions for forming the ester bond are also capable of forming the ester bond between FmocKyn(Boc,CHO)OH and peptide **1.2** (Chapter 1, scheme 1.1); however, the resulting peptide, **1.3**, is formed as a 2:3 mixture of epimers.

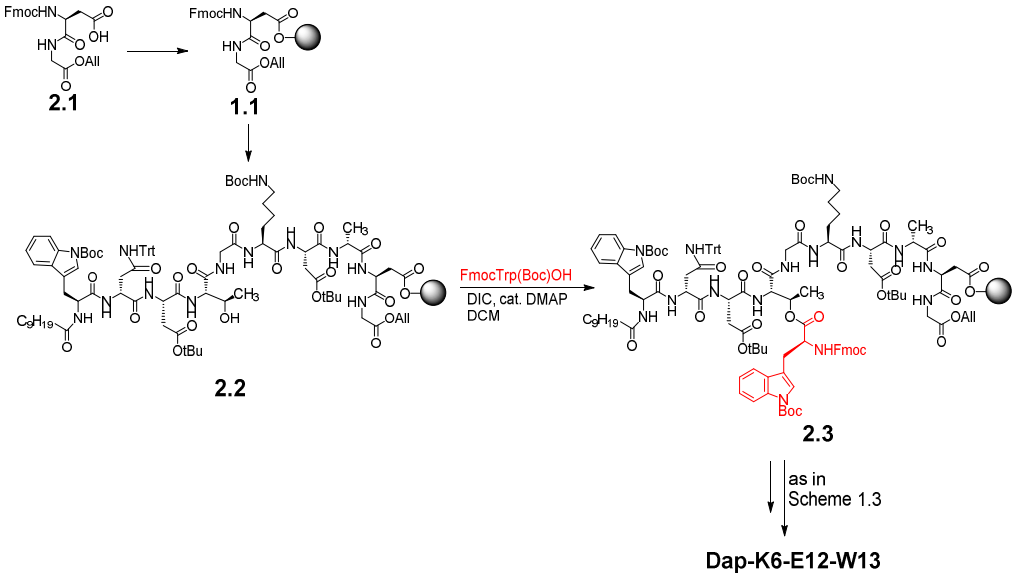

Scheme 2.1. Synthesis of Dap-K6-E12-W13.

The approach used to prepare Dap-K6-E12-W13 in scheme 2.1 was applied to the synthesis of Dap-E12-W13 (scheme 2.2). The synthesis was initiated by attaching a suitably protected Asp9Gly10 dipeptide (**2.1**) to 2-ClTrtCl polystyrene resin (2-ClTrtCl-PS) via the side chain of the Asp residue. Fmoc-based SPPS was used to introduce residues 1-8 using Fmoc amino acid (4 equiv), using O-(1H-6-chlorobenzotriazole-1-yl)-1,1,3,3-tetramethyluronium hexafluorophosphate (HCTU, 4 equiv) and 4-methylmorpholine (4 equiv) as coupling agent. The decanoic tail was introduced using decanoic acid (4 equiv), diisopropylcarbodiimide (DIC, 4 equiv) and hydroxybenzotriazole (HOBt, 4 equiv). FmocTrp(Boc)OH was successfully coupled to the side chain of Thr4 in peptide **2.4**, using

DIC/HOBt/cat. DMAP in DCM to give the desired peptide, **2.5**, in quantitative yield. It was found that the esterification could be achieved equally well with or without Triton. Fmoc SPPS was used to introduce residues 12 and 11 using 2-methylpiperidine (2-MP) for Fmoc removal to minimize C-O bond aminolysis. The allyl group in Gly10 was then removed using dimethylbarbituric acid (DMBA) and cat. $Pd(PPh_3)_4$. The resulting peptide, **2.6**, was cyclized using PyAOP/HOAt/2,4,6-collidine in DMF with 0.1 % Triton X-100 (called the magic mixture).[86] Pure Dap-E12-W13 was obtained after side chain deprotection and cleavage from the resin and HPLC purification of the resulting crude peptide.

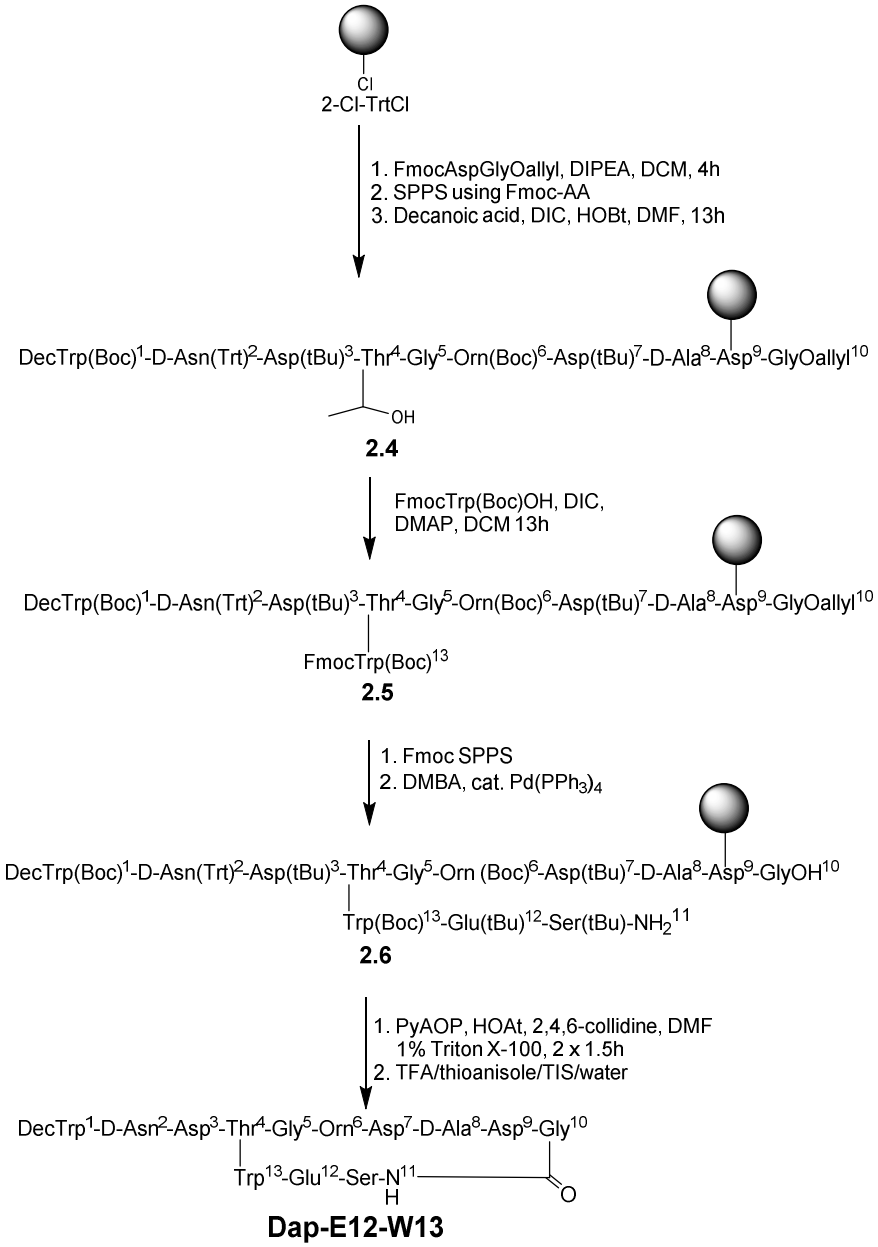

Scheme 2.2. Synthesis of DapE12W13 using the improved route.

The route outlined in scheme 2.2 was then applied to the synthesis of Dap-A6-E12-W13. When the esterification was done in the absence of Triton, 20% of unesterified peptide remained after two 13 h couplings. In the presence of 0.1 % Triton. the depsi bond

was formed with almost 100% efficiency after two 13 h couplings with very little epimerization. We also prepared Dap-A6-E12-W13 on TentaGel (2ClTrt-TG) resin. TentaGel resin is a copolymer consisting of a low crosslinked polystyrene matrix on which poly (ethylene glycol) (PEG) is grafted. Difficult couplings tend to proceed more readily on TentaGel as PEG is more hydrophilic than polystyrene and the PEG linker allows for more space between the resin and the peptide. Overall, this results in less peptide aggregation during SPPS and hence better coupling yields. For the synthesis of Dap-A6-E12-W13 on Tentagel resin, the esterification reaction proceeded with almost 100% efficiency after two 13 h couplings with or without 0.1 % Triton.

The procedure described in scheme 2.2 was then applied to the synthesis of the rest of the Ala variants (table 2.1). L- and D-Ala was used as appropriate so as to preserve the regular stereochemistry of the residue in question. The D-Ala residue at position 8 was substituted with L-Ala, and Asp9 was converted to an Asn residue using a Rink amide linker on polystyrene. Obviously, Thr4 cannot be changed to Ala due to the fact that the side chain of Thr4 is needed to form the ester linkage. 2ClTrt-PS resin was used rather than the analogous TentaGel resin for most of these syntheses due to the much higher cost and lower loading of 2ClTrt-TG resin compared to 2ClTrt-PS resin. In most cases the efficiency of the esterification reactions was greater than 90 % after two 13 h couplings when performed on 2ClTrt-PS resin (table 2.1). The only exceptions were Dap-A1-E12-W13 which required only one 13 h coupling to attain 90 % efficiency, Dap-A3-E12-W13 which required three 13 h couplings to attain 88 % efficiency and Dap-D-A2-E12-W13 which attained an efficiency of 81% after three 13 h couplings. To determine if the high esterification

efficiency observed during the synthesis of the Dap-A6-E12-W13 analog on TentaGel resin mentioned earlier was transferable to other Dap analogs, Dap-A5-E12-W13 was prepared using the TentaGel resin. In this case, the esterification reaction was formed greater than 95% efficiency after just one 13 h coupling in the absence of triton X-100.

Table 2.1. Alanine analogs of Dap-E12-W13 prepared via a route analogous to that outlined in scheme 2.2.

Dap analog	Resin	No. of Couplings[a]	0.1 %Triton	Esterification Efficiency (%)[b]
Dap-A1-E12-W13	2ClTrt-PS	1	yes	90
Dap-D-A2-E12-W13	2ClTrt-PS	3	yes	81
Dap-A3-E12-W13	2ClTrt-PS	3	yes	88
Dap-A5-E12-W13	TentaGel	1	no	>95
Dap-A6-E12-W13	2ClTrt-PS	2	no	80
Dap-A6-E12-W13	2ClTrt-PS	2	yes	>95
Dap-A6-E12-W13	TentaGel	2	no	>95
Dap-A6-E12-W13	TentaGel	2	yes	>95
Dap-L-A8-E12-W13	2ClTrt-PS	2	yes	95
Dap-L-N9-E12-W13	Rink amide-PS	3	no	85
Dap-A10-E12-W13	2ClTrt-PS	2	Yes	95
Dap-D-A11-E12-W13	2ClTrt-PS	2	Yes	91
Dap-A12-W13	2ClTrt-PS	2	Yes	92
Dap-E12-A13	2ClTrt-PS	2	Yes	>95

[a]Esterification reactions were performed using 10 equiv FmocTrp(Boc)OH, 10 equiv DIPCDI, 0.1 eq. DMAP CH_2Cl_2, rt) either with or without 0.1 % triton X-100. FmocAlaOH was used instead of FmocTrp(Boc)OH for the synthesis of the Dap-E12-A13 analog. [b]The percent efficiencies of the esterification reactions were determined by analytical RP-HPLC analysis of the released and deprotected peptides after the esterification reaction.[87]

2.3.2 In Vitro Antibacterial Activity of Dap-E12-W13 Analogs

The *in vitro* antibacterial activity of Dap-E12-W13 and its alanine analogs was examined against *B. subtilis* 1046 at physiological Ca^{2+} concentration (1.25 mM) and 5 mM Ca^{2+}. The results are shown in table 2.2. All of the alanine analogs exhibited higher MICs than Dap-E12-W13 at the lower Ca^{2+} concentration. Most of the analogs were more active at the higher Ca^{2+} concentration compared to the lower Ca^{2+} concentration. This observation is consistent with our previous studies (see chapter 1, section 1.4.2.3) where we found that Dap-E12-W13 and other analogs that are less active than Dap at physiological Ca^{2+} concentration, are usually more active at Ca^{2+} concentrations greater than physiological.[67]

Only three residues, D-Asn2, Orn6 and Ser11, in Dap-E12-W13 appear to be amenable to substitution with Ala, without major loss of activity. The A11 and A6 analogs were only 1.5-fold less active than Dap-E12-W13 while the D-Ala2 analog was about 4-fold less active than Dap-E12-W13. The Ala1 and Ala3 analogs showed some activity at 5 mM Ca^{2+} but were still 30-fold less active than Dap-E12-W13. The Ala13 analog was 100-fold less active than Dap-E12-W13 at 5 mM Ca^{2+}.

Table 2.2. *In vitro* antibacterial activity of Dap, Dap-E12-W13 and alanine analogs of Dap-E12-W13 against *B. subtilis* 1046.

	MIC (μg/mL)	
Dap analog	1.25 mM Ca^{2+}	5.0 mM Ca^{2+}
Daptomycin	0.75	0.5
Dap-E12-W13	3.5	1.0
Dap-A1-E12-W13	>100	30
Dap-D-A2-E12-W13	15	3
Dap-A3-E12-W13	>100	30
Dap-A5-E12-W13	35	4
Dap-A6-E12-W13	5	0.5
Dap-A7-E12-W13	>100[a]	>100[a]
Dap-L-A8-E12-W13	100	35
Dap-L-N9-E12-W13	>100	35
Dap-A10-E12-W13	>100	>100
Dap-D-A11-E12-W13	5	0.5
Dap-A12-W13	35	4
Dap-E12-A13	>100	100

[a]From reference 66

Our finding that Orn6 is amenable to substitution by Ala is consistent with previous reports that modifications can be made to Orn6 in Dap often without significant loss of activity.[88] The finding that the D-Ala11 analog was also amenable to Ala substitution was expected as it had been previously shown that substitution of D-Ser11 in Dap with D-Ala, using the biosynthetic approach, had little effect on activity.[59] Miao *et al*. have shown that substituting D-Asn2 with L-Asn2 resulted in a 10-fold reduction in activity suggesting that stereochemistry at this position is important to activity.[88] Besides this substitution, no other residues have been examined at this position. Our results with the D-Ala2 analog suggest that this position is amenable to substitution so long as stereochemistry is maintained.

The finding that positions 2, 6 and 11 are amenable to substitution in Dap-E12-W13 is consistent with the fact that these residues in Dap are not conserved in A54145 (figure 2.2), a closely related Ca^{2+}-dependent cLPA, which bears D-Asp, L-Ala and D-Gln at positions 2, 6 and 11 respectively, though stereochemistry is maintained at these positions.

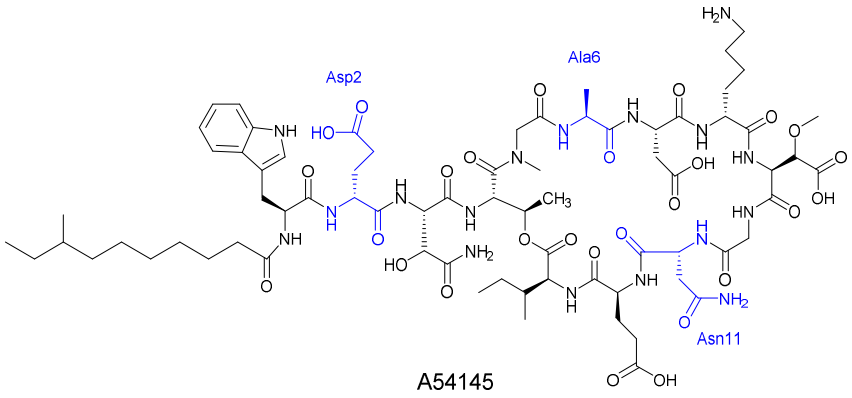

Figure 2.2. Structure of A54145

Our studies show that the Ala7, L-Ala8, Asn9 and Ala10 analogs of Dap-E12-W13 were inactive or active at only the highest concentration tested (100 ug/mL at 1.25 mM Ca^{2+}). This is consistent with the results of Grunewald *et al.* who reported that replacing Asp7 and Asp9 with Asn in a Dap-L-N2-E12 analog resulted in complete loss of activity,[58] and supports the hypothesis that the D-X-D-G motif in Dap is crucial to its activity most likely because it is directly involved in binding Ca^{2+}.

Replacing Glu12 with Ala did not have a catastrophic effect on activity. This suggests that Glu12 does not play a crucial role in determining activity and suggests that it does not have a major role in binding Ca^{2+}.

The L-Ala8 analog was significantly less active than Dap-E12-W13, which has D-Ala at this position. Nguyen *et al.* reported that substitution of D-Ala8 in Dap with D-Lys

or D-Ser resulted in very little loss of activity.[63] Moreover, these residues in A54145 are essentially reversed relative to Dap: L-Ala and D-Lys in A54145 are L-Orn6 and D-Ala8 in Dap. These results suggest that position 8 in Dap may also be amenable to variation so long as the correct stereochemistry is maintained.

Our results also show that residues Trp13 (Kyn in Dap), Asp3, and Trp1 are also very important for biological activity, as the corresponding Ala analogs were inactive at the highest concentration tested. Kyn13 in Dap has been substituted with Trp, Leu and Val and the resulting Trp13, Leu13 and Val13 analogs were 2- 4- and 8-fold less active than Dap, respectively.[59] The Taylor group has substituted Kyn13 in Dap with Tyr and the resulting analog was 30-fold less active than Dap.[67] Therefore, it appears that Dap can, to a certain degree, bear hydrophobic groups and certain aromatic residues at positions 1 and 13, but small residues, such as Ala, are not well tolerated.

2.3.3 Membrane Binding Studies

The interaction of Dap and Dap-E12-W13 with model membranes containing PG as a function of Ca^{2+} concentration can be monitored by following the increase in fluorescence and simultaneous blue shift of Kyn13 in Dap, or Trp1 and Trp13 in Dap-E12-W13, as these residues insert into the a-polar environment of the membrane.[39,85]

The intrinsic fluorescence of Dap (λ_{em} = 400-600 nm) and Dap-E12-W13 (λ_{em} = 300-400 nm) in the presence of DMPC/DMPG (1:1) LUVs and DOPG/DOPC (1:1) LUVs as a function of Ca^{2+} concentration is shown in figure 2.3 (we will be referring to these types of plots as membrane binding curves (MBCs)). With the DM LUVs, the fluorescence intensity of Dap does not increase significantly between 0-0.10 mM Ca^{2+}. As the Ca^{2+}

concentration increases from 0.1-1.0 mM, the fluorescence intensity of Dap rapidly increases and then levels off above 1 mM. This is a typical MBC for Dap using DMPC/DMPG (1:1) LUVs.[85] Dap-E12-W13 exhibits a similar binding curve, though it appears to respond to Ca^{2+} at slightly lower concentrations of Ca^{2+}. A possible reason why the MBC for Dap is slightly different from the MBC for Dap-E12-W13 is because we are not following the fluorescence of the same residues in the two peptides: in Dap-E12-W13, the fluorescence intensity of both Trp1 and Trp13 is being monitored, while Kyn13 is being monitored with Dap. In either case, it has been suggested that it is the second step of Dap's MOA that this increase in fluorescence above 0.05-0.1 mM Ca^{2+} is monitoring: the binding of the second Ca^{2+}, oligomer formation and deeper membrane insertion.[89]

When DO LUVs are used, the MBCs are different from the MBCs obtained using DM LUVs. With DO LUVs, both peptides appear to be very sensitive to Ca^{2+}, as the fluorescence of both peptides increases rapidly between 0-0.1 mM Ca^{2+} and levels off above 0.1 mM. So it appears that Dap and Dap-E12-W13 interact more avidly with LUVs composed of DO lipids than DM lipids. This has been noted previously in the Taylor and Palmer groups for Dap. The reason behind this is not known.

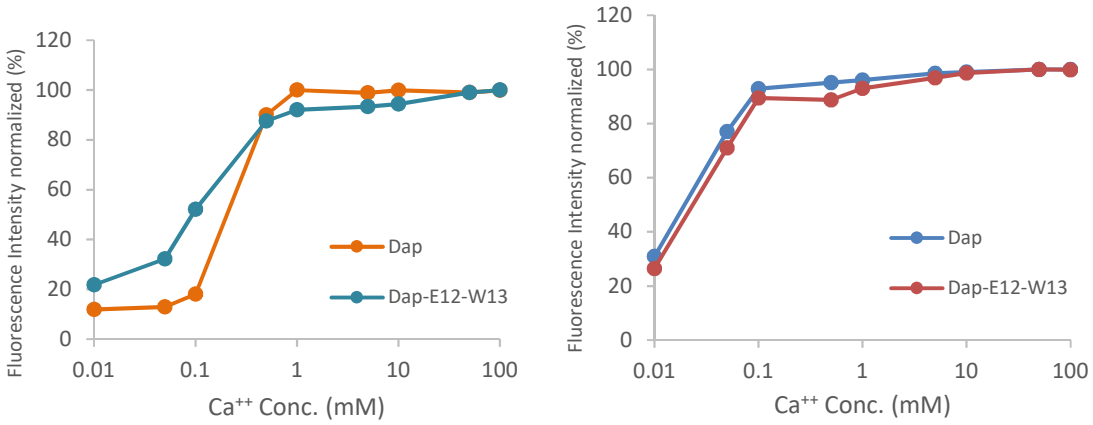

Figure 2.3. MBCs of Dap and Dap-E12-W13 in the presence of DMPC/DMPG (1:1) LUVs (*on the left*) and DOPG/DOPC (1:1) LUVs (*on the right*).

MBCs were obtained for the Dap analogs listed in table 2.2 using DMPC/DMPG (1:1) and DOPC/DOPG (1:1) LUVs. The fluorescence of the Trp residues at position1 and/or 13 was monitored. The MBCs for these analogs are given in Appendix B or are shown and discussed below.

The fluorescence spectra for Dap-A6-E12-W13, which is only 1.5-fold less active than Dap-E12-W13 (table 2.2), in the presence of DM and DO LUVs at different Ca^{2+} concentrations and the associated MBCs are given in figure 2.4. The MBCs of Dap-E12-W13 are also shown. The MBCs of Dap-A6-E12-W13 and Dap-E12-W13 with DM and DO LUVs are very similar which suggests that they have a similar affinity for Ca^{2+}.

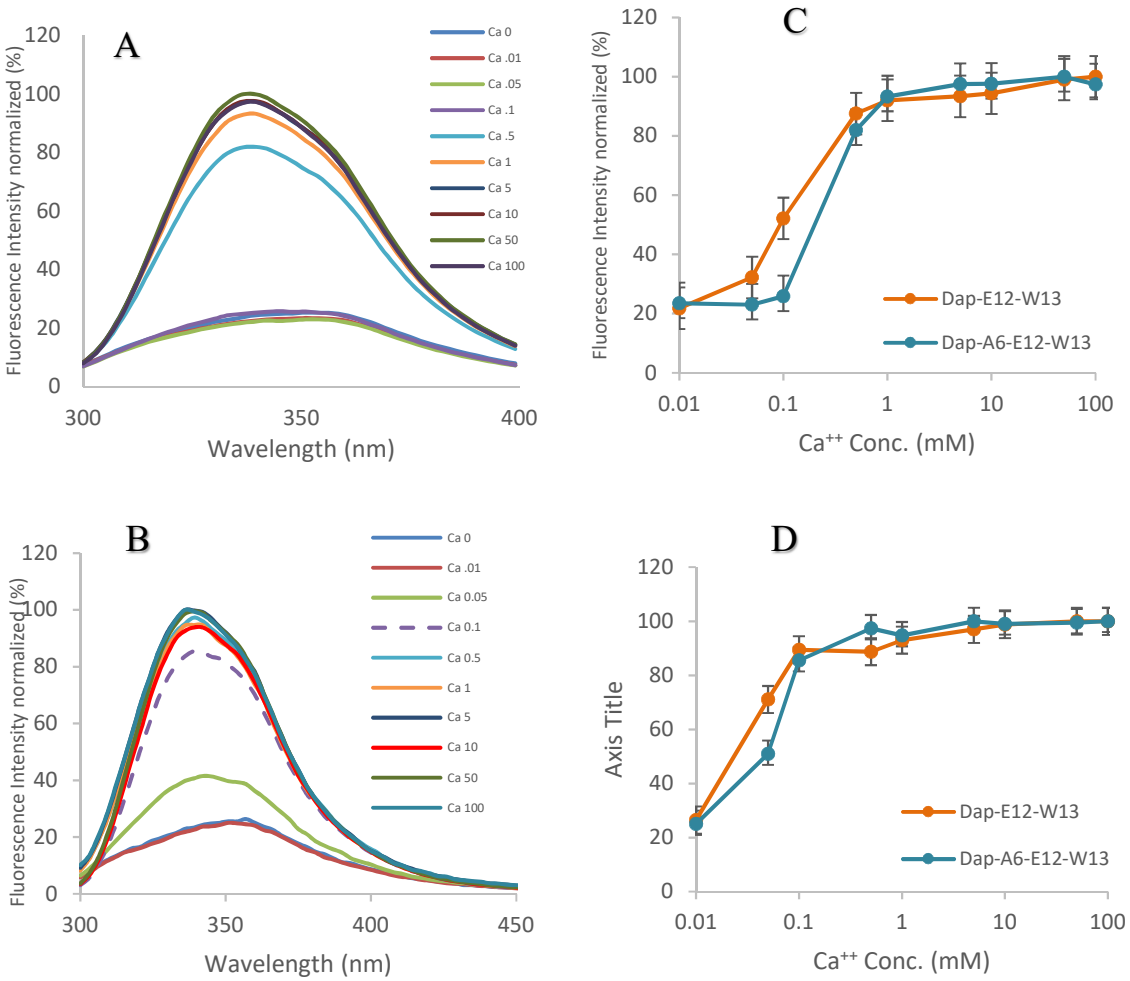

Figure 2.4. Fluorescence spectra of Dap-A6-E12-W13 in the presence of *(A)* DMPC/DMPG (1:1) liposomes, *(B)* DOPC/DOPG (1:1) liposomes with increasing Ca^{2+} concentration (mM) at 37 °C. *(C)* and *(D)*: MBCs of Dap-A6-E12-W13 and Dap-E12-W13 on DMPC/DMPC and DOPC/DOPG liposomes. Error bars represent the standard deviation of three different experiments.

Another analog found to have antibacterial activity comparable to Dap-E12-W13 is Dap-A11-E12-W13. The fluorescence spectra for Dap-A11-E12-W13 in the presence of DM and DO LUVs at different Ca^{2+} concentrations and the associated MBCs are given in figure 2.5. The MBCs of Dap-E12-W13 are also shown. The MBCs of Dap-A11-E12-W13

and Dap-E12-W13 with DM and DO LUVs are very similar which suggests that they have a similar affinity for Ca^{2+}.

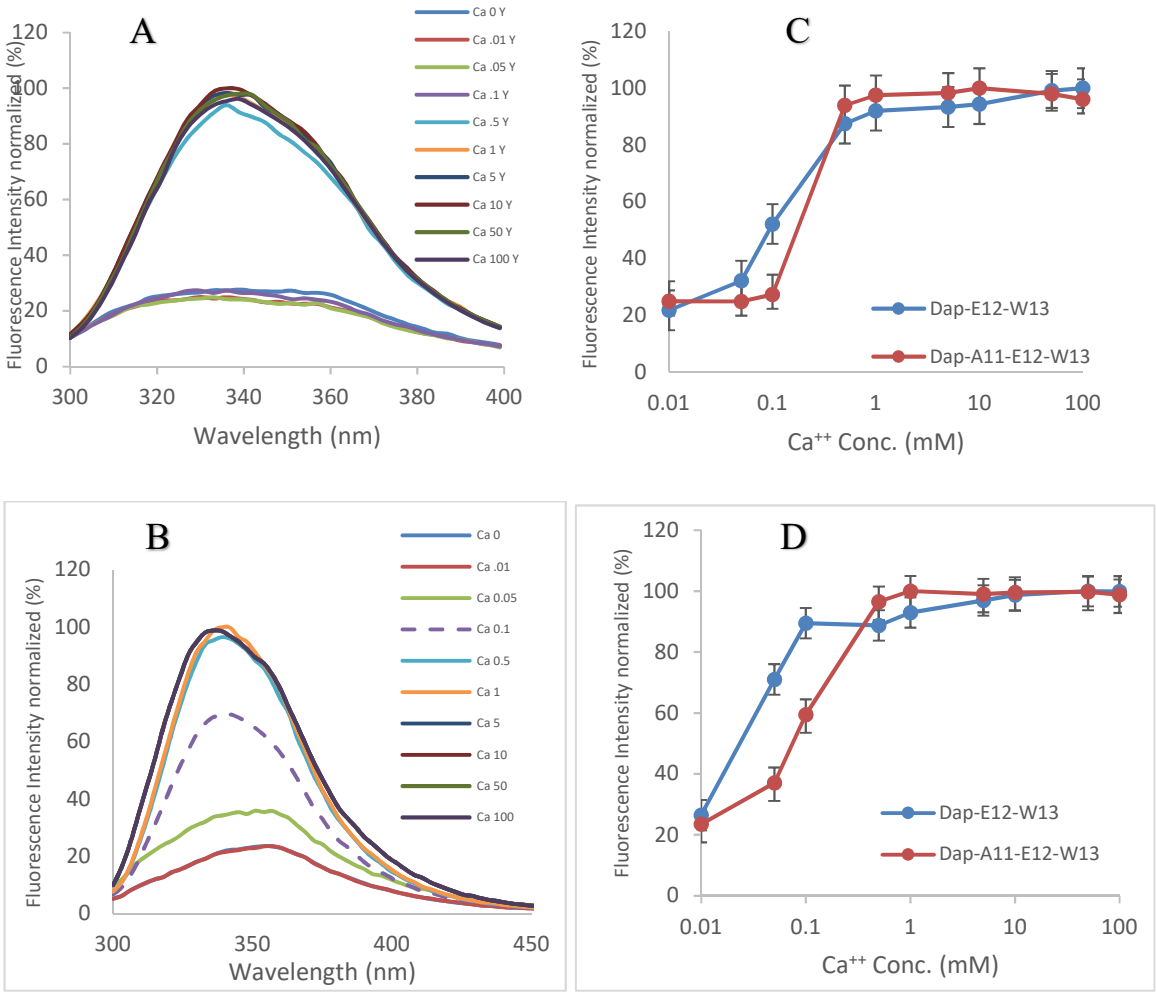

Figure 2.5. Fluorescence spectra of Dap-A11-E12-W13 in the presence of *(A)* DMPC/DMPG (1:1) liposomes, *(B)* DOPC/DOPG (1:1) liposomes, and increasing Ca^{2+} concentration (mM) at 37 °C. *(C)* and *(D):* MBCs of Dap-A11-E12-W13 and Dap-E12-W13 on DMPC/DMPC and DOPC/DOPG liposomes. Error bars represent the standard deviation of three different experiments.

The fluorescence spectra for Dap-A8-E12-W13, which is 35-fold less active than Dap-E12-W13 (table 2.2), in the presence of DM and DO LUVs at different Ca^{2+} concentrations and the associated MBCs are given in figure 2.6. The MBCs of Dap-E12-

W13 are also shown. The MBCs of Dap-A8-E12-W13 are very different from that of Dap-E12-W13 in that it takes much higher concentrations of Ca^{2+} to achieve maximal binding of Dap-A8-E12-W13 to the LUVs compared to Dap-E12-W13. This suggests that Dap-A8-E12-W13 has a lower affinity for Ca^{2+} than Dap-E12-W13 and/or Ca^{2+}-bound Dap-A8-E12-W13 has a lower affinity for the LUVs than Ca^{2+}-bound Dap-E12-W13. The lower affinity of Dap-A8-E12-W13 for Ca^{2+} and/or the LUVs might be the reason for the reduced activity of this analog.

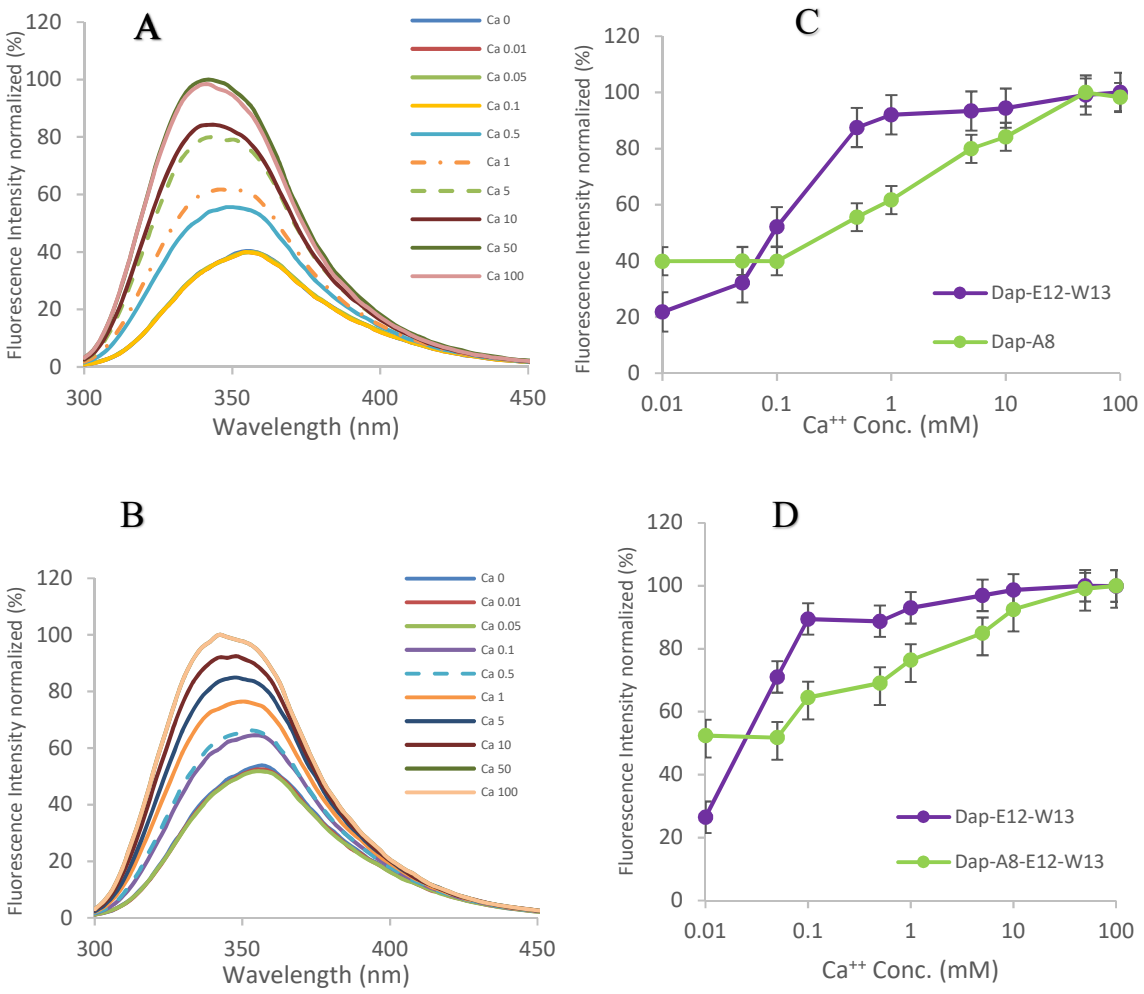

Figure 2.6. Fluorescence spectra of Dap-A8-E12-W13 in the presence of *(A)* DMPC:DMPG (1:1) liposomes, *(B)* DOPC/DOPG (1:1) liposomes, and increasing Ca^{2+} concentration (mM) at 37 °C. *(C)* and *(D):* MBCs of Dap-A8-E12-W13 and Dap-E12-W13 on DMPC/DMPC and DOPC/DOPG liposomes. Error bars represent the standard deviation of three different experiments.

The Ca^{2+} concentration needed for Dap and Dap analogs obtained in this study to fully associate with DMPC/DMPG (1:1) and DOPC/DOPG (1:1) LUVs (as determined from the MBCs) and their MICs are given in table 2.3. From the data in this table it can be seen that there is a correlation between MIC and the Ca^{2+} concentration required for Dap

and Dap analogs to fully associate with the LUVs: the higher the MIC the higher the concentration of Ca^{2+} required to achieve full membrane insertion. These results suggest that a high affinity for Ca^{2+}, whether at the first stage of Daps MOA (binding of the first Ca^{2+}) or at the second stage of Daps MOA (binding of the second Ca^{2+}, followed by deep membrane insertion), is required in order for the peptides to exhibit good biological activity.

Table 2.3. Ca^{2+} concentration needed for Dap and Dap analogs to fully associate with DMPC/DMPG (1:1) and DOPC/DOPG (1:1) LUVs and the MICs of these analogs.

		Ca^{2+} concentration needed for maximal membrane binding (mM)	
Dap analog	MIC[a] (μg/mL)	DMPC/DMPG LUVs	DOPC/DOPG LUVs
Daptomycin	0.75	1	0.1
Dap-E12-W13	3.5	1	0.1
Dap-A1-E12-W13	>100	50	100
Dap-D-A2-E12-W13	15	5	0.5
Dap-A3-E12-W13	>100	50	50
Dap-A5-E12-W13	35	10	10
Dap-A6-E12-W13	5	1	0.1
Dap-L-A8-E12-W13	100	50	50
Dap-L-N9-E12-W13	>100	10	50
Dap-A10-E12-W13	>100	50	50
Dap-D-A11-E12-W13	5	0.5	0.5
Dap-A12-W13	35	5	1
Dap-E12-A13	>100	50	50

[a]1.25 mM Ca^{2+}

For those analogs whose MICs were ≥ 100 μg/mL, high Ca^{2+} concentrations (50-100 mM) were required for maximal membrane interaction regardless of the type of lipid (DM or DO). However, the Dap-N9-E12-W13 analog was an exception. This analog was

inactive at 100 μg/mL, but required only 10 mM Ca^{2+} to achieve maximal interactions with the DM liposomes (figure 2.7). Although it required 50 mM Ca^{2+} to achieve maximal interactions with the DO liposomes, it was more sensitive to Ca^{2+} with the DO liposomes than the other inactive analogs. This analog appears to be capable of binding Ca^{2+} and inserting into the membrane relatively well. This suggests that Asp9 of the DXDG motif is not essential for Ca^{2+} binding and/or membrane insertion, yet is essential for activity and stoichiometry. Perhaps this analog can bind Ca^{2+}, insert into the membrane but cannot form a functional oligomer. ITC studies on this analog would be helpful in determining its Ca^{2+} affinity. Fluorescence studies, similar to those performed on Dap (see Chapter 1, section 1.3), using Dap-N9-E12-W13 labelled with a fluorophore on the Orn residue, would be helpful in determining the extent of oligomer formation of this analog.

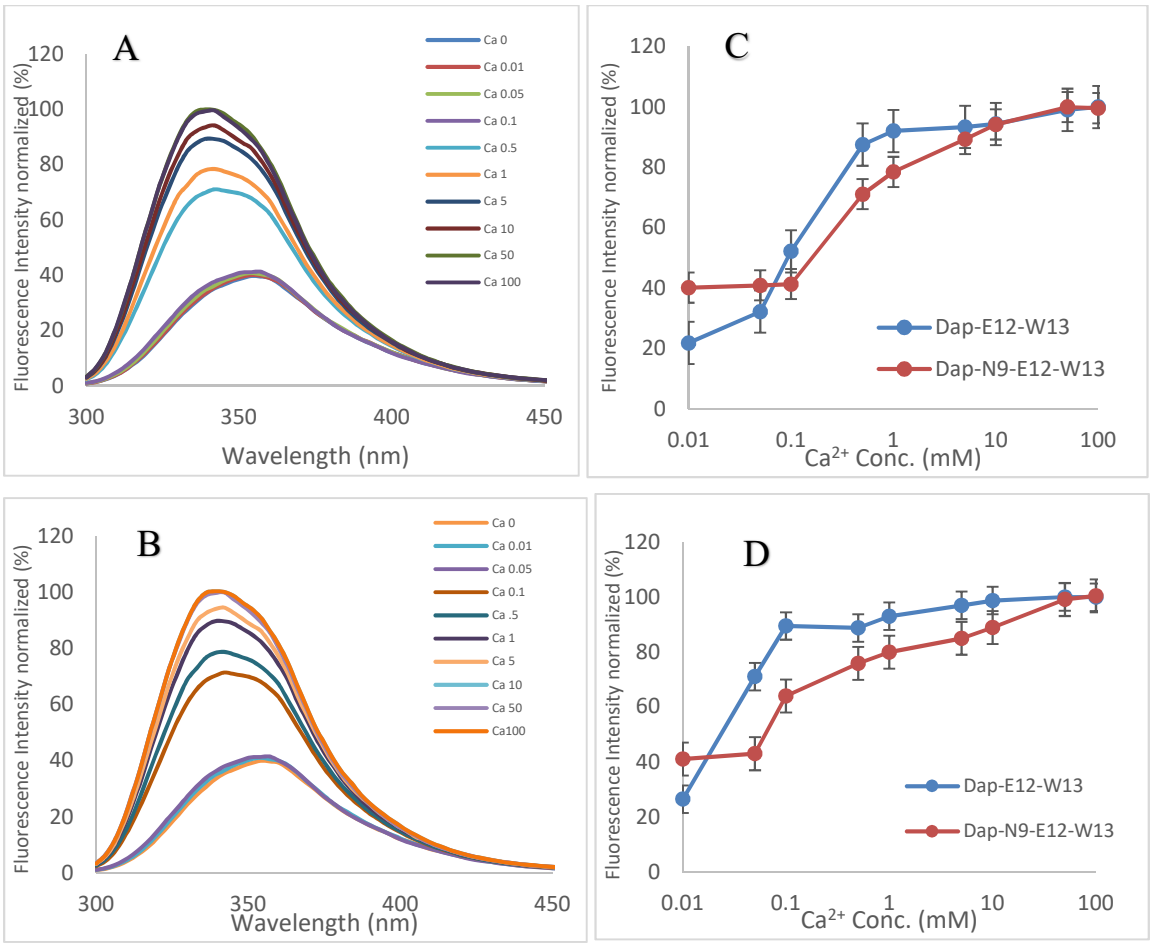

Figure 2.7. Fluorescence spectra of Dap-N9-E12-W13 in the presence of *(A)* DMPC/DMPG (1:1) liposomes, *(B)* DOPC/DOPG (1:1) liposomes with increasing Ca^{2+} concentration (mM) at 37 °C. *(C)* and *(D)*: MBCs of Dap-N9-E12-W13 and Dap-E12-W13 on DMPC/DMPC and DOPC/DOPG liposomes. Error bars represent the standard deviation of two different experiments.

Like Dap and Dap-E12-W13, *all* of the analogs required lower Ca^{2+} concentrations to *initiate* interactions with the DO LUVs as compared to the DM LUVs. These results suggest that the greater sensitivity of these peptides to Ca^{2+} with the DO LUVs is due to an interaction between the decanoyl tail of the peptide and the lipids of the LUVs.

2.3.4 Dap-K6-X11-E12-W13 Analogs

From the above Ala scan of Dap and from studies by Cubists Pharmaceuticals on Dap-X8 analogs (see chapter 1 section 1.4.2), it appears that four positions in Dap are amenable to substitution: positions 2, 6, 8, and 11. As one of the ultimate objectives of this work is to obtain a Dap analog with improved activity against Dap-resistant bacteria and active in the presence of lung surfactant, we decided to begin making analogs of Dap starting with position 11.

While the SAR studies presented in sections 2.3.1-3 were in progress, it was discovered by Robert Taylor, a graduate student in the Taylor and Palmer groups, that Dap-K6-E12-W13 (see section 2.3.1) is almost as active as Dap at physiological Ca^{2+} concentration and was about 2.3-fold more active than Dap-E12-W13 at physiological Ca^{2+} concentration (table 2.4). Therefore, it was decided to use Dap-K6-E12-W13 as the lead for the preparation of position 11 analogs.

Table 2.4. *In vitro* antibacterial activity of daptomycin, Dap-K6-E12-W13 and Dap-E12-W13 against *B. subtilis* 1046 and PY79.

	MICs (ug/mL)[a]		
Strain	**Daptomycin**	**Dap-K6-E12-W13**	**Dap-E12-W13**
B. subtilis 1046	0.75 (0.5)	1.5 (1.0)	3.5 (1.0)
B. subtilis PY79	0.75 (0.75)	1.5 (0.75)	4.5 (3.0)

[a]MICs presented outside brackets were obtained at 1.25 mM Ca^{2+}. MICs presented inside brackets were obtained at 5.0 mM Ca^{2+}.

Seventeen amino acids, as their D-isomers, were substituted for D-Ser11 in Dap-K6-E12-W13. We did not prepare the Lys11 analog, as it had already been shown by researchers at Cubist that Dap can tolerate this residue at position 11 with little loss of

activity.[59] The Ala11 analog was also not prepared, as we had already demonstrated above that Ala could be accommodated at position 11 in Dap-E12-W13.

The analogs were prepared using the same approach as outlined in scheme 2.2 for Dap-E12-W13. In brief, a large quantity of peptide **2.7** was prepared (scheme 2.3). This was achieved using automated Fmoc SPPS, with the exception of the formation of the depsi bond and the installation of Glu12, which were installed manually. The resin was then sectioned into 17 smaller vessels, which were used to install the 17 D-amino acids at position 11 (peptides of type **2.8**). The resulting peptides were cyclized, deprotected, cleaved from the resin and purified by HPLC as previously described. The HPLC chromatograms and mass spectra of these analogs are given in Appendix C.

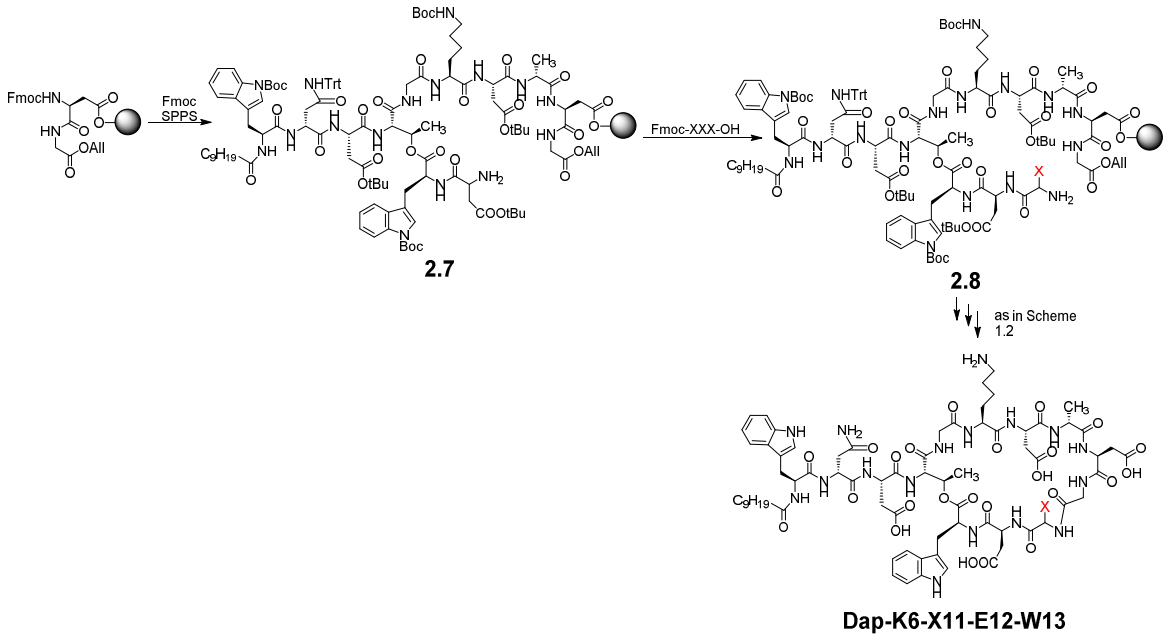

Scheme 2.3. Synthesis of Dap-K6-X11-E12-W13 peptides.

The *in vitro* antibacterial activity of the Dap-K6-X11-E12-W13 peptides were determined against *B. subtilis* 1046 at physiological Ca^{2+} concentration (1.25 mM) and 5 mM Ca^{2+}. The results are shown in table 2.5. None of the analogs were more active than Dap-K6-E12-W13; however, some interesting results were obtained.

Table 2.5. *In vitro* antibacterial activity of Dap, Dap-K6-E12-W13, Dap-A11-E12-W13, and Dap-K6-X11-E12-W13 against *B. subtilis* 1046.

		MIC (ug/mL)	
Entry	Dap analog	1.25 mM Ca^{2+}	5.0 mM Ca^{2+}
1	Daptomycin	0.75	0.5
2	Dap-K6-E12-W13	1.5	0.5
3	Dap-A11-E12-W13	5	0.5
4	Dap-K6-D-H11-E12-W13	1.5	1
5	Dap-K6-D-R11-E12-W13	2.5	0.5
6	Dap-K6-D-N11-E12-W13	2.5	0.5
7	Dap-K6-D-Q11-E12-W13	30	1.5
8	Dap-K6-D-T11-E12-W13	4	0.85
9	Dap-K6-D-C11-E12-W13	4	1.5
10	Dap-K6-D-M11-E12-W13	4	0.5
11	Dap-K6-G11-E12-W13	4	2.5
12	Dap-K6-D-D11-E12-W13	30	7.5
13	Dap-K6-D-E11-E12-W13	75	30
14	Dap-K6-D-L11-E12-W13	30	1.5
15	Dap-K6-D-V11-E12-W13	30	0.85
16	Dap-K6-D-allo-I1e-E12-W13	30	4
17	Dap-K6-D-F11-E12-W13	100	4
18	Dap-K6-D-Y11-E12-W13	75	10
19	Dap-K6-D-W11-E12-W13	>100	>100
20	Dap-K6-D-P11-E12-W13	>100	30

Particularly surprising was the finding that the His11 analog (entry 4) was as active as Dap-K6-E12-W13 at physiological Ca^{2+} concentration. Moreover, the Arg11 analog (entry 5) was less than 2-fold less active than Dap-K6-E12-W13 at physiological Ca^{2+} concentration. Therefore, it appears that Dap can accommodate positively charged residues at position 11 very well. Perhaps they are interacting with a phosphate group of a lipid in the membrane. In contrast, negatively charged residues at position 11 were quite detrimental to activity, with the Asp11 (entry 12) and Glu 11 (entry 13) analogs being 20- and 50-fold less active than the parent peptide, respectively. In the case of the Asp11 analog, the large loss of activity was due to the extra negative charge, as the Asn11 analog (entry 6) was almost as active as Dap-K6-E12-W13 at physiological Ca^{2+} concentration. However, this was not the case with the Gln11 analog, which was 20-fold less active than the parent peptide suggesting that the larger size (compared to Asp or Ser) and the negative charge contributed the reduced activity of the Glu analog.

Ser11 can be replaced with a Thr residue (entry 8) with only a 2.5-fold loss of activity, indicating that the addition of a methyl group to the side chain of Ser does not significantly affect activity. The Cys analog (entry 9) was also only 2.5-fold less active than the parent compound, indicating that the OH group of Ser11 can be replaced with an SH without causing a serious deleterious effect on activity. Moreover, the Met analog (entry 10) was as active as the Cys analog.

Gly11 (entry 11) was also only 2.5-fold less active than Dap-K6-E12-W13, indicating that a side chain at position 11 was not crucial to the antibacterial activity.

Although an Ala residue can be accommodated at position 11, the incorporation of hydrophobic, branched residues (Leu (entry 14), Val (entry 15), and D-allo-Ile (entry 16)), was detrimental to activity. The incorporation of uncharged aromatic residues (Phe (entry 17), Tyr (entry 18), and Trp (entry 19)) at position 11 resulted in a large decrease in activity.

The Pro analog (entry 20) was one of the least active, showing no activity at 100 μg/mL. This is probably due to the proline causing a significant change in the overall 3-D structure of the peptide which probably significantly affected the ability of the analog to bind Ca^{2+}.

Chapter 3
Summary and Future Work

3.1 Summary

Daps unresolved MOA, the increasing appearance of Dap resistant bacteria, and the inability of Dap to treat community-acquired pneumonia stresses the need for the development and study of new Dap analogs. To begin addressing these issues, an SAR study, in the form of an alanine scan, was performed on Dap-E12-W13, a relatively active and synthetically accessible analog of Dap. This was done to determine which amino acids can be substituted with alanine without significantly adversely affecting Dap's biological activity and which amino acids are important for Dap's ability to interact with membranes. The analogs were prepared using a solid phase approach, which requires only Fmoc building blocks, recently developed in the Taylor group. It was found that the formation of the ester bond and the on-resin cyclization was more readily achieved when the peptides were prepared using Tenta-gel resin as opposed to standard polystyrene resin. The antibacterial activities of the peptides revealed that positions 2, 6, and 11 were amenable to substitution. It is also likely, based on the work of Cubist Pharmaceuticals, that position 8 is also amenable to substitution so long as the correct stereochemistry is maintained. Membrane binding studies with the Ala analogs revealed that the ability of the analogs to act as an antibiotic was closely related to their ability to bind calcium and interact with membranes.

Since the Ala scan revealed that position 11 was amenable to substitution, we prepared analogs of Dap-K6-E12-W13, an analog with activity approaching that of Dap, in

which Ser 11 was replaced with 17 of the common 20 amino acids. Although none of these analogs were more active than the parent peptide, these studies revealed that position 11 was particularly amenable to substitution with positively charged amino acids (His, Arg, Lys) as these substitutions resulted in either no or minimal loss of activity. Moreover, the Asn, Thr, Cys, Met and Gly analogs were also relatively active being only 2.7-fold less active than Dap-K6-E12-W13.

3.2 Future Work

Membrane permeabilization studies, as mentioned in Chapter 1, section 1.3, will be conducted on selected analogs derived from the Ala scan to determine how the substitution affects membrane permeabilization. Membrane binding curves will be obtained for the position 11 analogs of Dap-K6-E12-W13 to determine if these substitutions affect calcium affinity and membrane binding. These studies will be followed up with membrane permeabilization studies on selected analogs. We will also determine the biological activity of these analogs in the presence of synthetic lung surfactant and with Dap-resistant bacteria.

More Dap analogs will be prepared and their antimicrobial activity, in the presence and absence of lung surfactant, as well as their ability to interact with and permeabilize membranes, will be determined. For these studies, we will be substituting positions 2, 6 and 8 in Dap-K6-E12-W13 with the other common acids.

As mentioned in Chapter 1, section 1.3, Dap derivatives bearing fluorescent tags on the Orn residue and lipid tail have proven to be very useful as tools for studying Dap's MOA. It would be helpful for MOA studies if a fluorophore could be attached to another position in Dap. Unfortunately, in native Dap, the Orn residue and the lipid tail are the only

two places that a fluorescent tag can be easily attached. However, in this thesis, we have shown that the Dap-K6-C11-E12-W13 analog was quite active. Since it is relatively easy to append fluorescent dyes to Cys residues, we will append fluorescent tags to Dap-K6-C11-E12-W13. If such derivatives are biologically active, then it should be possible to use these fluorescent peptides to further study Dap's MOA.

Letter of Copyright Permissions

The authors of the journal article "Daptomycin forms cation-and size-selective pores in model membranes," Dr. Michael Palmer, gave permission for Figure 1.4 to be used in this thesis. (Zhang, T.; Muraih, J. K.; MacCormick, B.; Silverman, J.; Palmer, M. *Biochimica et Biophysica Acta (BBA)-Biomembranes* **2014***, 1838*, 2425-2430.)

The authors of the journal article "The action mechanism of Daptomycin," Dr. Scott Taylor and Dr. Michael Palmer, gave permission for Figure 1.5 to be used in this thesis. (Taylor, S.D.; Palmer, M. *Bioorganic Med. Chem.* **2016**, *24*, 6253–6268.)

The authors of the journal article "Daptomycin, a Bacterial Lipopeptide Synthesized by a Nonribosomal Machinery" Dr. Mohamed A. Marahiel, gave permission for Figure 1.6 to be used in this thesis. (Robbel, L.; Marahiel, M. A. *J. Biol. Chem.* **2010***, 285*, 27501-27508.)

Permission for Table 1.2:

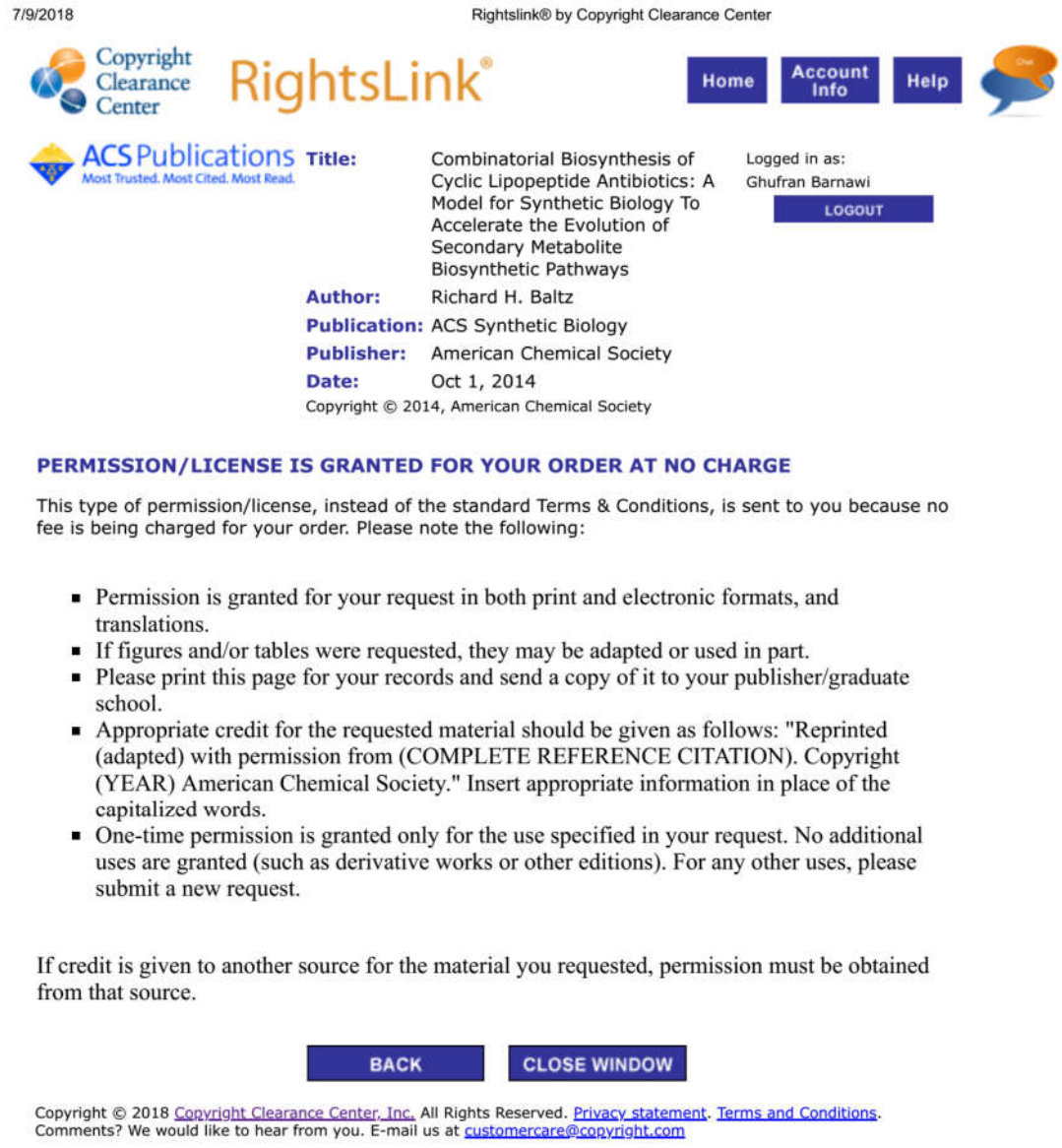

7/9/2018 Rightslink® by Copyright Clearance Center

Copyright Clearance Center RightsLink®

Home | Account Info | Help

ACS Publications Most Trusted. Most Cited. Most Read.

Title: Combinatorial Biosynthesis of Cyclic Lipopeptide Antibiotics: A Model for Synthetic Biology To Accelerate the Evolution of Secondary Metabolite Biosynthetic Pathways

Logged in as: Ghufran Barnawi

LOGOUT

Author: Richard H. Baltz

Publication: ACS Synthetic Biology

Publisher: American Chemical Society

Date: Oct 1, 2014

Copyright © 2014, American Chemical Society

PERMISSION/LICENSE IS GRANTED FOR YOUR ORDER AT NO CHARGE

This type of permission/license, instead of the standard Terms & Conditions, is sent to you because no fee is being charged for your order. Please note the following:

- Permission is granted for your request in both print and electronic formats, and translations.
- If figures and/or tables were requested, they may be adapted or used in part.
- Please print this page for your records and send a copy of it to your publisher/graduate school.
- Appropriate credit for the requested material should be given as follows: "Reprinted (adapted) with permission from (COMPLETE REFERENCE CITATION). Copyright (YEAR) American Chemical Society." Insert appropriate information in place of the capitalized words.
- One-time permission is granted only for the use specified in your request. No additional uses are granted (such as derivative works or other editions). For any other uses, please submit a new request.

If credit is given to another source for the material you requested, permission must be obtained from that source.

BACK CLOSE WINDOW

Copyright © 2018 Copyright Clearance Center, Inc. All Rights Reserved. Privacy statement. Terms and Conditions.
Comments? We would like to hear from you. E-mail us at customercare@copyright.com

References

1. Dougherty, T. J.; Pucci, M. J. *Antibiotic discovery and development; Springer Science & Business Media,* **2011**.

2. Strebhardt, K.; Ullrich, A. Paul Ehrlich's magic bullet concept: 100 years of progress. *Nature Reviews Cancer* **2008***, 8*, 473.

3. Voegtlin, C. The pharmacology of arsphenamine (salvarsan) and related arsenicals. *Physiol. Rev.* **1925***, 5*, 63-94.

4. Krafts, K.; Hempelmann, E.; Skórska-Stania, A. From methylene blue to chloroquine: a brief review of the development of an antimalarial therapy. *Parasitol. Res.* **2012***, 111*, 1-6.

5. Marshall, E. Historical perspectives in chemotherapy. *Adv. Chemother.* **1964***, 13*, 1-8.

6. Tampa, M.; Sarbu, I.; Matei, C.; Benea, V.; Georgescu, S. R. Brief history of syphilis. *J. Med. Life.* **2014***, 7*, 4-10.

7. Waksman, S. A. What is an antibiotic or an antibiotic substance? *Mycologia* **1947***, 39*, 565-569.

8. Chain, E. The early years of the penicillin discovery. *Trends Pharmacol. Sci.* **1979***, 1*, 6-11.

9. Bennett, J. W.; Chung, K. Alexander Fleming and the discovery of penicillin. **2001**.

10. Ligon, B. L. In *In Penicillin: its discovery and early development;* Seminars in pediatric infectious diseases; Elsevier: 2004; Vol. 15, pp 52-57.

11. Zetterström, R. Selman A. Waksman (1888–1973) Nobel Prize in 1952 for the discovery of streptomycin, the first antibiotic effective against tuberculosis. *Acta Paediatrica* **2007***, 96*, 317-319.

12. Lewis, K. Platforms for antibiotic discovery. *Nature reviews Drug discovery* **2013***, 12*, 371.

13. Schatz, A.; Bugie, E.; Waksman, S. A.; Hanssen, A. D.; Patel, R.; Osmon, D. R. The classic: streptomycin, a substance exhibiting antibiotic activity against Gram-positive and Gram-negative bacteria. *Clinical Orthopaedics and Related Research®* **2005***, 437*, 3-6.

14. Pelaez, F. The historical delivery of antibiotics from microbial natural products—can history repeat? *Biochem. Pharmacol.* **2006***, 71*, 981-990.

15. Aminov, R. I. A brief history of the antibiotic era: lessons learned and challenges for the future. *Frontiers in microbiology* **2010***, 1*, 134.

16. Zaffiri, L.; Gardner, J.; Toledo-Pereyra, L. H. History of antibiotics. From salvarsan to cephalosporins. *Journal of Investigative Surgery* **2012***, 25*, 67-77.

17. Maranan, M. C.; Moreira, B.; Boyle-Vavra, S.; Daum, R. S. Antimicrobial resistance in staphylococci. Epidemiology, molecular mechanisms, and clinical relevance. *Infect. Dis. Clin. North Am.* **1997***, 11*, 813-849.

18. Marchese, A.; Balistreri, G.; Tonoli, E.; Debbia, E. A.; Schito, G. C. Heterogeneous vancomycin resistance in methicillin-resistant Staphylococcus aureus strains isolated in a large Italian hospital. *J. Clin. Microbiol.* **2000***, 38*, 866-869.

19. Foster, T. J. The Staphylococcus aureus "superbug". *J. Clin. Invest.* **2004***, 114*, 1693-1696.

20. Jia, B.; Raphenya, A. R.; Alcock, B.; Waglechner, N.; Guo, P.; Tsang, K. K.; Lago, B. A.; Dave, B. M.; Pereira, S.; Sharma, A. N. CARD 2017: expansion and model-centric curation of the comprehensive antibiotic resistance database. *Nucleic Acids Res.* **2016**, gkw1004.

21. Debono, M.; Barnhart, M.; Carrell, C.; Hoffman, J.; Hamill, R. In A21978C, a complex of new acidic peptide antibiotics: factor definition and preliminary chemical characterization; Program and Abstracts of 20th Intersci. *Conference on Antimicrobial Agents and Chemtherapy*; **1980**.

22. Counter, F.; Ensminger, P.; Howard, L. In A21978C, a complex of new acidic peptide antibiotics: biological activity and toxicity*;* Program and Abstracts of 20th Intersci. *Conference on Antimicrobial Agents and Chemtherapy*; **1980**.

23. Eisenstein, B.; Oleson Jr, F.; Baltz, R. Clin Infect Dis 50 Suppl 1. *S10-15* **2010**.

24. Silverman, J. A.; Mortin, L. I.; VanPraagh, A. D.; Li, T.; Alder, J. Inhibition of daptomycin by pulmonary surfactant: in vitro modeling and clinical impact. *J. Infect. Dis.* **2005***, 191*, 2149-2152.

25. Debono, M.; Barnhart, M.; Carrell, C.; Hoffmann, J.; Occolowitz, J.; Abbott, B.; Fukuda, D.; Hamill, R.; Biemann, K.; Herlihy, W. A21978C, a complex of new acidic peptide antibiotics: isolation, chemistry, and mass spectral structure elucidation. *J. Antibiot.* **1987***, 40*, 761-777.

26. Taylor, S. D.; Palmer, M. The action mechanism of daptomycin. *Bioorg. Med. Chem.* **2016***, 24*, 6253-6268.

27. Canepari, P.; Boaretti, M.; Lleó, M. M.; Satta, G. Lipoteichoic acid as a new target for activity of antibiotics: mode of action of daptomycin (LY146032). *Antimicrob. Agents Chemother.* **1990***, 34*, 1220-1226.

28. Hachmann, A. B.; Angert, E. R.; Helmann, J. D. Genetic analysis of factors affecting susceptibility of Bacillus subtilis to daptomycin. *Antimicrob. Agents Chemother.* **2009***, 53*, 1598-1609.

29. Hachmann, A. B.; Sevim, E.; Gaballa, A.; Popham, D. L.; Antelmann, H.; Helmann, J. D. Reduction in membrane phosphatidylglycerol content leads to daptomycin resistance in Bacillus subtilis. *Antimicrob. Agents Chemother.* **2011***, 55*, 4326-4337.

30. Peleg, A. Y.; Miyakis, S.; Ward, D. V.; Earl, A. M.; Rubio, A.; Cameron, D. R.; Pillai, S.; Moellering Jr, R. C.; Eliopoulos, G. M. Whole genome characterization of the mechanisms of daptomycin resistance in clinical and laboratory derived isolates of Staphylococcus aureus. *PLoS One* **2012***, 7*, e28316.

31. Papahadjopoulos, D.; Poste, G.; Schaeffer, B. Fusion of mammalian cells by unilamellar lipid vesicles: influence of lipid surface charge, fluidity and cholesterol. *Biochimica et Biophysica Acta (BBA)-Biomembranes* **1973***, 323*, 23-42.

32. Lakey, J. H.; Ptak, M. Fluorescence indicates a calcium-dependent interaction between the lipopeptide antibiotic LY 146032 and phospholipid membranes. *Biochemistry (N. Y.)* **1988***, 27*, 4639-4645.

33. Jung, D.; Rozek, A.; Okon, M.; Hancock, R. E. Structural transitions as determinants of the action of the calcium-dependent antibiotic daptomycin. *Chem. Biol.* **2004***, 11*, 949-957.

34. Zhang, T.; Muraih, J. K.; Mintzer, E.; Tishbi, N.; Desert, C.; Silverman, J.; Taylor, S.; Palmer, M. Mutual inhibition through hybrid oligomer formation of daptomycin and the semisynthetic lipopeptide antibiotic CB-182,462. *Biochimica et Biophysica Acta (BBA)-Biomembranes* **2013***, 1828*, 302-308.

35. Lee, M.; Hung, W.; Hsieh, M.; Chen, H.; Chang, Y.; Huang, H. W. Molecular State of the Membrane-Active Antibiotic Daptomycin. *Biophys. J.* **2017***, 113*, 82-90.

36. Strieker, M.; Marahiel, M. A. The structural diversity of acidic lipopeptide antibiotics. *ChemBioChem* **2009***, 10*, 607-616.

37. Takagi, T.; Nemoto, T.; Konishi, K.; Yazawa, M.; Yagi, K. The amino acid sequence of the calmodulin obtained from sea anemone (Metridium senile) muscle. *Biochem. Biophys. Res. Commun.* **1980***, 96*, 377-381.

38. Grünewald, J.; Sieber, S. A.; Mahlert, C.; Linne, U.; Marahiel, M. A. Synthesis and derivatization of daptomycin: a chemoenzymatic route to acidic lipopeptide antibiotics. *J. Am. Chem. Soc.* **2004***, 126*, 17025-17031.

39. Jung, D.; Rozek, A.; Okon, M.; Hancock, R. E. Structural transitions as determinants of the action of the calcium-dependent antibiotic daptomycin. *Chem. Biol.* **2004***, 11*, 949-957.

40. Ball, L.; Goult, C. M.; Donarski, J. A.; Micklefield, J.; Ramesh, V. NMR structure determination and calcium binding effects of lipopeptide antibiotic daptomycin. *Organic & biomolecular chemistry* **2004***, 2*, 1872-1878.

41. Rotondi, K. S.; Gierasch, L. M. A well-defined amphipathic conformation for the calcium-free cyclic lipopeptide antibiotic, daptomycin, in aqueous solution. *Peptide Science: Original Research on Biomolecules* **2005***, 80*, 374-385.

42. Piazza, M. NMR Studies of Protein and Peptide Structure and Dynamics. *UWSpace* **2016**.

43. Allen, N. E.; Hobbs, J. N.; Alborn, W. E.,Jr Inhibition of peptidoglycan biosynthesis in gram-positive bacteria by LY146032. *Antimicrob. Agents Chemother.* **1987***, 31*, 1093-1099.

44. Silverman, J. A.; Perlmutter, N. G.; Shapiro, H. M. Correlation of daptomycin bactericidal activity and membrane depolarization in Staphylococcus aureus. *Antimicrob. Agents Chemother.* **2003***, 47*, 2538-2544.

45. Muraih, J. K.; Palmer, M. Estimation of the subunit stoichiometry of the membrane-associated daptomycin oligomer by FRET. *Biochimica et Biophysica Acta (BBA)-Biomembranes* **2012***, 1818*, 1642-1647.

46. Muraih, J. K.; Harris, J.; Taylor, S. D.; Palmer, M. Characterization of daptomycin oligomerization with perylene excimer fluorescence: stoichiometric binding of phosphatidylglycerol triggers oligomer formation. *Biochimica et Biophysica Acta (BBA)-Biomembranes* **2012***, 1818*, 673-678.

47. Zhang, T.; Muraih, J. K.; Tishbi, N.; Herskowitz, J.; Victor, R. L.; Silverman, J.; Uwumarenogie, S.; Taylor, S. D.; Palmer, M.; Mintzer, E. Cardiolipin prevents membrane translocation and permeabilization by daptomycin. *J. Biol. Chem.* **2014***, 289*, 11584-11591.

48. Zhang, T.; Muraih, J. K.; MacCormick, B.; Silverman, J.; Palmer, M. Daptomycin forms cation-and size-selective pores in model membranes. *Biochimica et Biophysica Acta (BBA)-Biomembranes* **2014***, 1838*, 2425-2430.

49. Clement, N. R.; Gould, J. M. Pyranine (8-hydroxy-1, 3, 6-pyrenetrisulfonate) as a probe of internal aqueous hydrogen ion concentration in phospholipid vesicles. *Biochemistry (N. Y.)* **1981***, 20*, 1534-1538.

50. Muller, A.; Wenzel, M.; Strahl, H.; Grein, F.; Saaki, T. N.; Kohl, B.; Siersma, T.; Bandow, J. E.; Sahl, H. G.; Schneider, T.; Hamoen, L. W. Daptomycin inhibits cell envelope synthesis by interfering with fluid membrane microdomains. *Proc. Natl. Acad. Sci. U. S. A.* **2016**.

51. Laganas, V.; Alder, J.; Silverman, J. A. In vitro bactericidal activities of daptomycin against Staphylococcus aureus and Enterococcus faecalis are not mediated by inhibition of lipoteichoic acid biosynthesis. *Antimicrob. Agents Chemother.* **2003***, 47*, 2682-2684.

52. Wolf, D.; Dominguez-Cuevas, P.; Daniel, R. A.; Mascher, T. Cell envelope stress response in cell wall-deficient L-forms of Bacillus subtilis. *Antimicrob. Agents Chemother.* **2012***, 56*, 5907-5915.

53. Knight-Connoni, V.; Mascio, C.; Chesnel, L.; Silverman, J. Discovery and development of surotomycin for the treatment of Clostridium difficile. *J. Ind. Microbiol. Biotechnol.* **2016***, 43*, 195-204.

54. Mascio, C. T.; Chesnel, L.; Thorne, G.; Silverman, J. A. Surotomycin demonstrates low in vitro frequency of resistance and rapid bactericidal activity in Clostridium difficile, Enterococcus faecalis, and Enterococcus faecium. *Antimicrob. Agents Chemother.* **2014***, 58*, 3976-3982.

55. Hill, J.; Siedlecki, J.; Parr, I.; Morytko, M.; Yu, X.; Zhang, Y.; Silverman, J.; Controneo, N.; Laganas, V.; Li, T. Synthesis and biological activity of N-acylated ornithine analogues of daptomycin. *Bioorg. Med. Chem. Lett.* **2003***, 13*, 4187-4191.

56. Siedlecki, J.; Hill, J.; Parr, I.; Yu, X.; Morytko, M.; Zhang, Y.; Silverman, J.; Controneo, N.; Laganas, V.; Li, T. Array synthesis of novel lipodepsipeptide. *Bioorg. Med. Chem. Lett.* **2003***, 13*, 4245-4249.

57. He, Y.; Li, J.; Yin, N.; Herradura, P. S.; Martel, L.; Zhang, Y.; Pearson, A. L.; Kulkarni, V.; Mascio, C.; Howland, K. Reduced pulmonary surfactant interaction of daptomycin analogs via tryptophan replacement with alternative amino acids. *Bioorg. Med. Chem. Lett.* **2012***, 22*, 6248-6251.

58. Grunewald, J.; Marahiel, M. A. Chemoenzymatic and template-directed synthesis of bioactive macrocyclic peptides. *Microbiol. Mol. Biol. Rev.* **2006***, 70*, 121-146.

59. Baltz, R. H. Combinatorial biosynthesis of cyclic lipopeptide antibiotics: a model for synthetic biology to accelerate the evolution of secondary metabolite biosynthetic pathways. *ACS synthetic biology* **2012***, 3*, 748-758.

60. Baltz, R. H. Daptomycin: mechanisms of action and resistance, and biosynthetic engineering. *Curr. Opin. Chem. Biol.* **2009***, 13*, 144-151.

61. Robbel, L.; Marahiel, M. A. Daptomycin, a bacterial lipopeptide synthesized by a nonribosomal machinery. *J. Biol. Chem.* **2010***, 285*, 27501-27508.

62. Nguyen, K. T.; Ritz, D.; Gu, J. Q.; Alexander, D.; Chu, M.; Miao, V.; Brian, P.; Baltz, R. H. Combinatorial biosynthesis of novel antibiotics related to daptomycin. *Proc. Natl. Acad. Sci. U. S. A.* **2006***, 103*, 17462-17467.

63. Nguyen, K. T.; He, X.; Alexander, D. C.; Li, C.; Gu, J. Q.; Mascio, C.; Van Praagh, A.; Mortin, L.; Chu, M.; Silverman, J. A.; Brian, P.; Baltz, R. H. Genetically engineered lipopeptide antibiotics related to A54145 and daptomycin with improved properties. *Antimicrob. Agents Chemother.* **2010***, 54*, 1404-1413.

64. Lam, H. Y.; Zhang, Y.; Liu, H.; Xu, J.; Wong, C. T.; Xu, C.; Li, X. Total synthesis of daptomycin by cyclization via a chemoselective serine ligation. *J. Am. Chem. Soc.* **2013***, 135*, 6272-6279.

65. Laurens, H.; Bruin, G. A combined solid-and solution-phase approach provides convenient access to analogues of the calcium-dependent lipopeptide antibiotics. *Organic & biomolecular chemistry* **2014***, 12*, 913-918.

66. Lohani, C. R.; Taylor, R.; Palmer, M.; Taylor, S. D. Solid-phase total synthesis of daptomycin and analogs. *Org. Lett.* **2015***, 17*, 748-751.

67. Lohani, C. R.; Taylor, R.; Palmer, M.; Taylor, S. D. Solid-phase synthesis and in vitro biological activity of a Thr4→ Ser4 analog of daptomycin. *Bioorg. Med. Chem. Lett.* **2015***, 25*, 5490-5494.

68. Lohani, C. R.; Rasera, B.; Scott, B.; Palmer, M.; Taylor, S. D. α-Azido Acids in Solid-Phase Peptide Synthesis: Compatibility with Fmoc Chemistry and an Alternative Approach to the Solid Phase Synthesis of Daptomycin Analogs. *J. Org. Chem.* **2016***, 81*, 2624-2628.

69. Taylor, S. D.; Lohani, C. R. A Fresh Look at the Staudinger Reaction on Azido Esters: Formation of 2 H-1, 2, 3-Triazol-4-ols from α-Azido Esters Using Trialkyl Phosphines. *Org. Lett.* **2016***, 18*, 4412-4415.

70. Mishra, N. N.; McKinnell, J.; Yeaman, M. R.; Rubio, A.; Nast, C. C.; Chen, L.; Kreiswirth, B. N.; Bayer, A. S. In vitro cross-resistance to daptomycin and host defense cationic antimicrobial peptides in clinical methicillin-resistant Staphylococcus aureus isolates. *Antimicrob. Agents Chemother.* **2011***, 55*, 4012-4018.

71. Mishra, N. N.; Bayer, A. S. Correlation of cell membrane lipid profiles with daptomycin resistance in methicillin-resistant Staphylococcus aureus. *Antimicrob. Agents Chemother.* **2013***, 57*, 1082-1085.

72. Tran, T. T.; Munita, J. M.; Arias, C. A. Mechanisms of drug resistance: daptomycin resistance. *Ann. N. Y. Acad. Sci.* **2015***, 1354*, 32-53.

73. Tran, T. T.; Panesso, D.; Gao, H.; Roh, J. H.; Munita, J. M.; Reyes, J.; Diaz, L.; Lobos, E. A.; Shamoo, Y.; Mishra, N. N.; Bayer, A. S.; Murray, B. E.; Weinstock, G. M.; Arias, C. A. Whole-genome analysis of a daptomycin-susceptible enterococcus faecium strain and its daptomycin-resistant variant arising during therapy. *Antimicrob. Agents Chemother.* **2013***, 57*, 261-268.

74. Fukushima, T.; Szurmant, H.; Kim, E.; Perego, M.; Hoch, J. A. A sensor histidine kinase co-ordinates cell wall architecture with cell division in Bacillus subtilis. *Mol. Microbiol.* **2008***, 69*, 621-632.

75. Sathappa, M.; Alder, N. N. The ionization properties of cardiolipin and its variants in model bilayers. *Biochimica et Biophysica Acta (BBA)-Biomembranes* **2016***, 1858*, 1362-1372.

76. Wecke, T.; Zuhlke, D.; Mader, U.; Jordan, S.; Voigt, B.; Pelzer, S.; Labischinski, H.; Homuth, G.; Hecker, M.; Mascher, T. Daptomycin versus Friulimicin B: in-depth profiling of Bacillus subtilis cell envelope stress responses. *Antimicrob. Agents Chemother.* **2009***, 53*, 1619-1623.

77. Arias, C. A.; Panesso, D.; McGrath, D. M.; Qin, X.; Mojica, M. F.; Miller, C.; Diaz, L.; Tran, T. T.; Rincon, S.; Barbu, E. M. Genetic basis for in vivo daptomycin resistance in enterococci. *N. Engl. J. Med.* **2011***, 365*, 892-900.

78. D'Costa, V. M.; Mukhtar, T. A.; Patel, T.; Koteva, K.; Waglechner, N.; Hughes, D. W.; Wright, G. D.; De Pascale, G. Inactivation of the lipopeptide antibiotic daptomycin by hydrolytic mechanisms. *Antimicrob. Agents Chemother.* **2012***, 56*, 757-764.

79. Bertsche, U.; Weidenmaier, C.; Kuehner, D.; Yang, S. J.; Baur, S.; Wanner, S.; Francois, P.; Schrenzel, J.; Yeaman, M. R.; Bayer, A. S. Correlation of daptomycin resistance in a clinical Staphylococcus aureus strain with increased cell wall teichoic acid production and D-alanylation. *Antimicrob. Agents Chemother.* **2011***, 55*, 3922-3928.

80. Bertsche, U.; Yang, S.; Kuehner, D.; Wanner, S.; Mishra, N. N.; Roth, T.; Nega, M.; Schneider, A.; Mayer, C.; Grau, T. Increased cell wall teichoic acid production and D-alanylation are common phenotypes among daptomycin-resistant methicillin-resistant Staphylococcus aureus (MRSA) clinical isolates. *PLoS One* **2013***, 8*, e67398.

81. Mishra, N. N.; Bayer, A. S.; Weidenmaier, C.; Grau, T.; Wanner, S.; Stefani, S.; Cafiso, V.; Bertuccio, T.; Yeaman, M. R.; Nast, C. C. Phenotypic and genotypic characterization of daptomycin-resistant methicillin-resistant Staphylococcus aureus strains: relative roles of mprF and dlt operons. *PLoS One* **2014***, 9*, e107426.

82. Fischer, A.; Yang, S.; Bayer, A. S.; Vaezzadeh, A. R.; Herzig, S.; Stenz, L.; Girard, M.; Sakoulas, G.; Scherl, A.; Yeaman, M. R. Daptomycin resistance mechanisms in clinically derived Staphylococcus aureus strains assessed by a combined transcriptomics and proteomics approach. *J. Antimicrob. Chemother.* **2011***, 66*, 1696-1711.

83. Kanazawa, K.; Sato, Y.; Ohki, K.; Okimura, K.; Uchida, Y.; Shindo, M.; Sakura, N. Contribution of each amino acid residue in polymyxin B3 to antimicrobial and lipopolysaccharide binding activity. *Chemical and Pharmaceutical Bulletin* **2009***, 57*, 240-244.

84. Wavreille, A.; Garaud, M.; Zhang, Y.; Pei, D. Defining SH2 domain and PTP specificity by screening combinatorial peptide libraries. *Methods* **2007***, 42*, 207-219.

85. Muraih, J. K.; Pearson, A.; Silverman, J.; Palmer, M. Oligomerization of daptomycin on membranes. *Biochimica et Biophysica Acta (BBA)-Biomembranes* **2011***, 1808*, 1154-1160.

86. Thakkar, A.; Trinh, T. B.; Pei, D. Global analysis of peptide cyclization efficiency. *ACS combinatorial science* **2013***, 15*, 120-129.

87. Barnawi, G.; Noden, M.; Taylor, R.; Lohani, C.; Beriashvili, D.; Palmer, M.; Taylor, S. D. An entirely fmoc solid phase approach to the synthesis of daptomycin analogs. *Peptide Science* **2018**.

88. Miao, V.; Coeffet-LeGal, M.; Brian, P.; Brost, R.; Penn, J.; Whiting, A.; Martin, S.; Ford, R.; Parr, I.; Bouchard, M. Daptomycin biosynthesis in Streptomyces roseosporus: cloning and analysis of the gene cluster and revision of peptide stereochemistry. *Microbiology* **2005***, 151*, 1507-1523.

89. Taylor, R.; Butt, K.; Scott, B.; Zhang, T.; Muraih, J. K.; Mintzer, E.; Taylor, S.; Palmer, M. Two successive calcium-dependent transitions mediate membrane binding and oligomerization of daptomycin and the related antibiotic A54145. *Biochimica et Biophysica Acta (BBA)-Biomembranes* **2016***, 1858*, 1999-2005.

Appendix A

HPLC Chromatograms and ESI$^+$ Mass spectra of Dap Alanine Analogs

Analytical HPLC gradient: 90% Acetonitrile and 10% H_2O (0.1% TFA) to 10% Acetonitrile and 90% H_2O (0.1% TFA) in over 50 min.

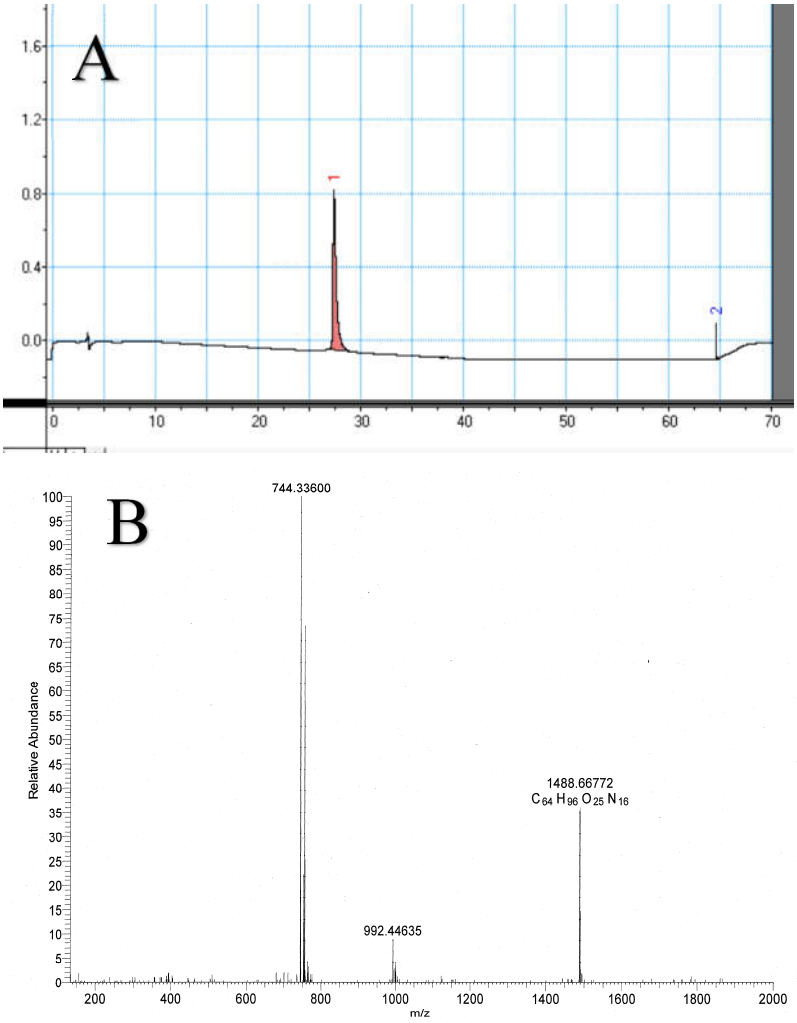

Figure A.1 (A) Analytical HPLC chromatogram of purified Dap-A1-E12-W13. (B) HRMS of purified Dap-A1-E12-W13, peak at *m/z* = 1488.66772 corresponds to $[M+H]^{2+}$ and *m/z* = 744.33600 corresponds to $[M+2H]^{2+}$.

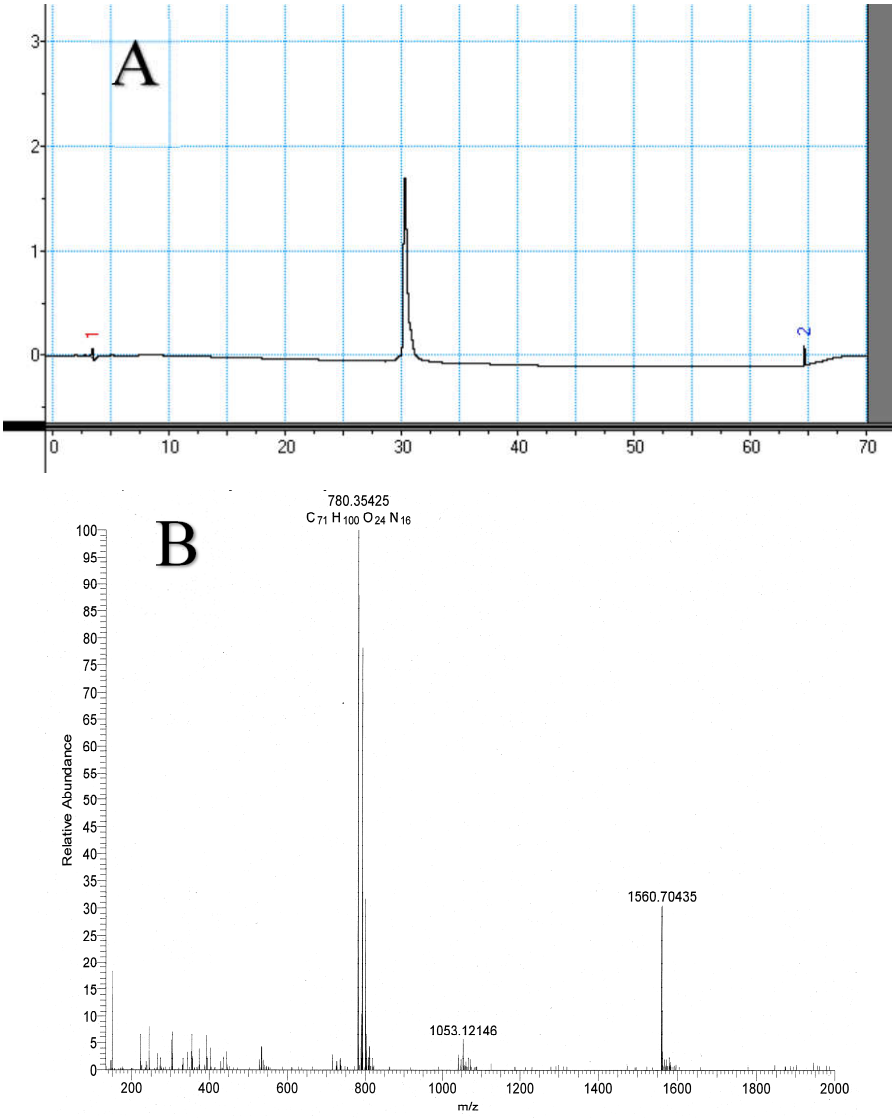

Figure A.2. (A) Analytical HPLC chromatogram of purified Dap-A2-E12-W13. (B) HRMS of purified Dap-A2-E12-W13, peak at *m/z* = 1560.7043 corresponds to $[M+H]^{2+}$ and *m/z* = 780.35425 corresponds to $[M+2H]^{2+}$.

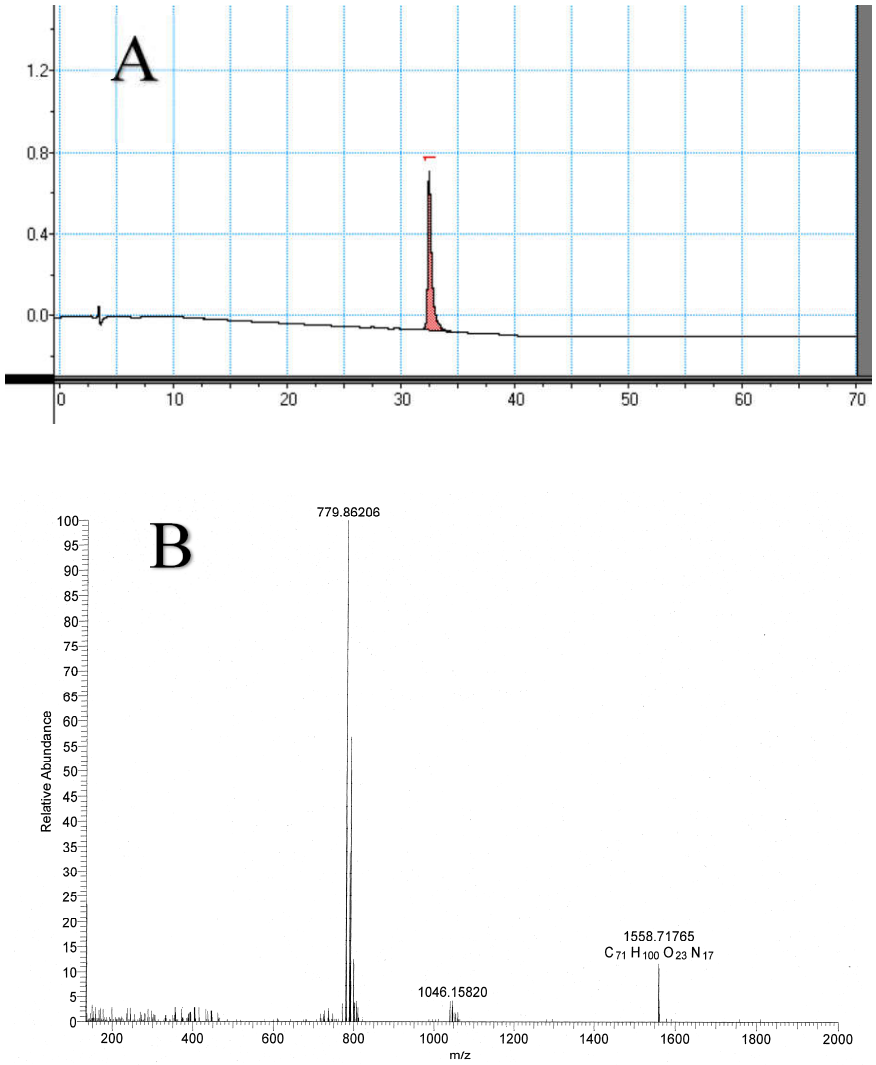

Figure A.3. (A) Analytical HPLC chromatogram of purified Dap-A3-E12-W13. (B) HRMS of purified Dap-A3-E12-W13, peak at *m/z* = 1558.71765 corresponds to $[M+H]^{2+}$ and *m/z* = 779.86206 corresponds to $[M+2H]^{2+}$.

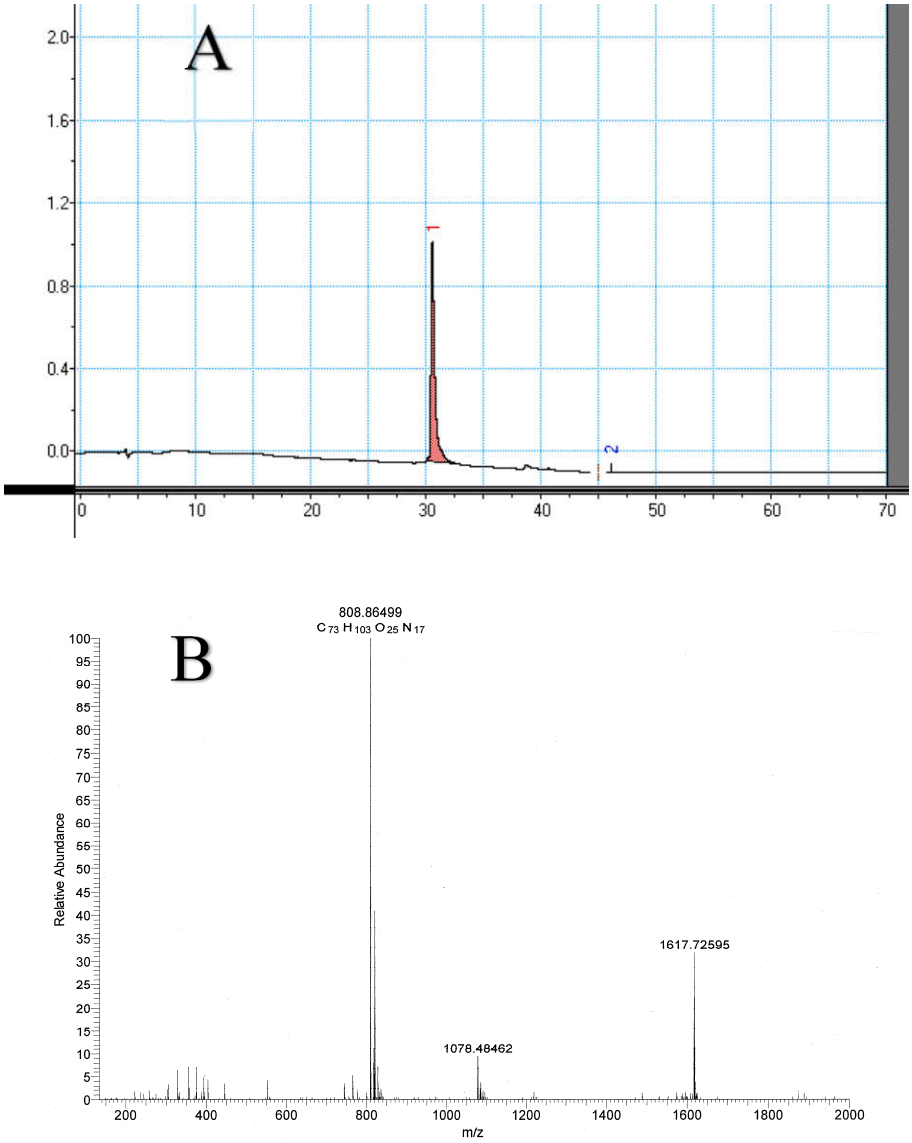

Figure A.4. (A) Analytical HPLC chromatogram of purified Dap-A5-E12-W13. (B) HRMS of purified Dap-A5-E12-W13, peak at *m/z* = 1617.72595 corresponds to $[M+H]^{2+}$ and *m/z* = 808.86499 corresponds to $[M+2H]^{2+}$.

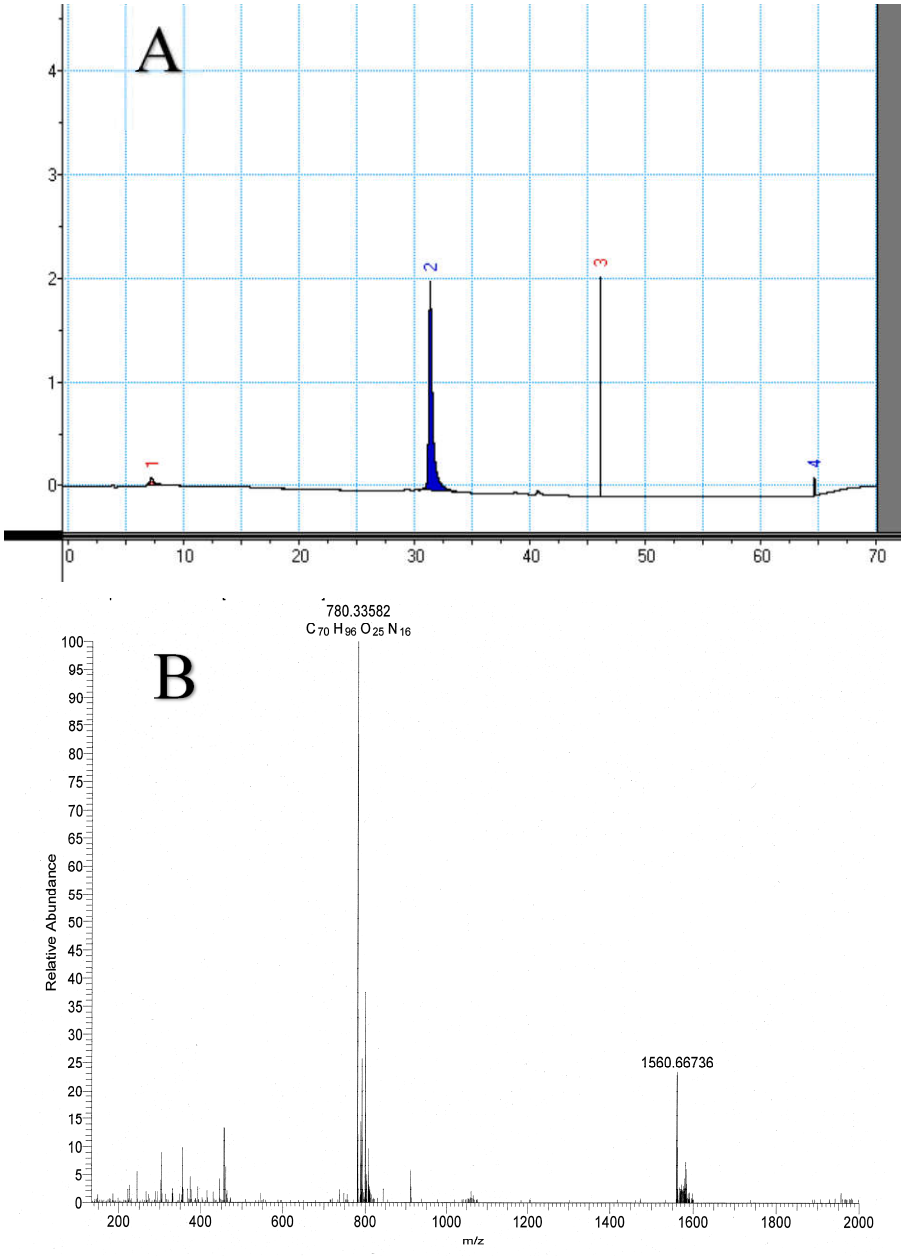

Figure A.5. (A) Analytical HPLC chromatogram of purified Dap-A6-E12-W13. (B) HRMS of purified Dap-A6-E12-W13, peak at *m/z* = 1560.66736 corresponds to $[M+H]^{2+}$ and *m/z* = 1560.66736 corresponds to $[M+2H]^{2+}$.

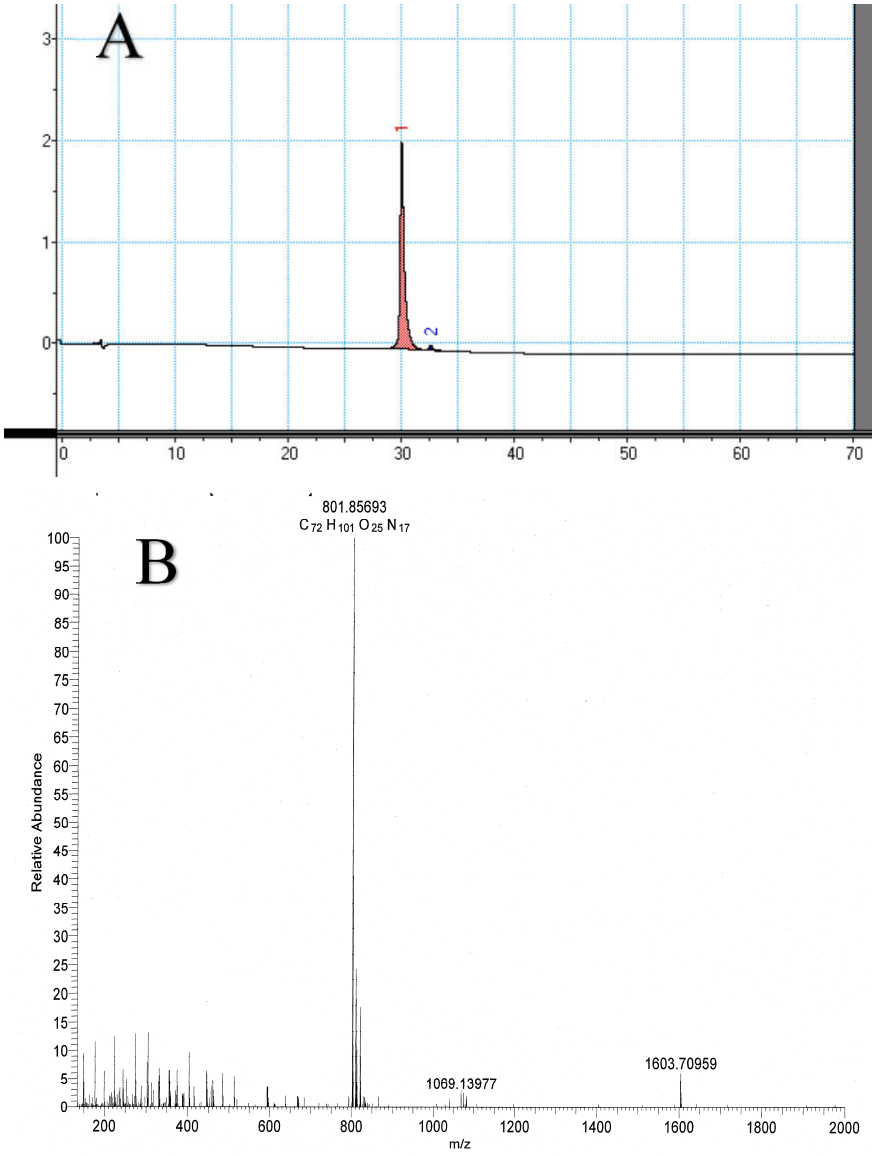

Figure A.6. (A) Analytical HPLC chromatogram of purified Dap-A8-E12-W13. (B) HRMS of purified Dap-A8-E12-W13, peak at *m/z* = 1603.709 corresponds to $[M+H]^{2+}$ and *m/z* = 801.85693 corresponds to $[M+2H]^{2+}$.

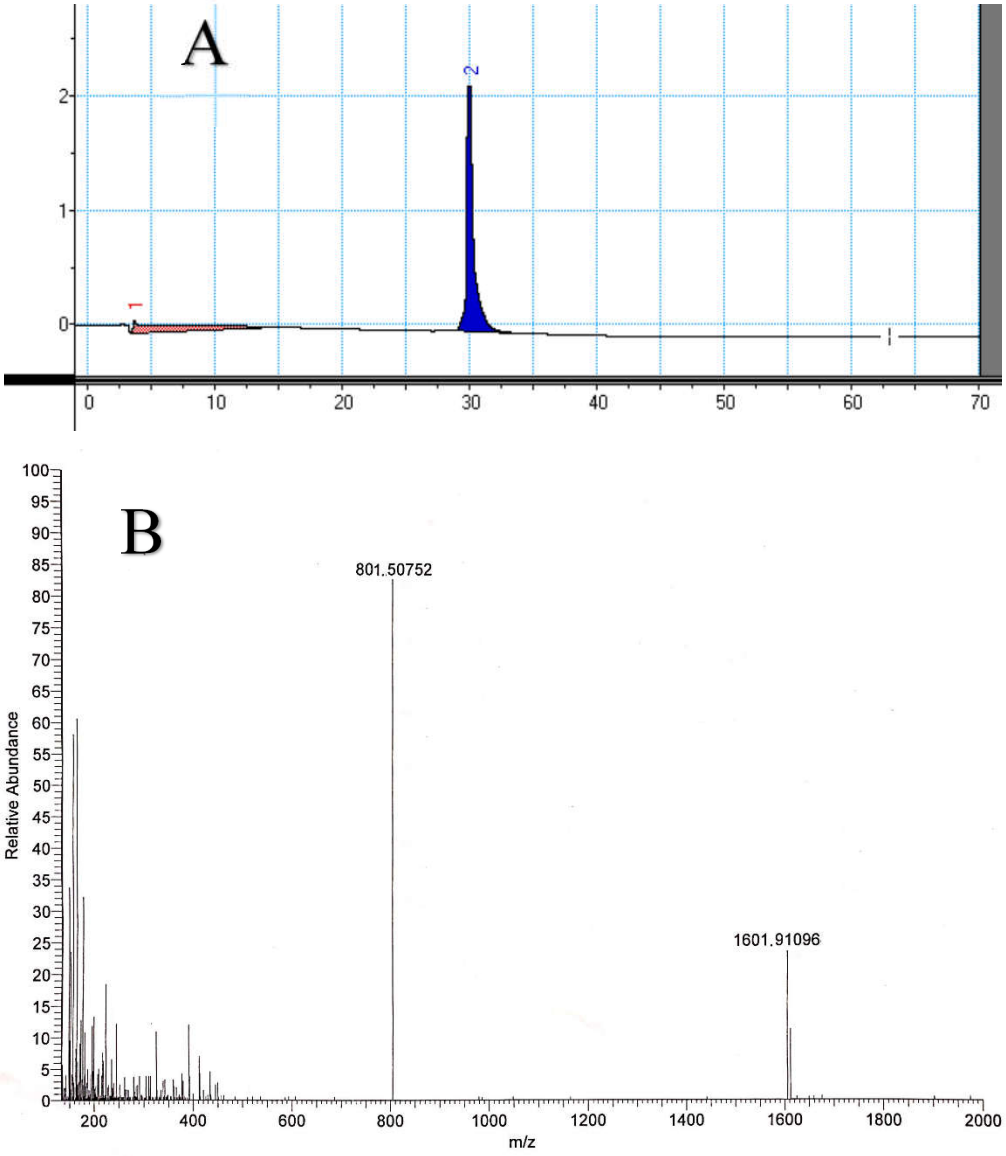

Figure A.7. (A) Analytical HPLC chromatogram of purified Dap–N9-E12-W13. (B) HRMS of purified Dap-N9-E12-W13, peak at *m/z* = 1601.91096 corresponds to $[M+H]^{2+}$ and *m/z* = 801.50752 corresponds to $[M+2H]^{2+}$.

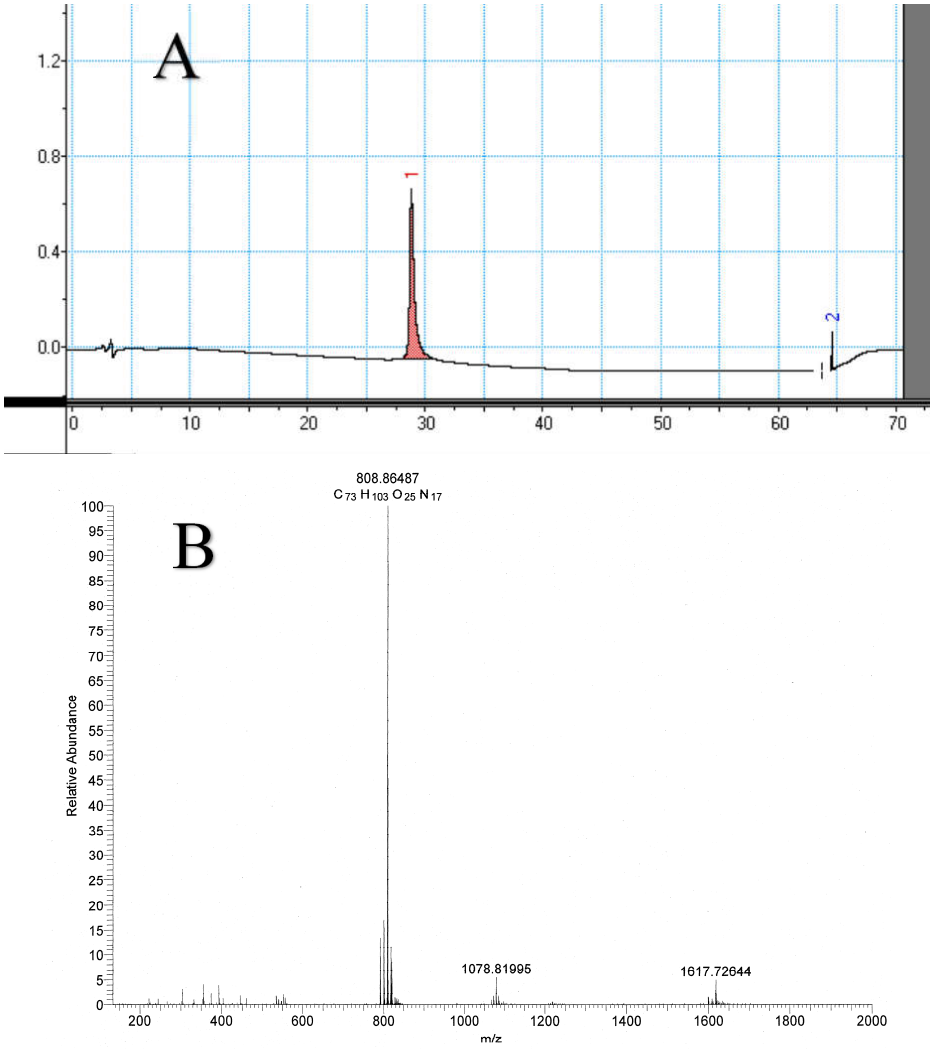

Figure A.8. (A) Analytical HPLC chromatogram of purified Dap -A10-E12-W13. (B) HRMS of purified Dap-A10-E12-W13, peak at *m/z* = 1617.72 corresponds to $[M+H]^{2+}$ and *m/z* = 808.86487 corresponds to $[M+2H]^{2+}$.

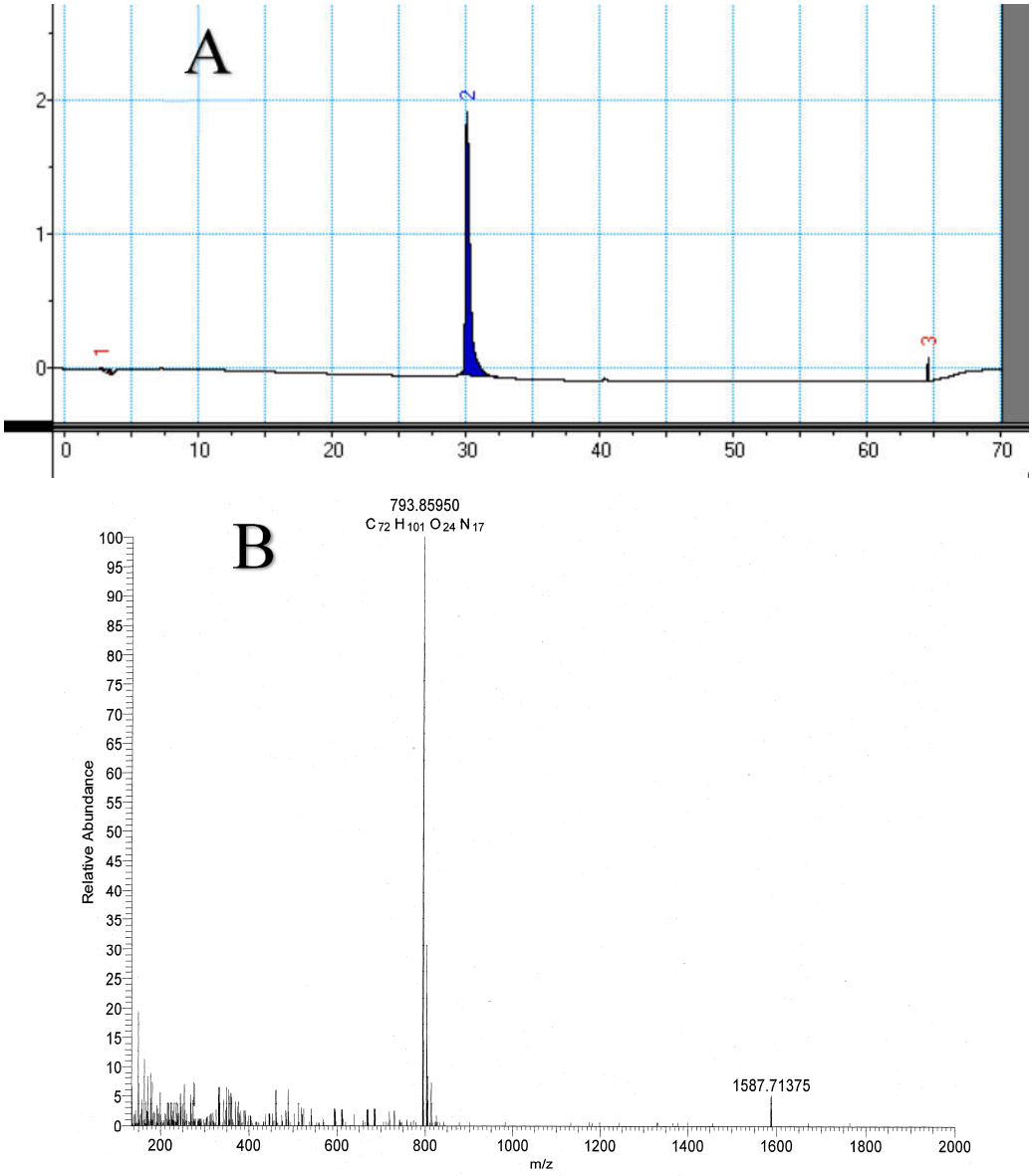

Figure A.9. (A) Analytical HPLC chromatogram of purified Dap -A11-E12-W13. (B) HRMS of purified Dap-A11-E12-W13, peak at *m/z* = 1587.713 corresponds to $[M+H]^{2+}$ and *m/z* = 793.85950 corresponds to $[M+2H]^{2+}$.

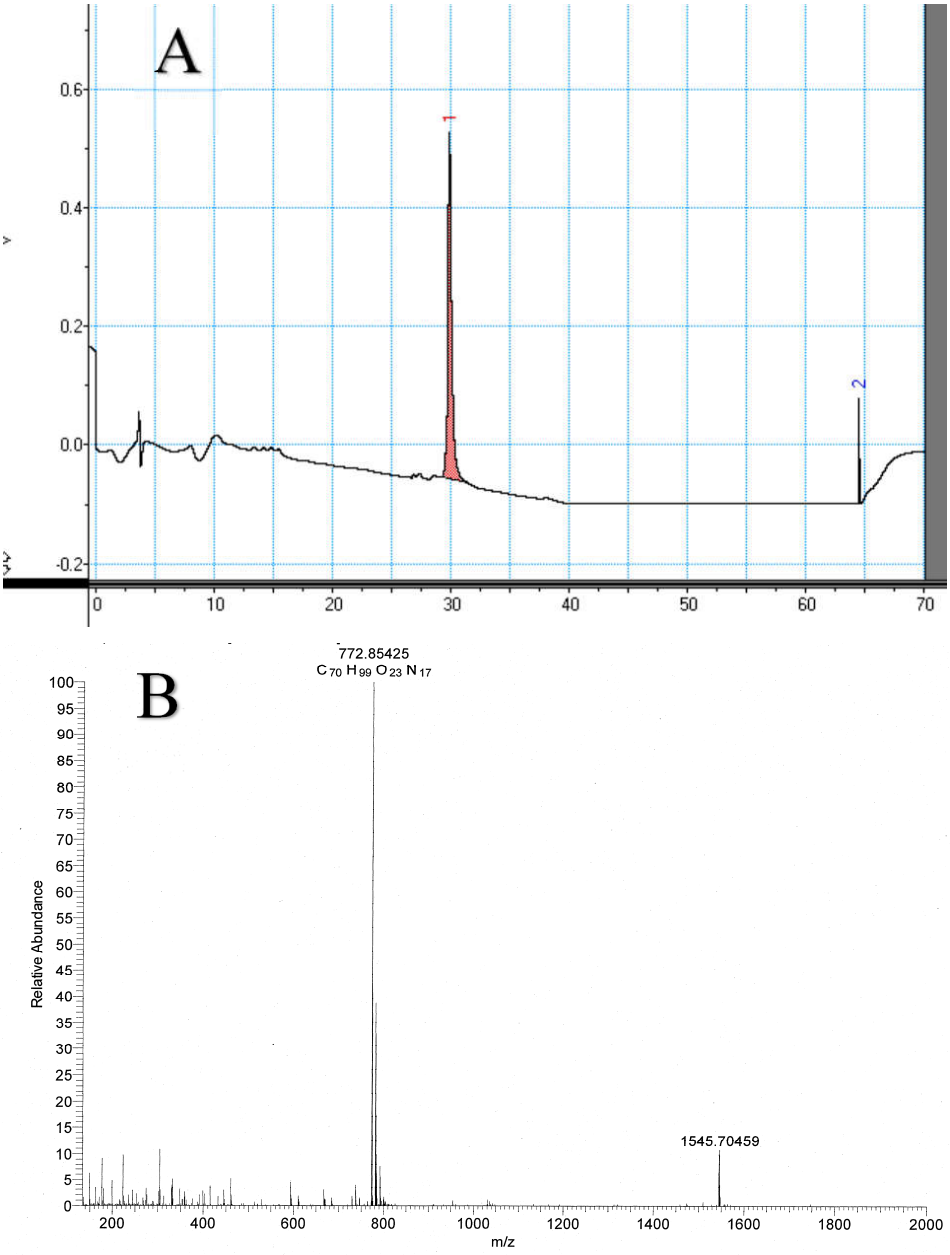

Figure A.10. (A) Analytical HPLC chromatogram of purified Dap-A12-W13. (B) HRMS of purified Dap-A12-W13, peak at *m/z* = 1545.7054 corresponds to $[M+H]^{2+}$ and *m/z* = 772.85425 corresponds to $[M+2H]^{2+}$.

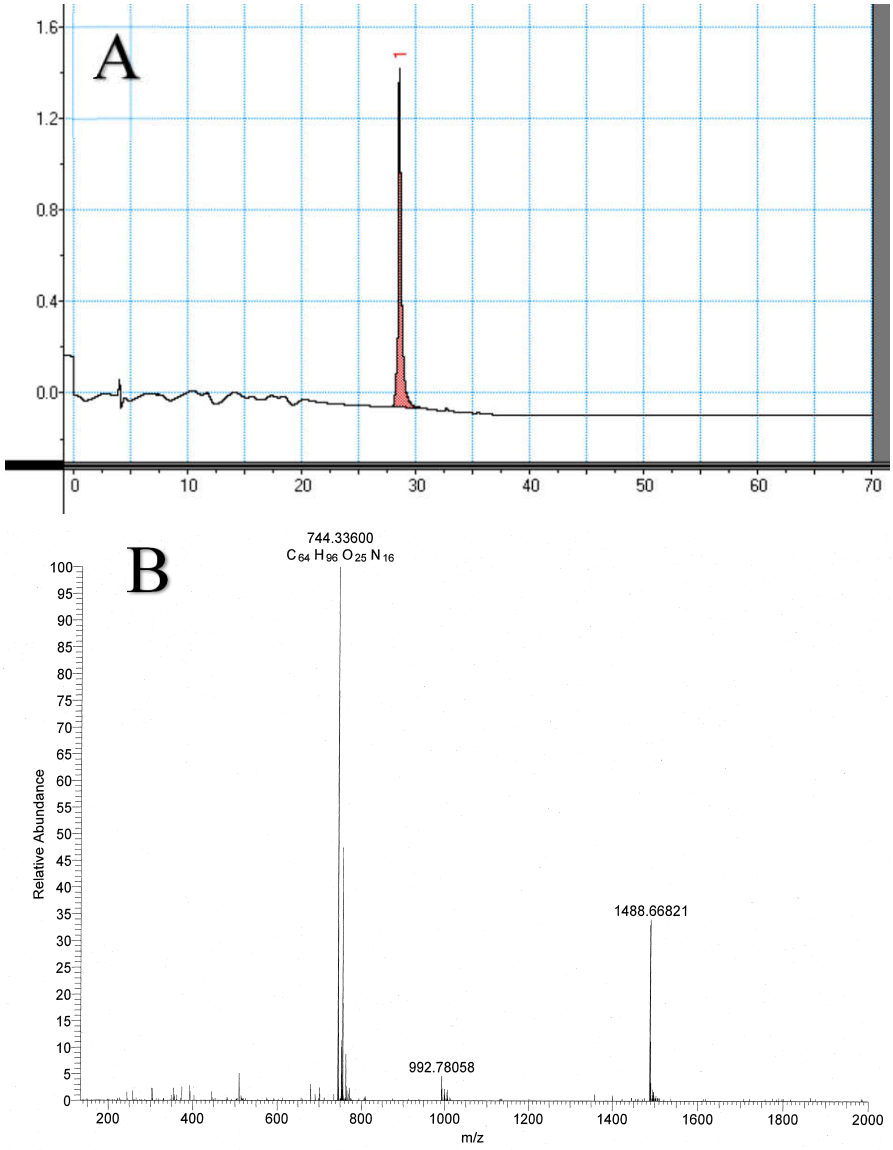

Figure A.11. (A) Analytical HPLC chromatogram of purified Dap-A13-E12. (B) HRMS of purified Dap-A13-E12, peak at *m/z* = 1488.66821 corresponds to $[M+H]^{2+}$ and *m/z* = 744.33600 corresponds to $[M+2H]^{2+}$.

Appendix B

Membrane Binding Curves of Dap Alanine Analogs

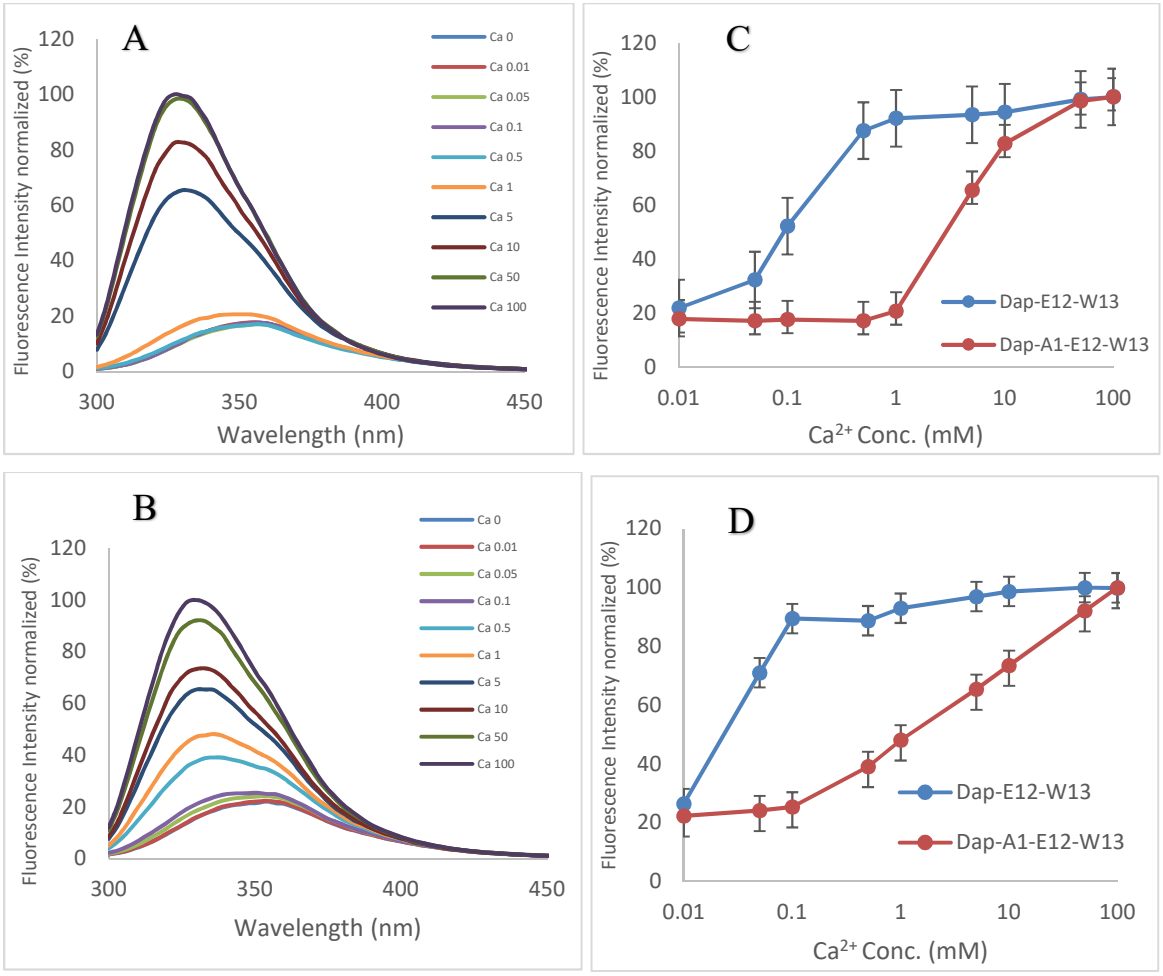

Figure B.1 Fluorescence spectra of Dap-A1-E12-W13 in the presence of *(A)* DMPC/DMPG (1:1) liposomes, *(B)* DOPC/DOPG (1:1) liposomes with increasing Ca^{2+} concentration (mM) at 37 °C. *(C)* and *(D)*: MBCs of Dap-A1-E12-W13 and Dap-E12-W13 on DMPC/DMPC and DOPC/DOPG liposomes. Error bars represent the standard deviation of three different experiments.

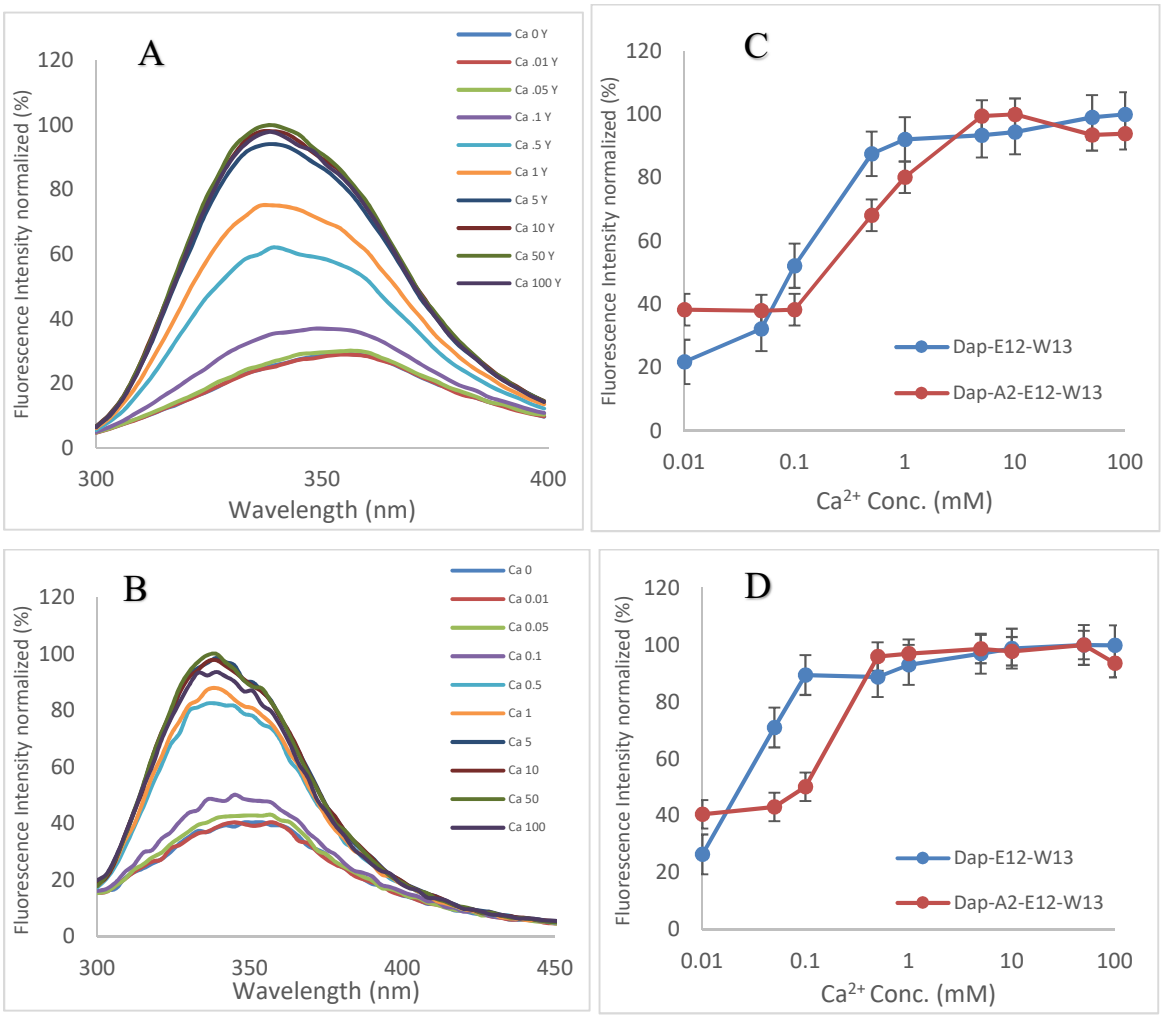

Figure B.2. Fluorescence spectra of Dap-A2-E12-W13 in the presence of *(A)* DMPC/DMPG (1:1) liposomes, *(B)* DOPC/DOPG (1:1) liposomes with increasing Ca^{2+} concentration (mM) at 37 °C. *(C)* and *(D)*: MBCs of Dap-A2-E12-W13 and Dap-E12-W13 on DMPC/DMPC and DOPC/DOPG liposomes. Error bars represent the standard deviation of three different experiments.

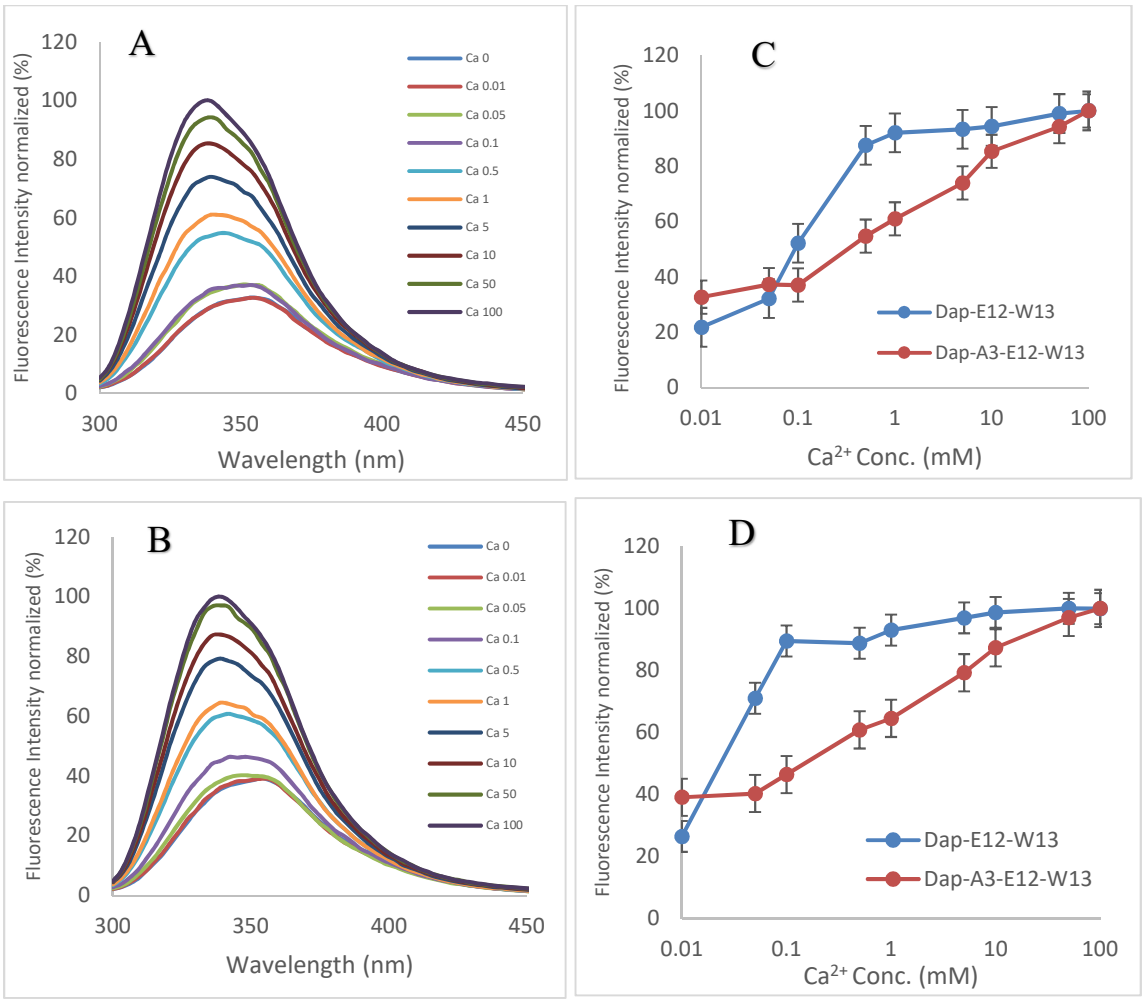

Figure B.3. Fluorescence spectra of Dap-A3-E12-W13 in the presence of *(A)* DMPC/DMPG (1:1) liposomes, *(B)* DOPC/DOPG (1:1) liposomes with increasing Ca^{2+} concentration (mM) at 37 °C. *(C)* and *(D)*: MBCs of Dap-A3-E12-W13 and Dap-E12-W13 on DMPC/DMPC and DOPC/DOPG liposomes. Error bars represent the standard deviation of three different experiments.

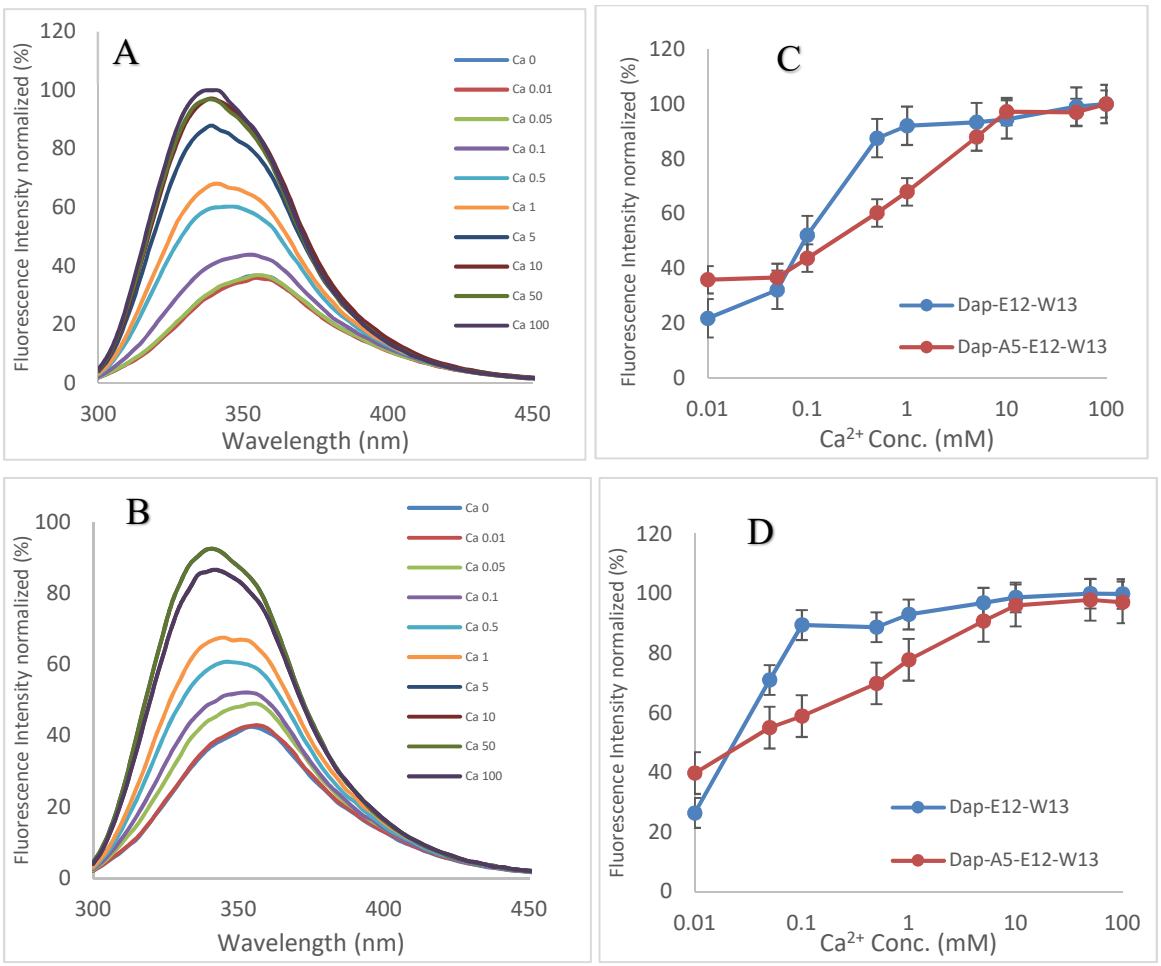

Figure B.4. Fluorescence spectra of Dap-A5-E12-W13 in the presence of *(A)* DMPC/DMPG (1:1) liposomes, *(B)* DOPC/DOPG (1:1) liposomes with increasing Ca^{2+} concentration (mM) at 37 °C. *(C)* and *(D)*: MBCs of Dap-A5-E12-W13 and Dap-E12-W13 on DMPC/DMPC and DOPC/DOPG liposomes. Error bars represent the standard deviation of three different experiments.

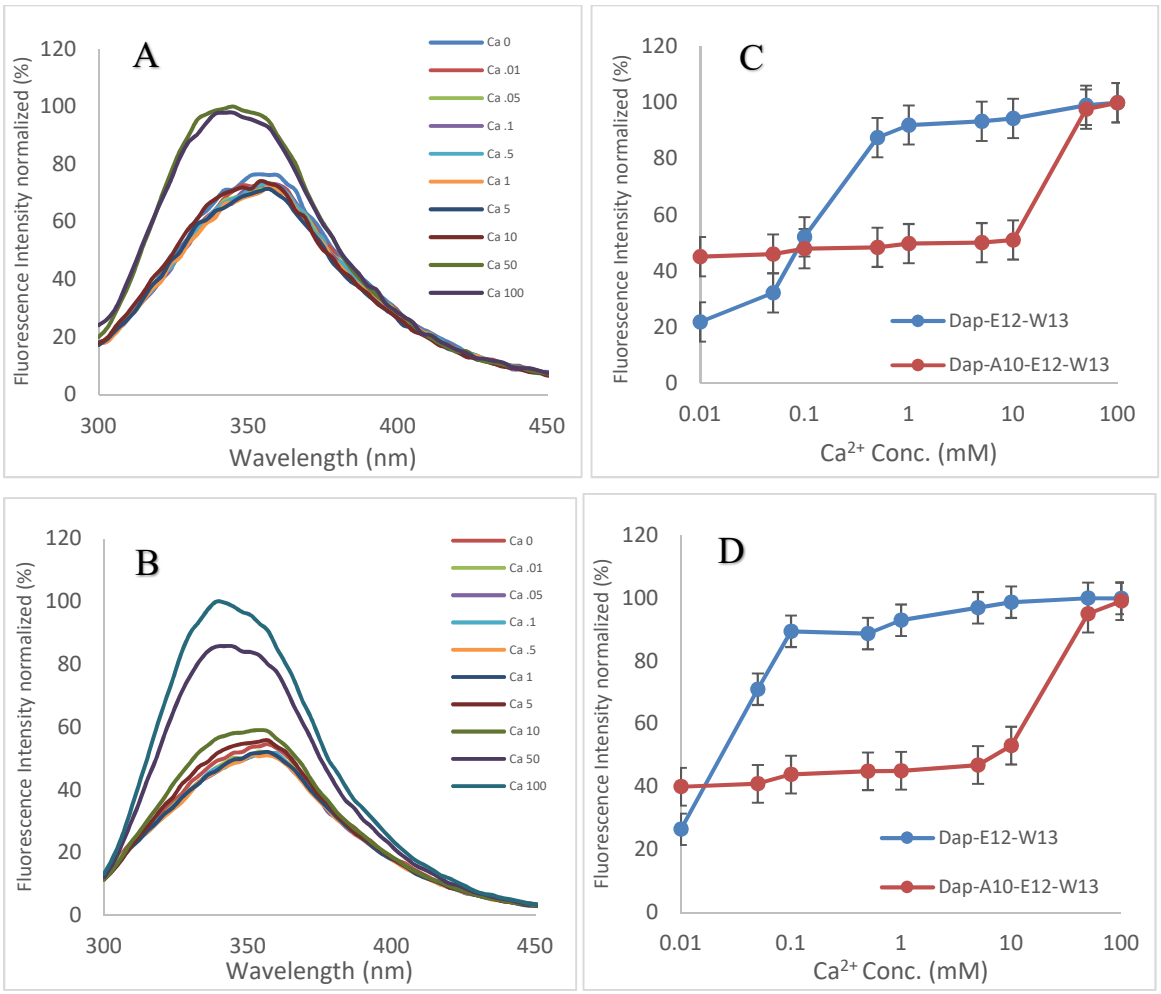

Figure B.5. Fluorescence spectra of Dap-A10-E12-W13 in the presence of *(A)* DMPC/DMPG (1:1) liposomes, *(B)* DOPC/DOPG (1:1) liposomes with increasing Ca^{2+} concentration (mM) at 37 °C. *(C)* and *(D)*: MBCs of Dap-A10-E12-W13 and Dap-E12-W13 on DMPC/DMPC and DOPC/DOPG liposomes. Error bars represent the standard deviation of three different experiments.

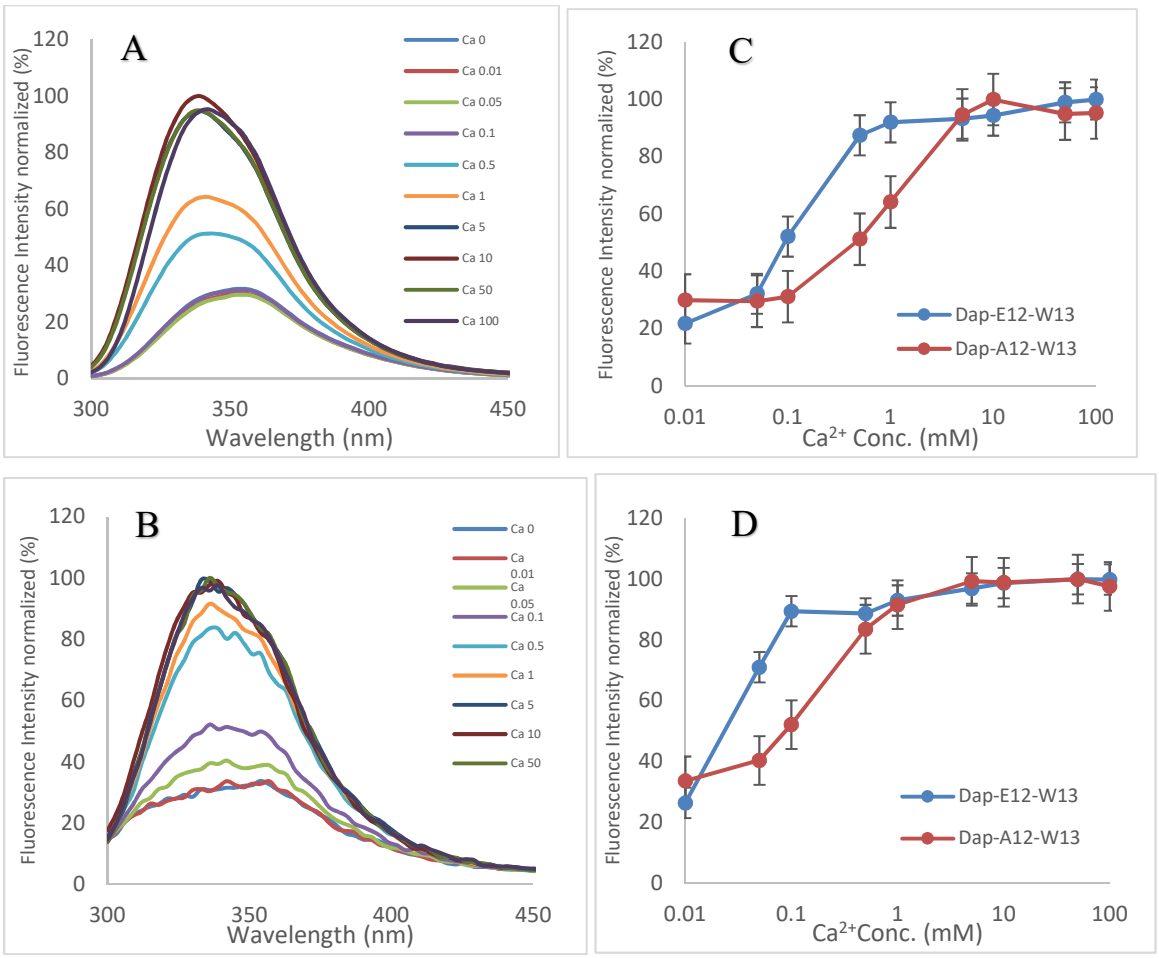

Figure B.6. Fluorescence spectra of Dap-A12-W13 in the presence of *(A)* DMPC/DMPG (1:1) liposomes, *(B)* DOPC/DOPG (1:1) liposomes with increasing Ca^{2+} concentration (mM) at 37 °C. *(C)* and *(D)*: MBCs of Dap-A12-W13 and Dap-E12-W13 on DMPC/DMPC and DOPC/DOPG liposomes. Error bars represent the standard deviation of three different experiments.

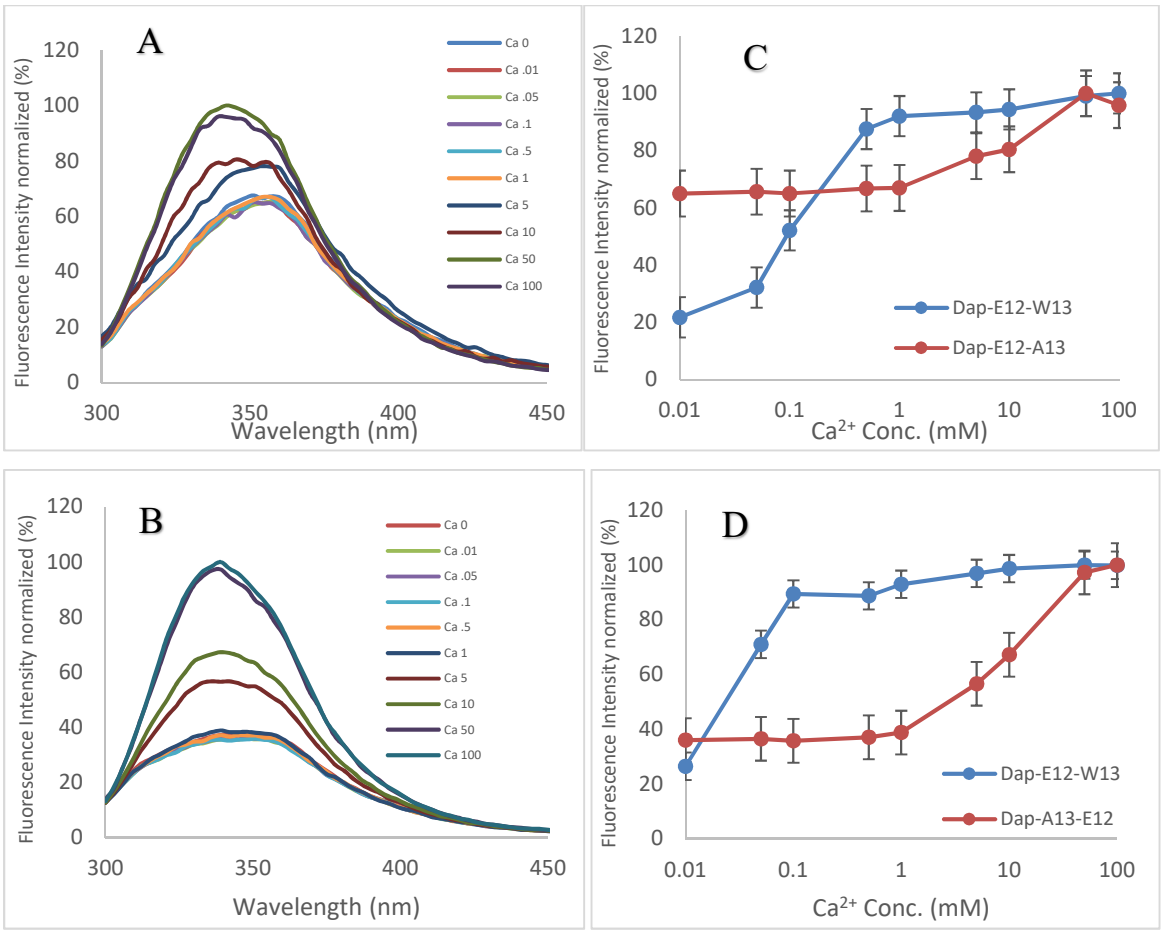

Figure B.7. Fluorescence spectra of Da-E12-A13 in the presence of *(A)* DMPC/DMPG (1:1) liposomes, *(B)* DOPC/DOPG (1:1) liposomes with increasing Ca^{2+} concentration (mM) at 37 °C. *(C)* and *(D)*: MBCs of Dap-E12-A13 and Dap-E12-W13 on DMPC/DMPC and DOPC/DOPG liposomes. Error bars represent the standard deviation of three different experiments.

Appendix C

HPLC Figures and ESI$^+$-MS of Dap-K6-X11-E12-W13 Analogs

Analytical HPLC gradient: 90% Acetonitrile and 10% H_2O (0.1% TFA) to 10% Acetonitrile and 90% H_2O (0.1% TFA) in over 50 min.

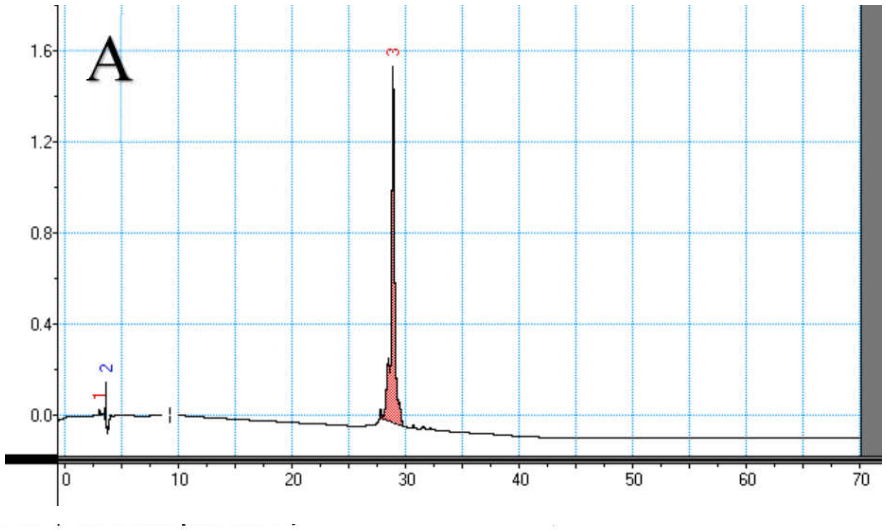

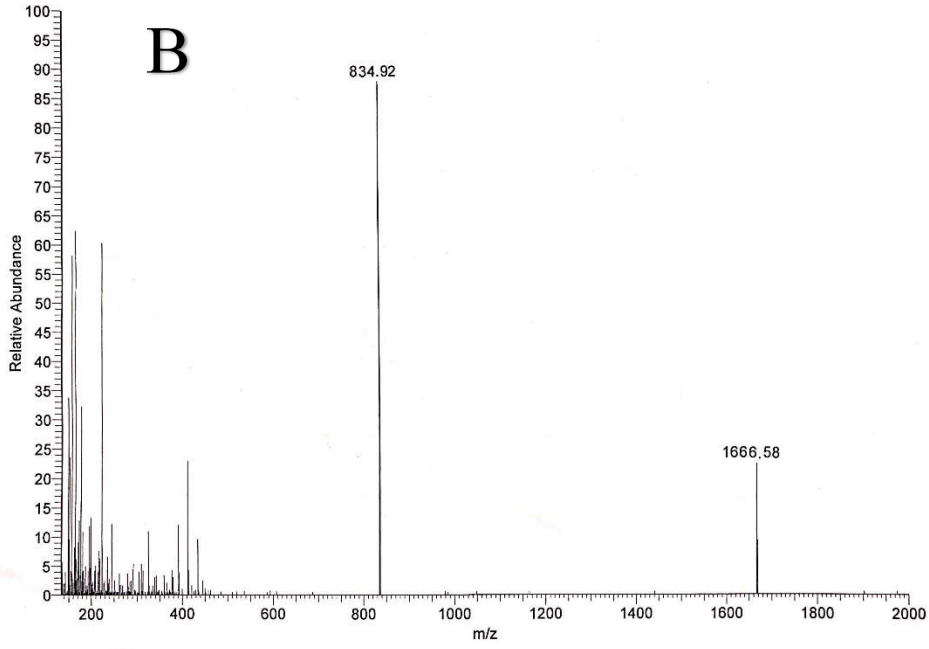

Figure C.1. (A) Analytical HPLC chromatogram of purified Dap-K6-D-H11-E12-W13. (B) HRMS of purified Dap-K6-D-H11-E12-W13, peak at *m/z* = 1666.58 corresponds to $[M+H]^{2+}$ and *m/z* = 834.92 corresponds to $[M+2H]^{2+}$.

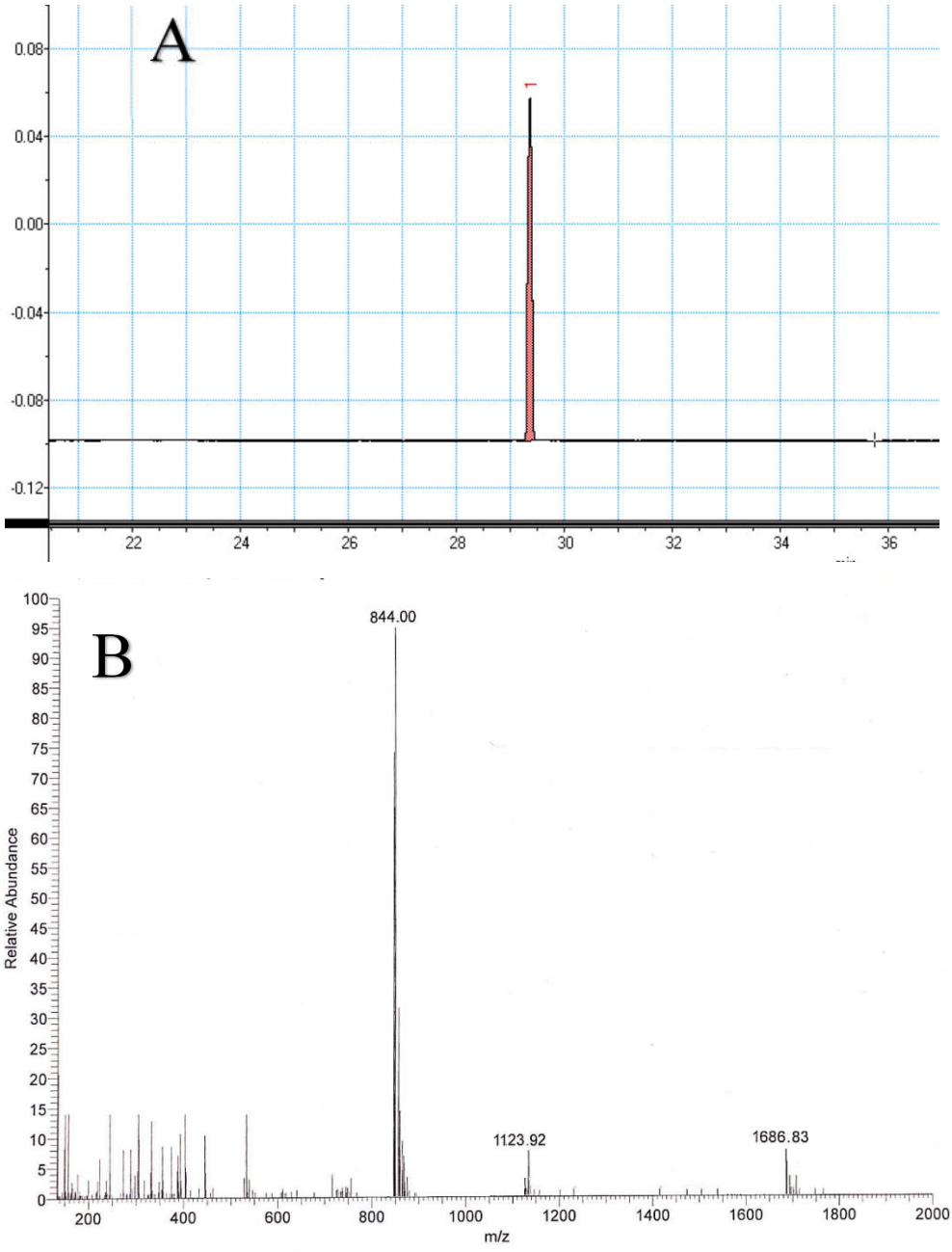

Figure C.2. (A) Analytical HPLC chromatogram of purified Dap-K6-D-R11-E12-W13. (B) HRMS of purified Dap-K6-D-R11-E12-W13, peak at *m/z* = 1686.83 corresponds to $[M+H]^{2+}$ and *m/z* = 844.00 corresponds to $[M+2H]^{2+}$.

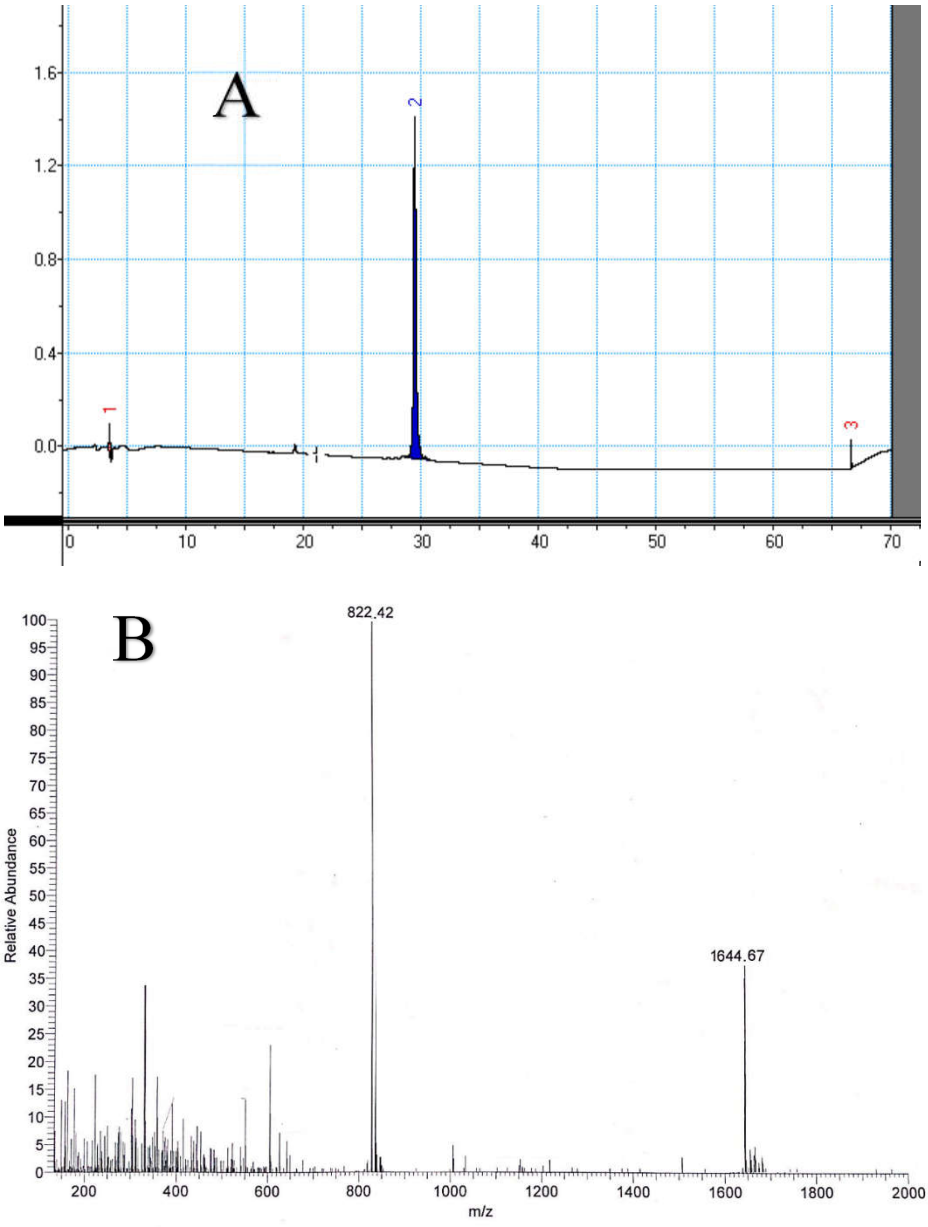

Figure C.3. (A) Analytical HPLC chromatogram of purified Dap-K6-D-N11-E12-W13. (B) HRMS of purified Dap-K6-D-N11-E12-W13, peak at *m/z* = 1644.67 corresponds to $[M+H]^{2+}$ and *m/z* = 822.42 corresponds to $[M+2H]^{2+}$.

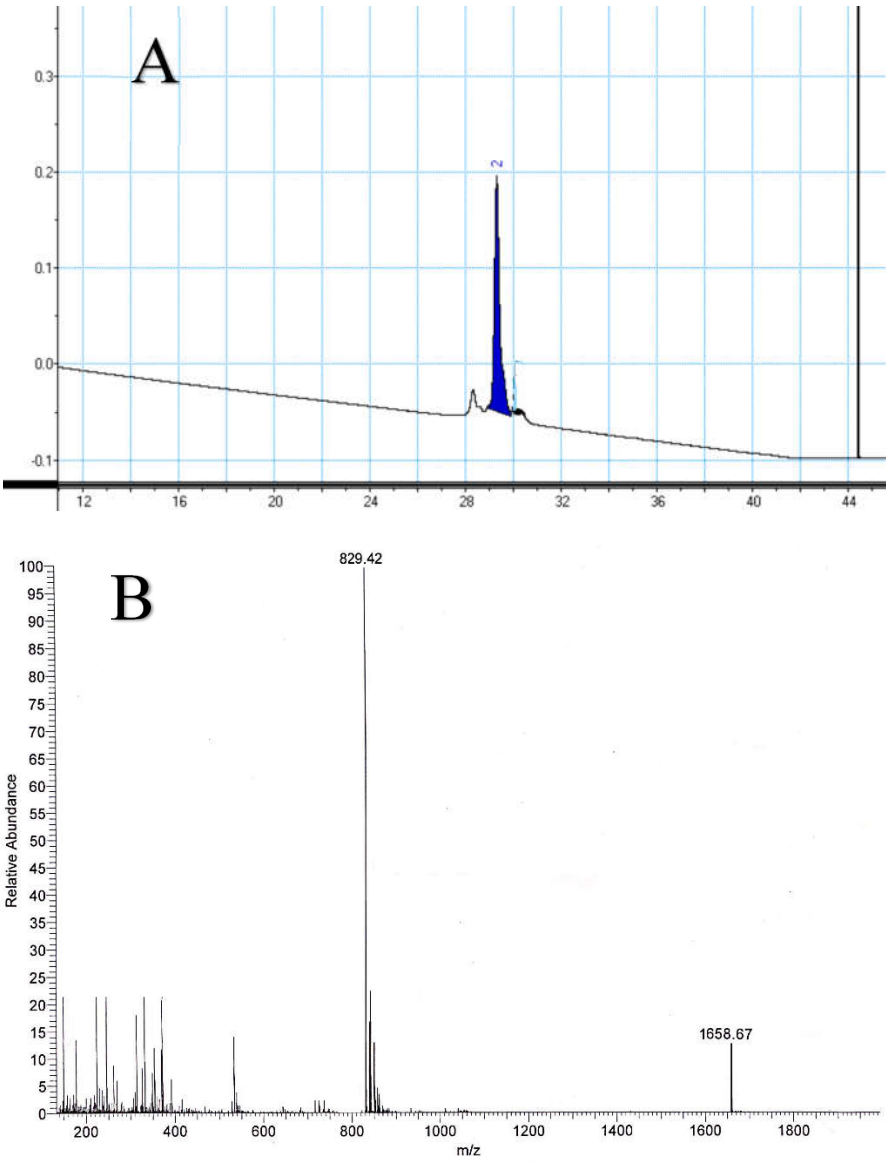

Figure C.4. (A) Analytical HPLC chromatogram of purified Dap-K6-D-Q11-E12-W13. (B) HRMS of purified Dap-K6-D-Q11-E12-W13, peak at *m/z* = 1658.67 corresponds to $[M+H]^{2+}$ and *m/z* = 829.42 corresponds to $[M+2H]^{2+}$.

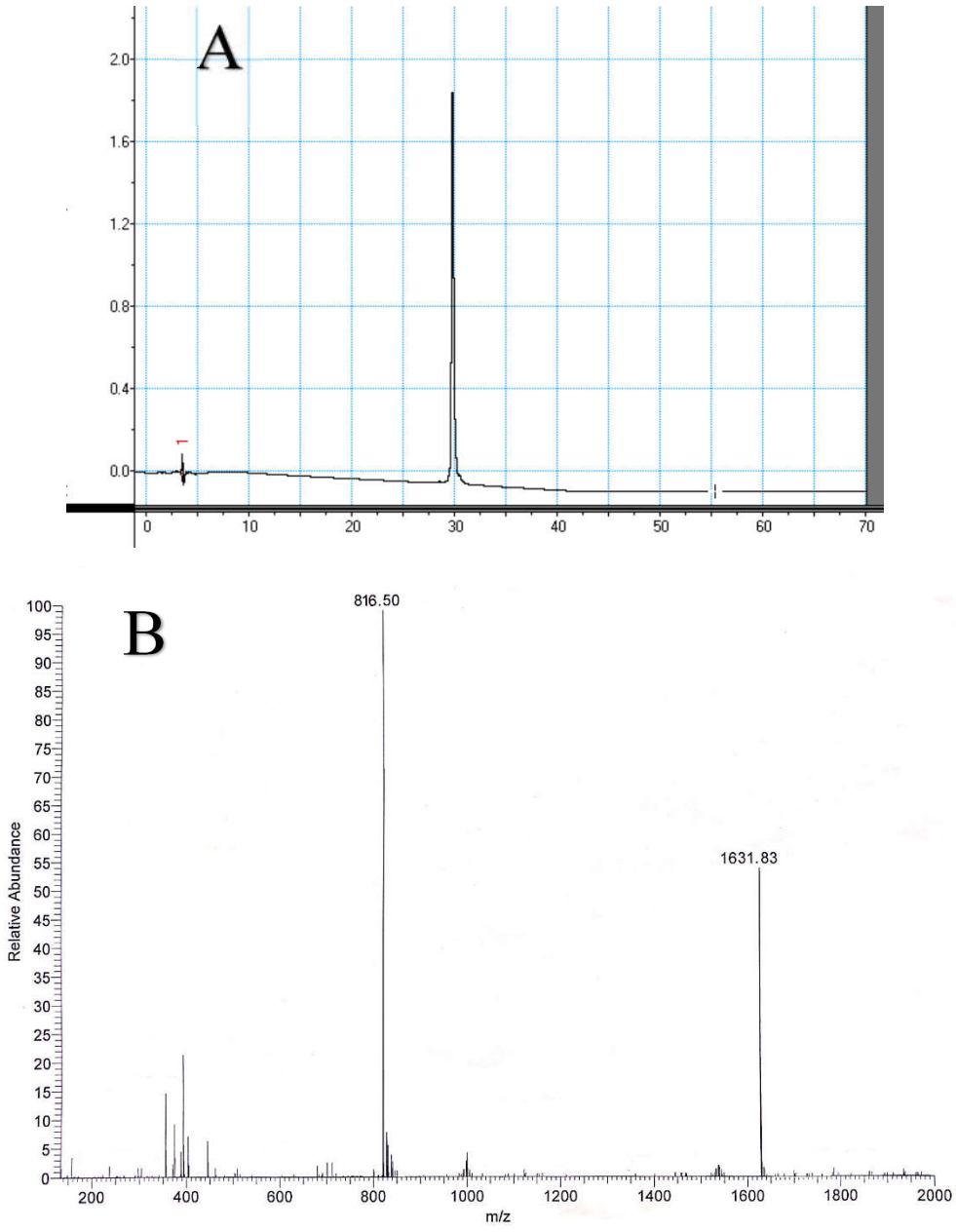

Figure C.5. (A) Analytical HPLC chromatogram of purified Dap-K6-D-T11-E12-W13. (B) HRMS of purified Dap-K6-D-T11-E12-W13, peak at *m/z* = 1631.83 corresponds to $[M+H]^{2+}$ and *m/z* = 816.50 corresponds to $[M+2H]^{2+}$.

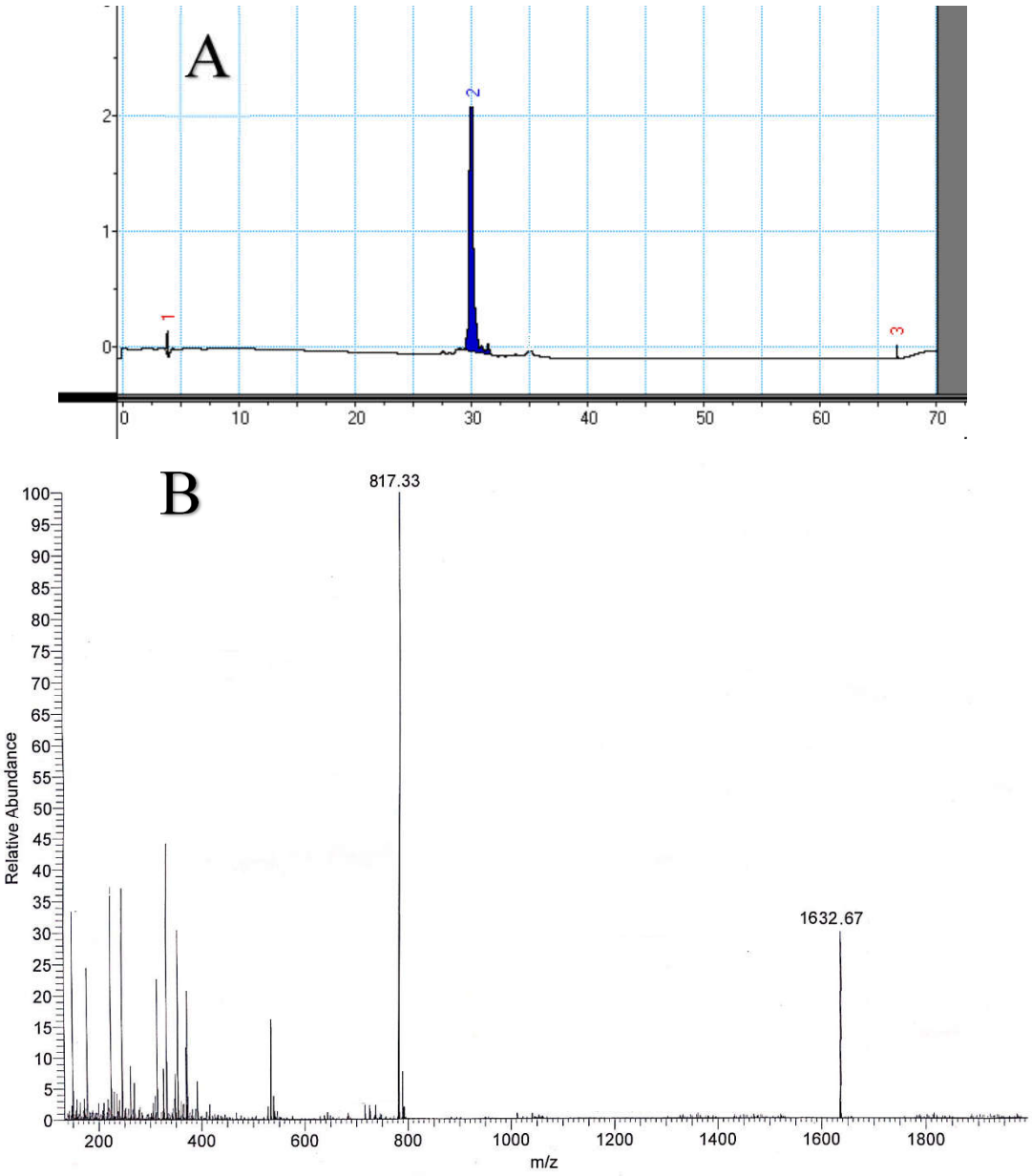

Figure C.6. (A) Analytical HPLC chromatogram of purified Dap-K6-D-C11-E12-W13. (B) HRMS of purified Dap-K6-D-C11-E12-W13, peak at *m/z* = 1632.67 corresponds to $[M+H]^{2+}$ and *m/z* = 817.33 corresponds to $[M+2H]^{2+}$.

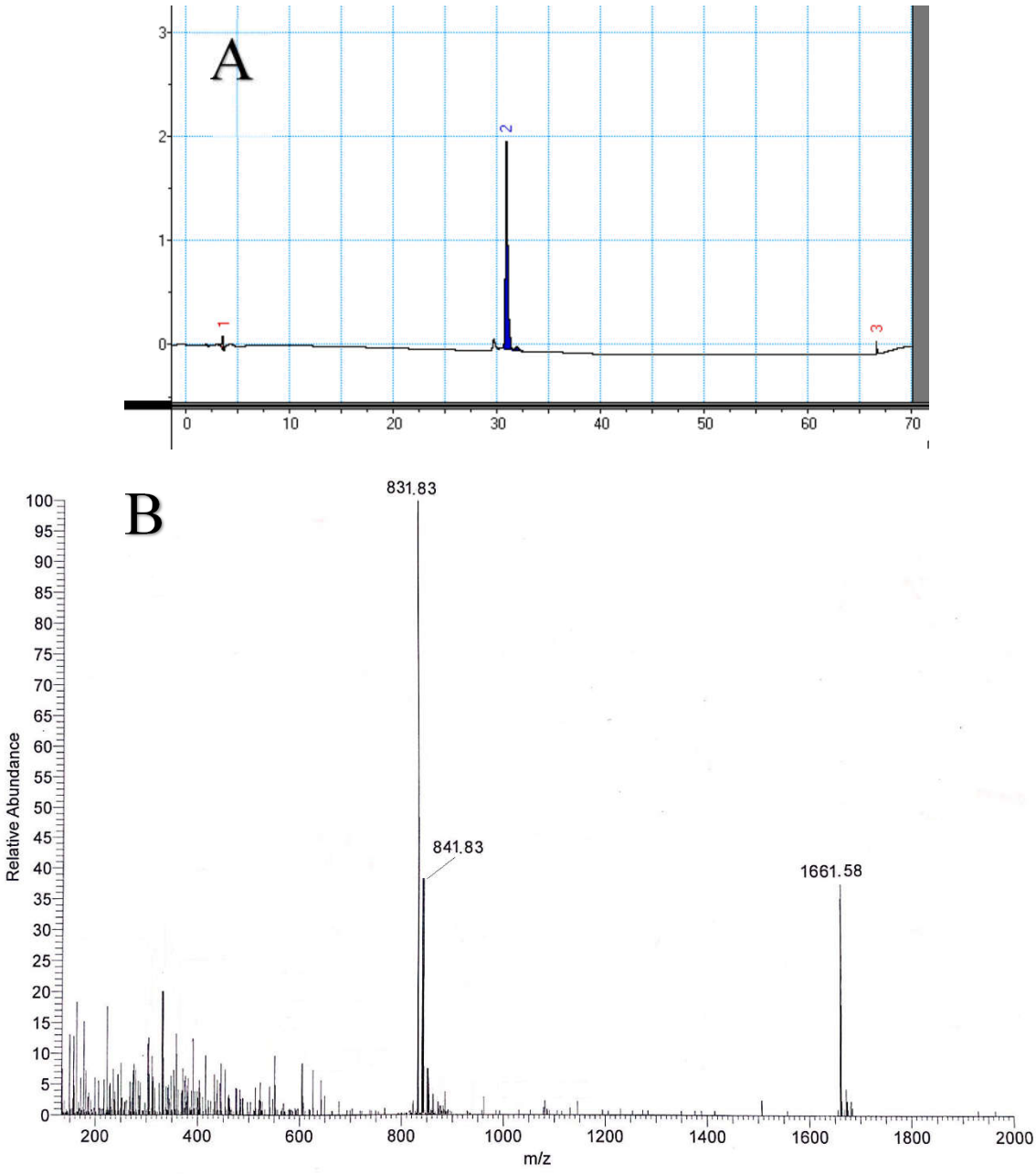

Figure C.7. (A) Analytical HPLC chromatogram of purified Dap-K6-D-M11-E12-W13. (B) HRMS of purified Dap-K6-D-M11-E12-W13, peak at *m/z* = 1661.58 corresponds to $[M+H]^{2+}$ and *m/z* = 831.83 corresponds to $[M+2H]^{2+}$.

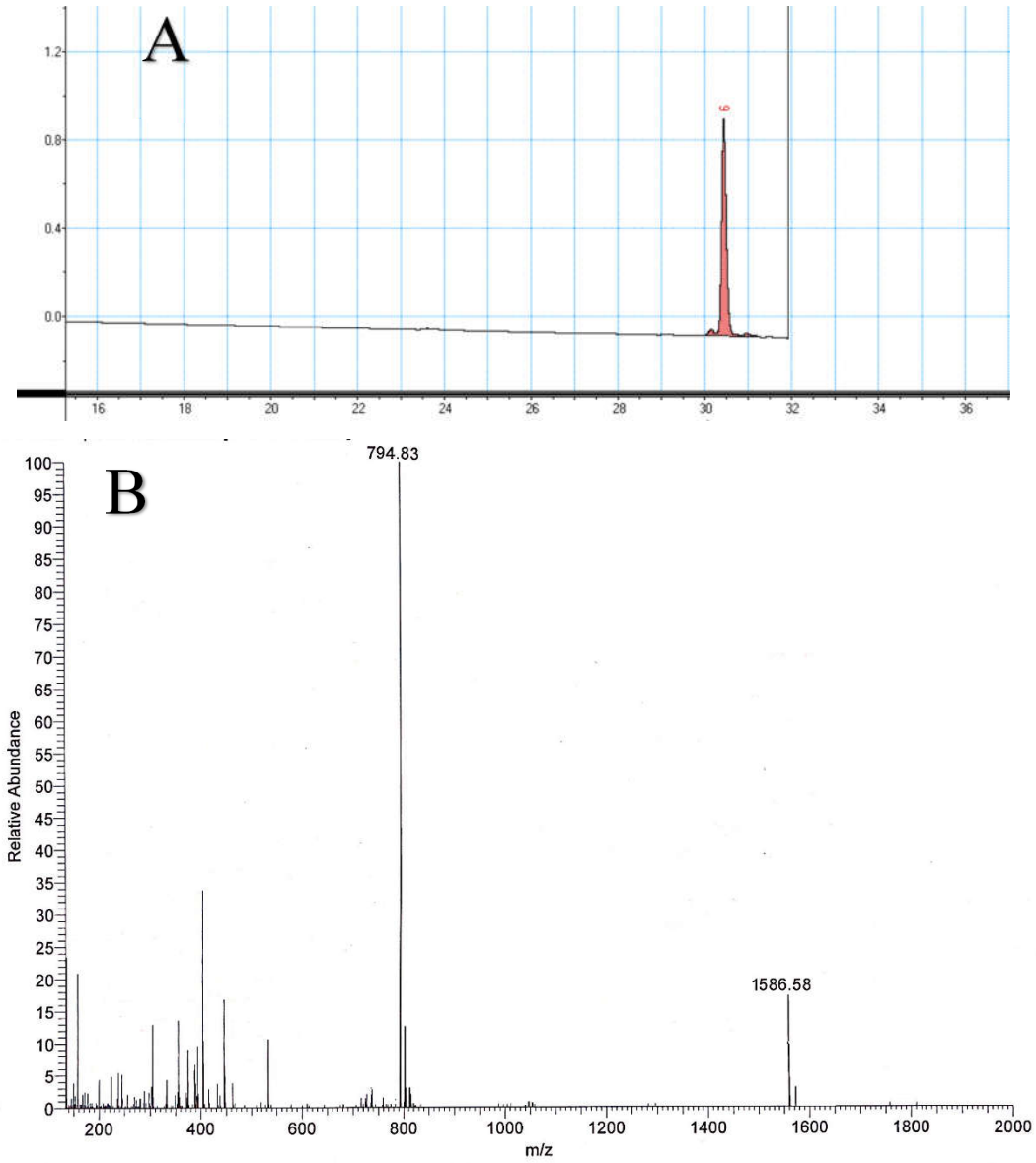

Figure C.8. (A) Analytical HPLC chromatogram of purified Dap-K6 -G11-E12-W13. (B) HRMS of purified Dap-K6-G11-E12-W13, peak at *m/z* = 1586.58 corresponds to $[M+H]^{2+}$ and *m/z* = 794.83 corresponds to $[M+2H]^{2+}$.

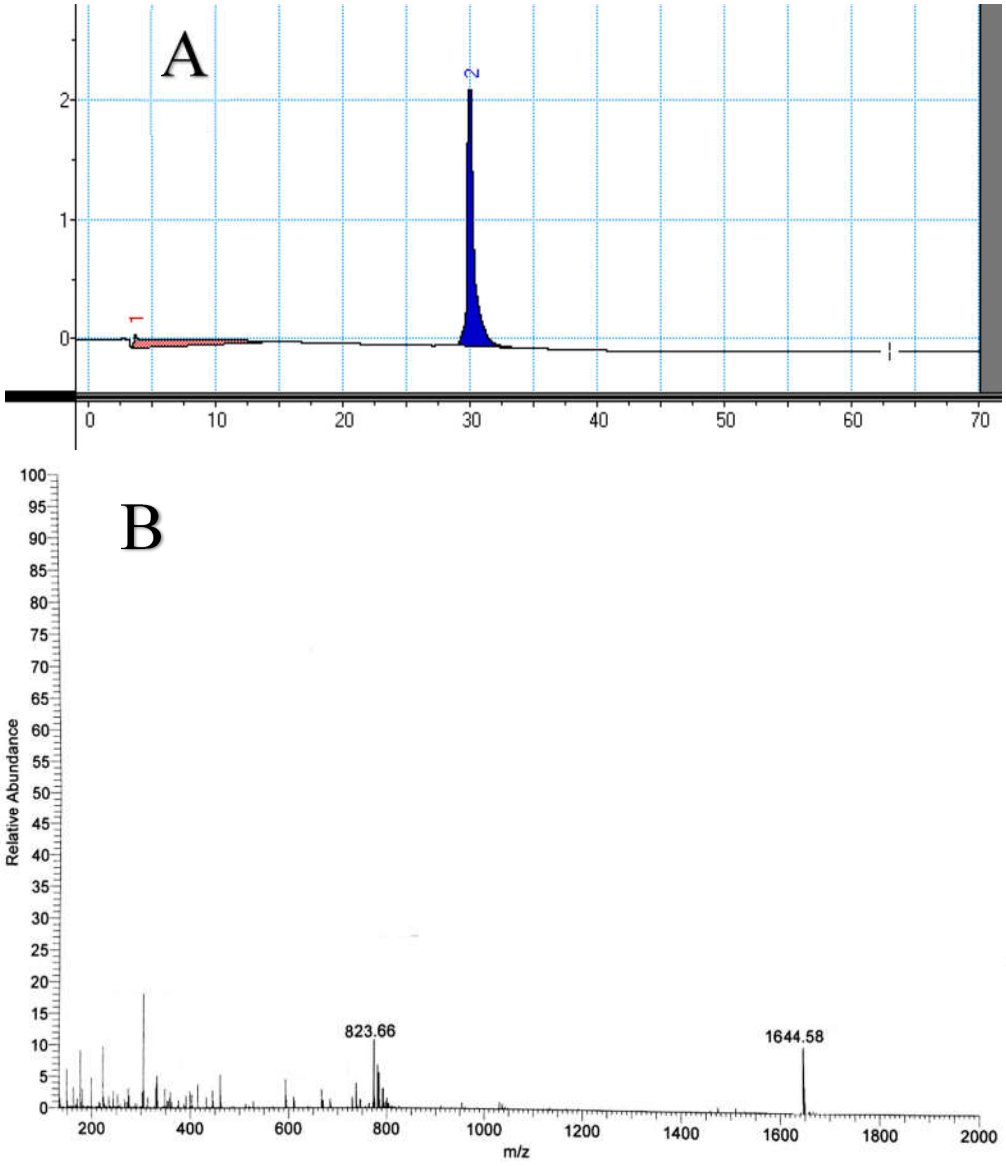

Figure C.9. (A) Analytical HPLC chromatogram of purified Dap-K6-D-D11-E12-W13. (B) HRMS of purified Dap-K6-D-D11-E12-W13, peak at *m/z* = 1644.58 corresponds to $[M+H]^{2+}$ and *m/z* = 823.66 corresponds to $[M+2H]^{2+}$.

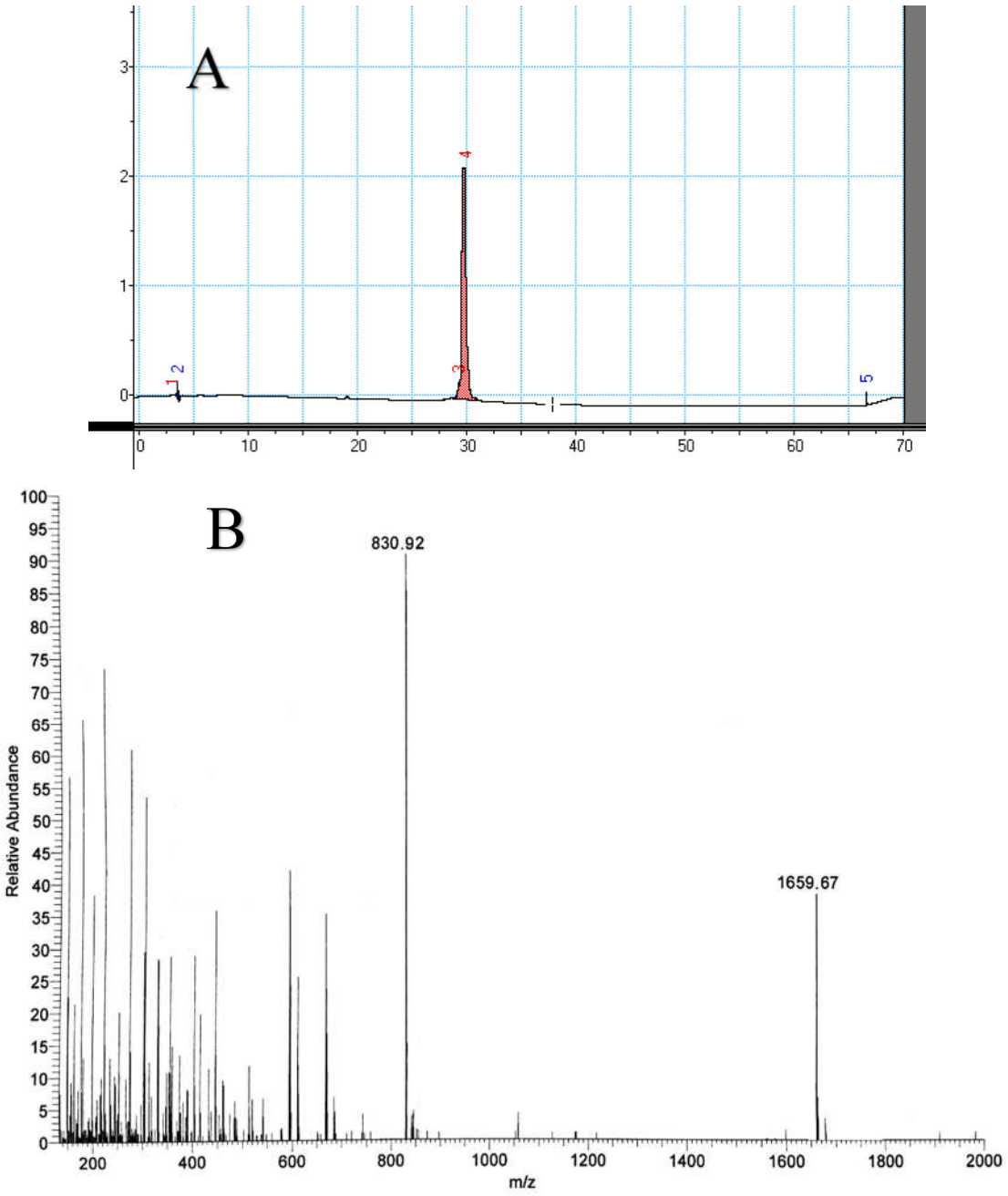

Figure C.10. (A) Analytical HPLC chromatogram of purified Dap-K6-D-E11-E12-W13. (B) HRMS of purified Dap-K6-D-E11-E12-W13, peak at *m/z* = 1659.67 corresponds to $[M+H]^{2+}$ and *m/z* = 830.92 corresponds to $[M+2H]^{2+}$.

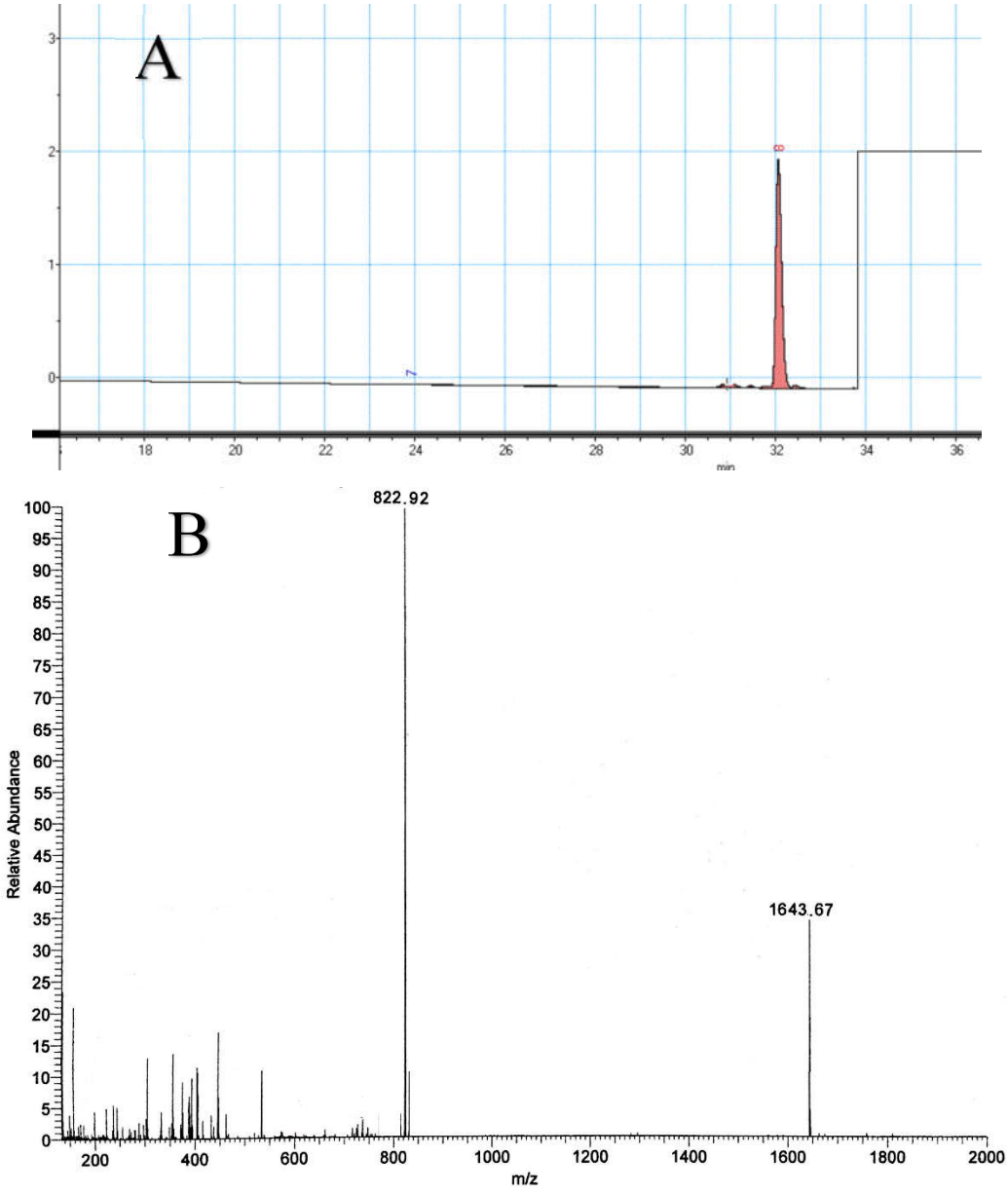

Figure C.11. (A) Analytical HPLC chromatogram of purified Dap-K6-D-L11-E12-W13. (B) HRMS of purified Dap-K6-D-L11-E12-W13, peak at *m/z* = 1643.67 corresponds to $[M+H]^{2+}$ and *m/z* = 822.92 corresponds to $[M+2H]^{2+}$.

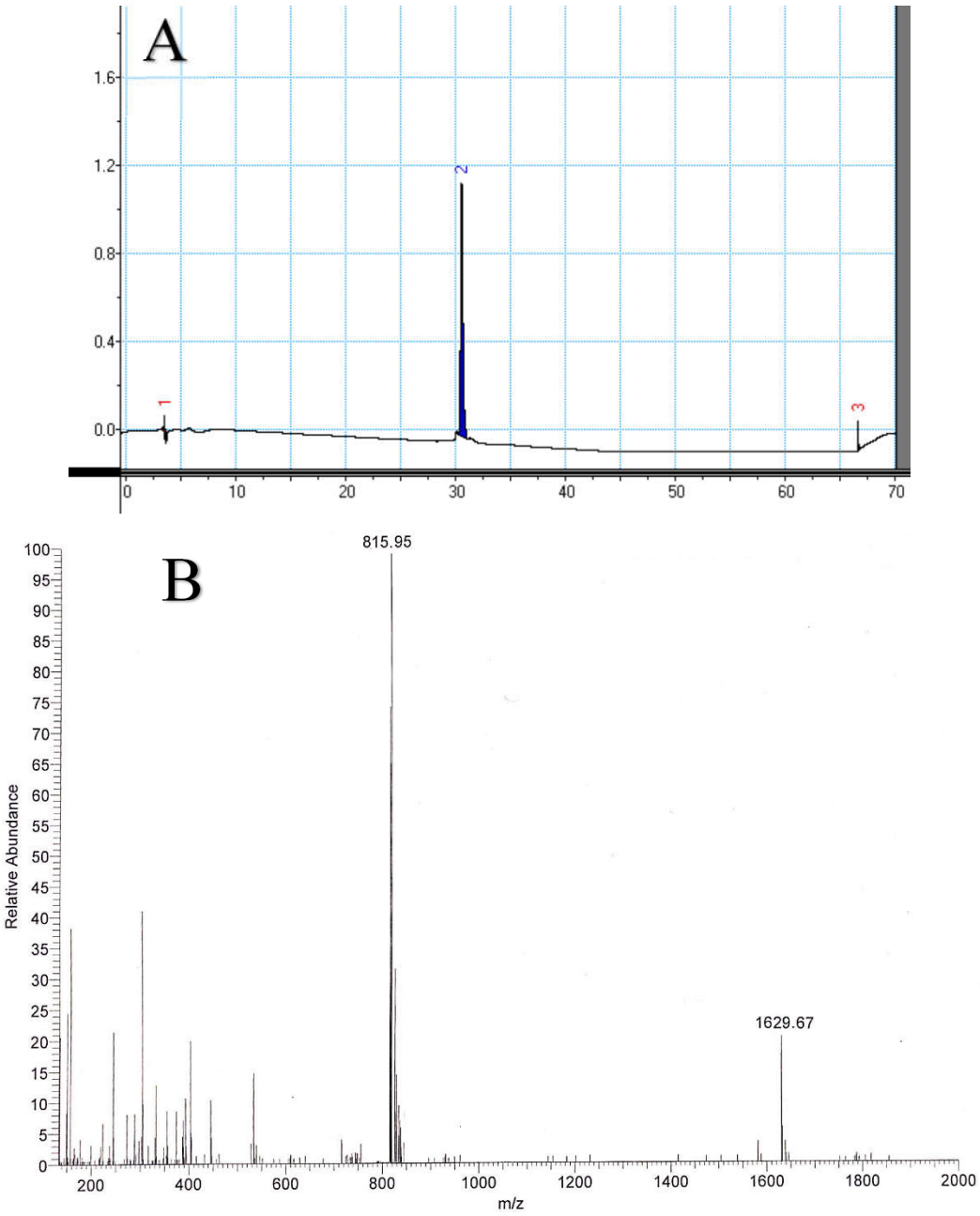

Figure C.12. (A) Analytical HPLC chromatogram of purified Dap-K6-D-V11-E12-W13. (B) HRMS of purified Dap-K6-D-V11-E12-W13, peak at *m/z* = 1629.67 corresponds to $[M+H]^{2+}$ and *m/z* = 815.95 corresponds to $[M+2H]^{2+}$.

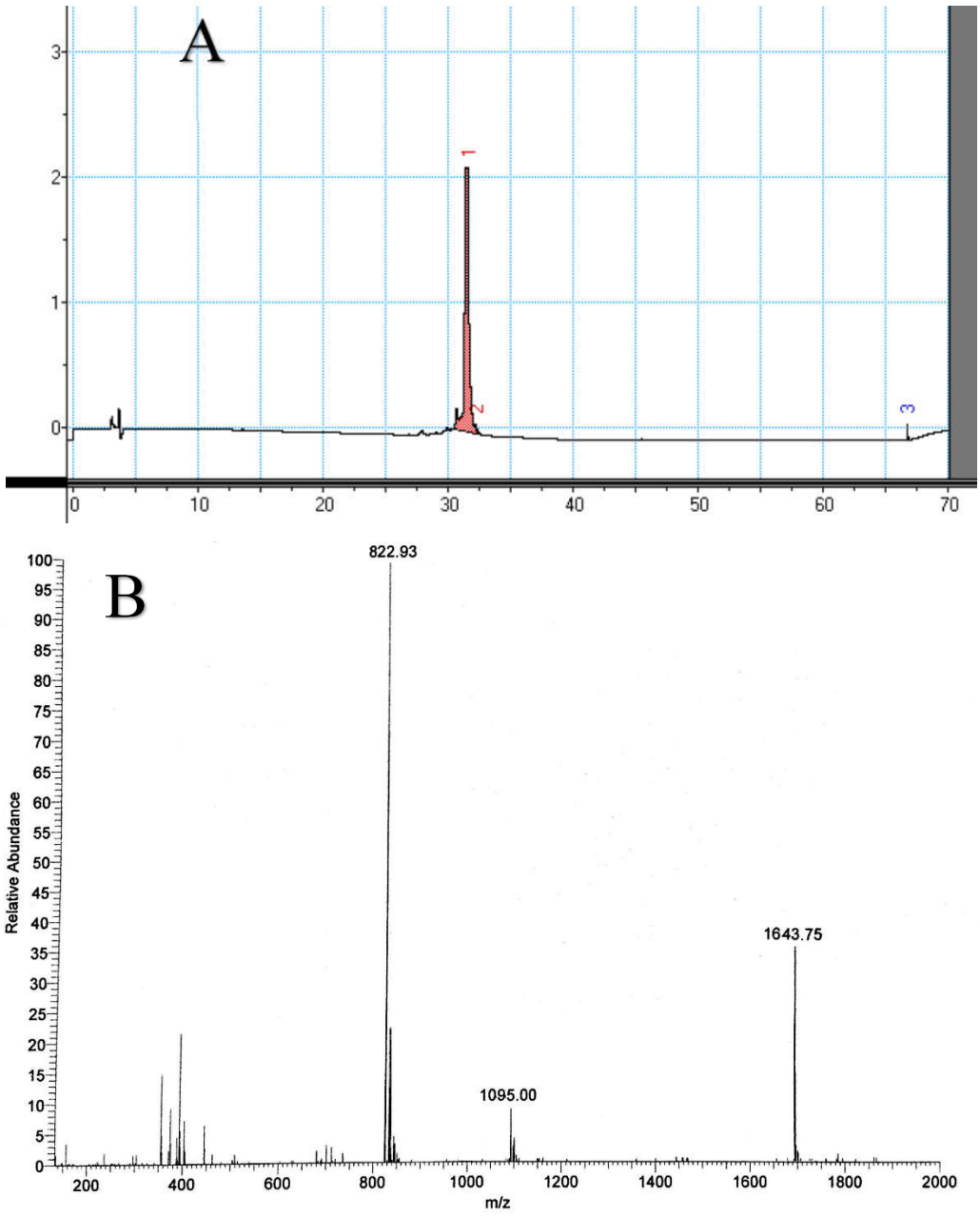

Figure C.13. (A) Analytical HPLC chromatogram of purified Dap-K6-D-allo-Ile11-E12-W13. (B) HRMS of purified Dap-K6-D-allo-Ile11-E12-W13, peak at *m/z* = 1643.75 corresponds to $[M+H]^{2+}$ and *m/z* = 822.93 corresponds to $[M+2H]^{2+}$.

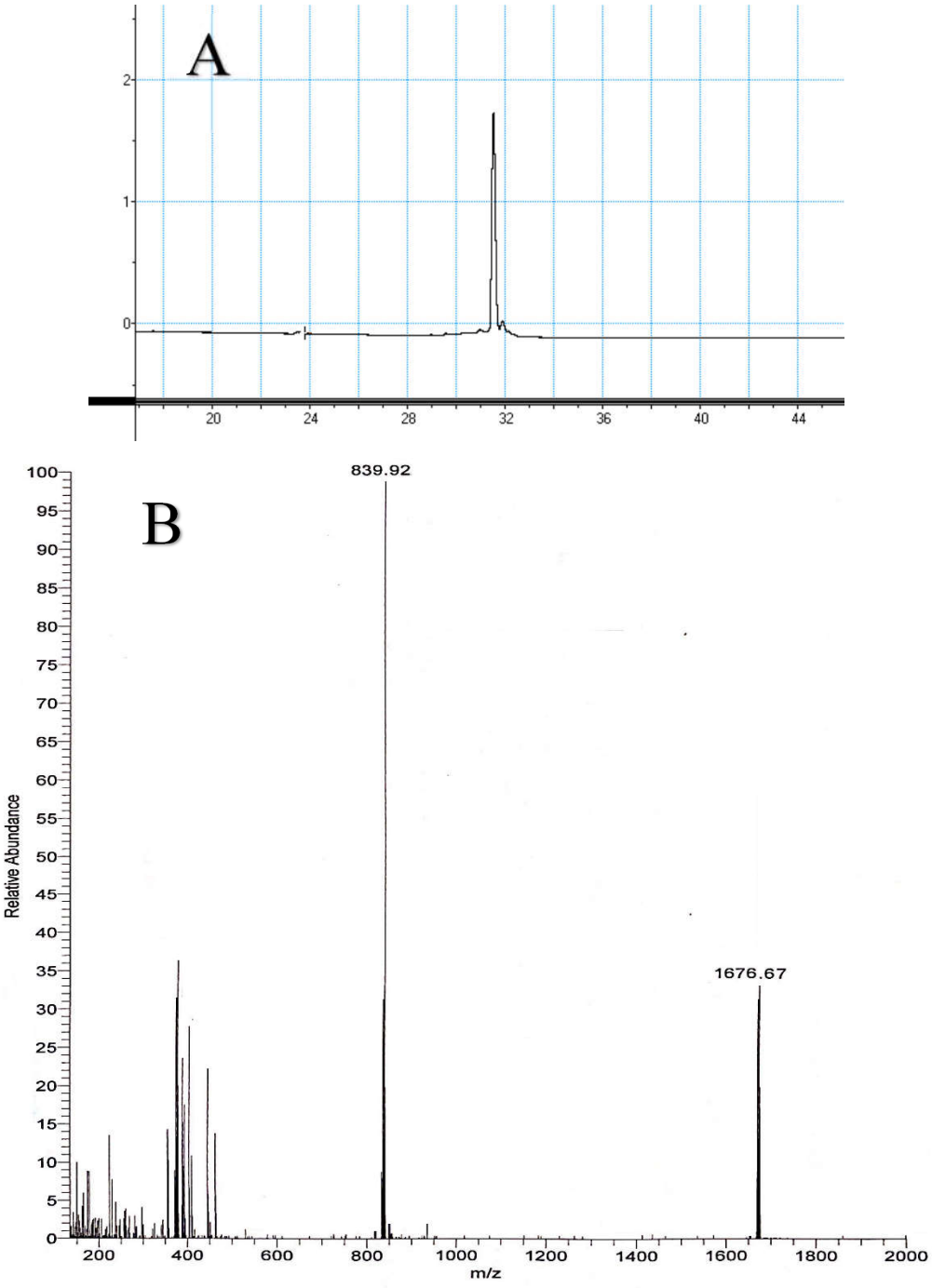

Figure C.14. (A) Analytical HPLC chromatogram of purified Dap-K6-D-F11-E12-W13. (B) HRMS of purified Dap-K6-D-F11-E12-W13, peak at *m/z* = 1676.67 corresponds to $[M+H]^{2+}$ and *m/z* = 839.92 corresponds to $[M+2H]^{2+}$.

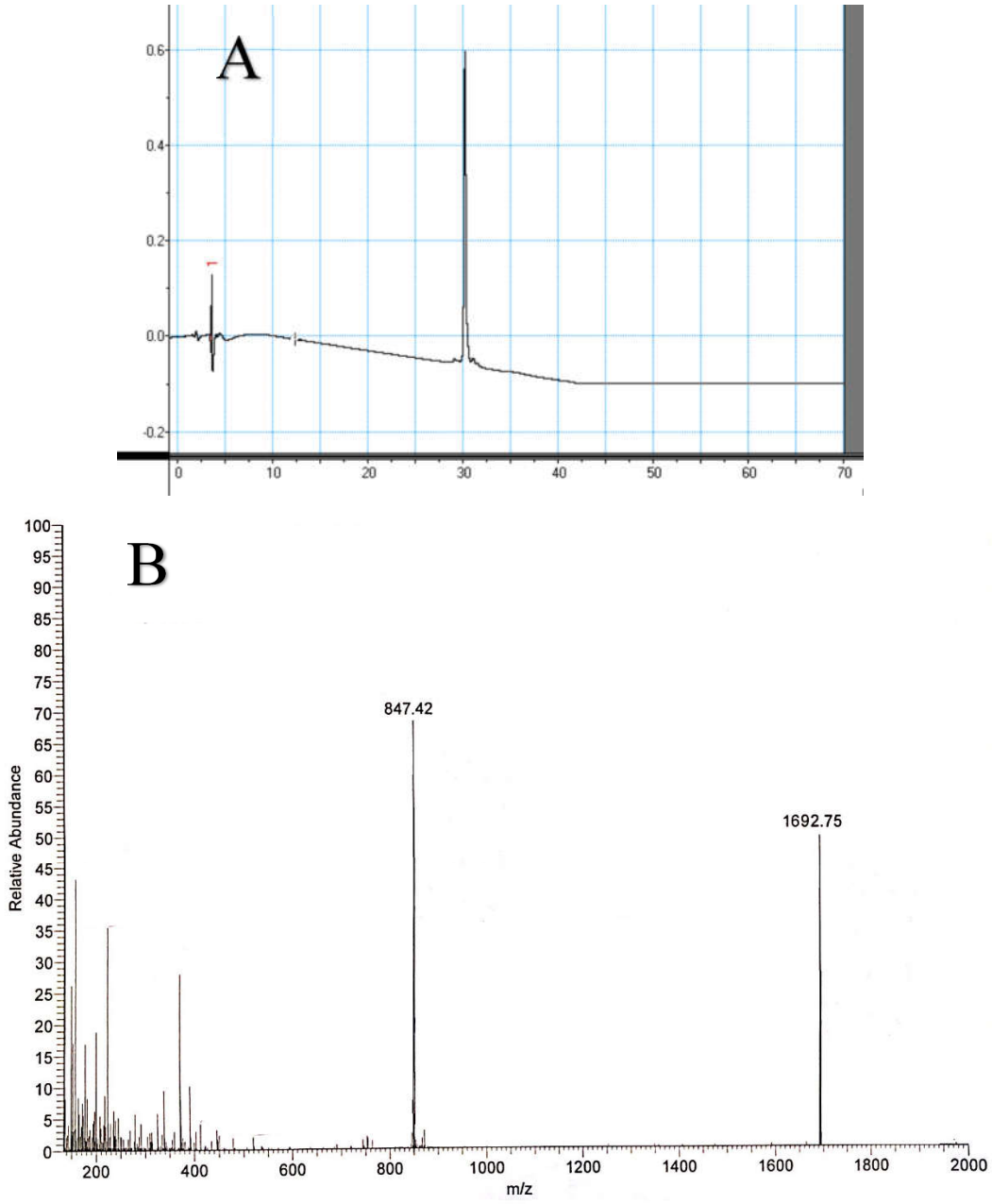

Figure C.15. (A) Analytical HPLC chromatogram of purified Dap-K6-D-Y11-E12-W13. (B) HRMS of purified Dap-K6-D-Y11-E12-W13, peak at *m/z* = 1692.75 corresponds to $[M+H]^{2+}$ and *m/z* = 847.42 corresponds to $[M+2H]^{2+}$.

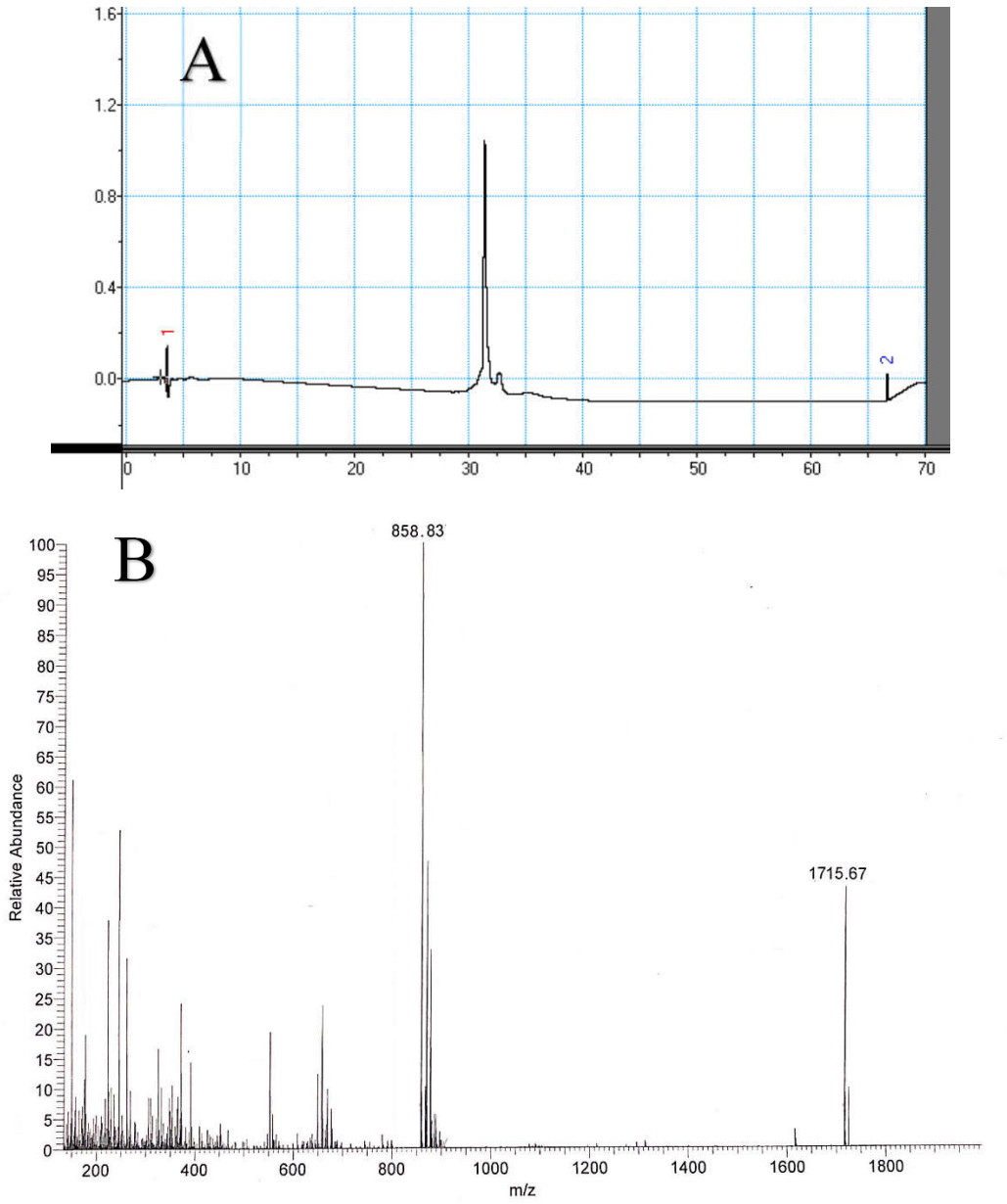

Figure C.16. (A) Analytical HPLC chromatogram of purified Dap-K6-D-W11-E12-W13. (B) HRMS of purified Dap-K6-D-W11-E12-W13, peak at *m/z* = 1715.67 corresponds to $[M+H]^{2+}$ and *m/z* = 858.83 corresponds to $[M+2H]^{2+}$.

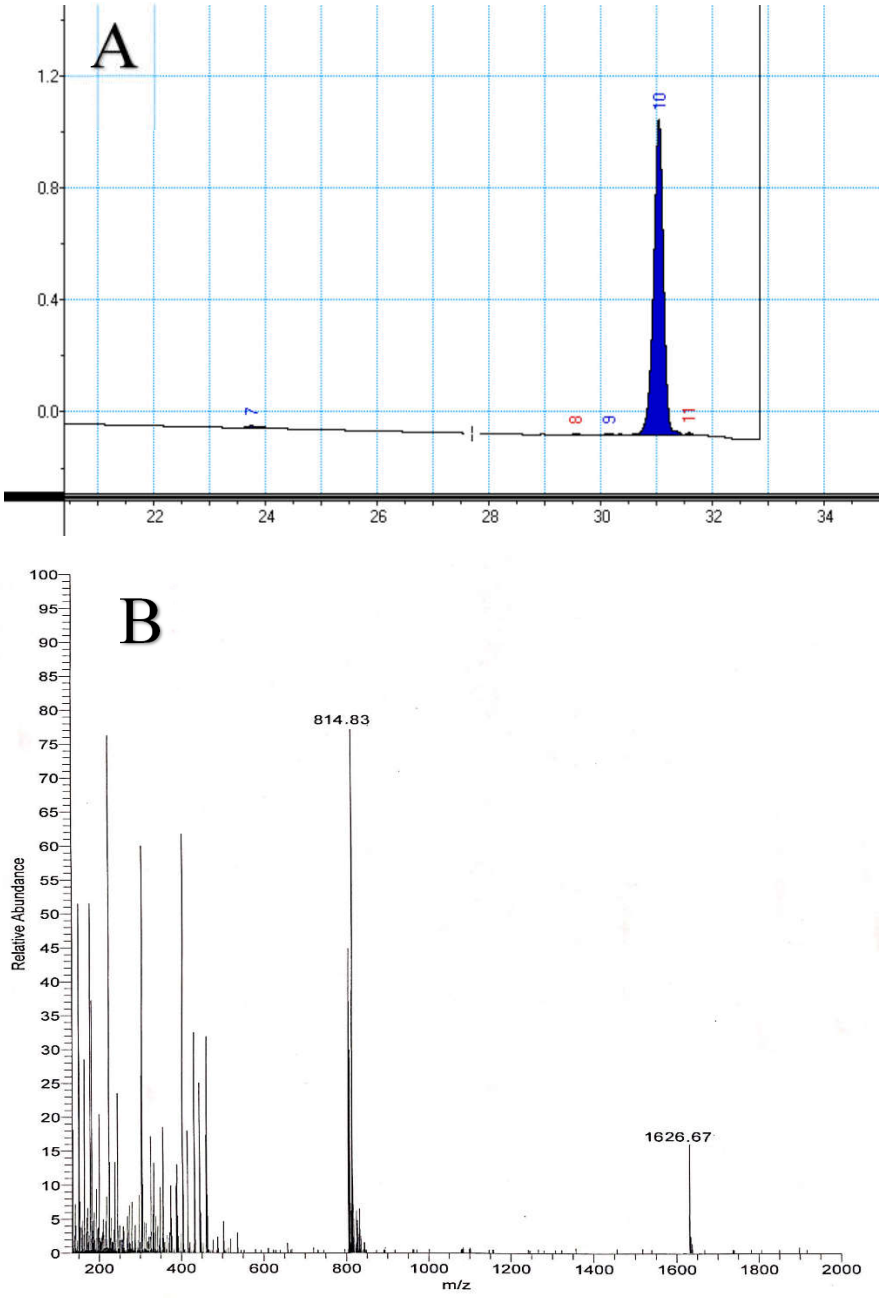

Figure C.17. (A) Analytical HPLC chromatogram of purified Dap-K6-D-P11-E12-W13. (B) HRMS of purified Dap-K6-D-P11-E12-W13, peak at *m/z* = 1626.67 corresponds to $[M+H]^{2+}$ and *m/z* = 814.83 corresponds to $[M+2H]^{2+}$.